BUCKLING OF COMPOSITE LAMINATES WITH RANDOM MATERIAL PROPERTIES

A Thesis Submitted

in Partial Fulfillment of the Requirements

for the Degree of

Master of Technology

by

K. SUBRAMANYAM RAJU

to the

DEPARTMENT OF AEROSPACE ENGINEERING

INDIAN INSTITUTE OF TECHNOLOGY KANPUR

December 1998

CERTIFICATE

It is certified that the work contained in this thesis entitled **Buckling of Composite Laminates with Random Material Properties**, by **K. Subramanyam Raju**, has been carried out under our supervision and that this work has not been submitted elsewhere for a degree.

N.G.R. Iyengar

Dr. N.G.R. Iyengar
Professor
Department of Aerospace Engg.
IIT Kanpur

D. Yadav

Dr. D. Yadav
Professor
Department of Aerospace Engg.
IIT Kanpur

December, 1998

Acknowledgement

I would like to this opportunity to express my sincere gratitude to my thesis supervisors Dr. N. G. R. Iyengar and Dr. D. Yadav for their sincere help, fruitful suggestions and inspiration during the entire course of this work. I am extremely thankful to them for giving me complete freedom of work, thus helping me to gain confidence and to work independently.

I sincerely thank to my friends Sri K. Ravi, Sri K. Ramu, Sri S. Valibabu, S. M. Vishnu and Raju

I am also very much thankful to my friends Srikanth, Sridhar, Bhaskar, Prasanth, Mishra and Kitey for their all round support, encouragement and suggestions.

I wish to express my indebtedness to my parents, sisters and uncles, brother and sister-in-law whose deep affection and inspiration have always guided me towards success.

Keerthipati Subramanyam Raju.

DEDICATED

TO

MY PARENTS

Abstract

Composite materials have large number of uncertain parameters associated with its manufacturing. It is not possible to control these completely. This results in variations in the properties of composite materials. For accurate modeling, the material properties are, therefore, considered as random variables. The influence of randomness in material properties on buckling behavior of graphite/epoxy composite laminate has been analyzed in the present study with the help of Monte Carlo Simulation and FEM. The analysis has been carried out for composite laminates with different edge conditions, aspect ratios(ARs), and ply-orientations to random material properties. The study has also been extended to plates with cut-outs using NASTRAN software. It has been found that the normalized buckling response of the composite plates with random materials is similar for various aspect ratios, edge conditions and ply-orientations. Further, for a given area of the cut-outs, the buckling load for a laminate with elliptical cut-out is lower than circular and rectangular cut-outs. The buckling load with circular cut-out is the highest.

Contents

List of Figures

List of Tables

Nomenclature

AR	: Aspect ratio of the plate (a/b)
CC	: Clamped - Clamped edge conditions
SS	: Simply Supported edge conditions
SD, σ	: Standard Deviation
RV	: Random Variable
a	: Length of the plate
b	: Breadth of the plate
d	: Diameter of the Cut-out
c/d	: Length of major and minor axes of the cut-
out	
h	: Thickness of the plate
μ	: Mean

Chapter 1

Introduction

The composite materials are formed by the combination of two or more materials on a macroscopic scale. The materials used in composites may be called as: reinforcing material and parent or matrix material. Structures made of such materials are called as composite structures.Composite structures can be fabricated to have better performance in engineering applications compared to the conventional metallic materials. . Some of the properties that can be improved by forming a composite are: stiffness and strength to weight ratios, corrosion resistance, thermal characteristics, fatigue life and wear resistance etc,. These are the reasons for composites finding applications in a variety of systems including aircraft and submarine structures, space structures, automobiles, sports equipment, medical prosthetic devices and electronic circuit boards.

Presently, aircrafts are being manufacturing with a very high percentage of components made from the composite materials. These results in reduction in structural weight consequently the payload can be increased for a given engine performance. Besides this, the range can be extended and operating efficiency improved. Space vehicles having plan forms like plates have been designed and built of high strength temperature resistant composite materials. Composite materials used for space vehicles provides structural efficiency, ease of fabrication and freedom from thermal distor-

tion.

All materials will have dispersion in material properties due to lack of complete control over manufacturing / fabrication / processing techniques employed. Composite materials experience larger dispersions in their material properties compared to conventional materials due to larger number of parameters involved in their fabrication. Also, the uncertainties involved in manufacturing and processing techniques employed for composites are more as compared to isotropic materials. These uncertainties can occur due to air entrapment, de-lamination, lack of resin, incomplete curing of resin, excess resin between layers etc,. Moreover, the different test methods provide variable property data. Zweben [1] illustrated the dispersion in test data as a result of conventional testing methods used for composites.

Considering the above aspects, the properties of structural materials in general and composites in particular, may be modeled as a random process. However, in conventional structural analysis generally used for composites, the material properties like elastic modulus, poisson's ratio etc. are commonly assumed to be deterministic quantities. Studies made by various researchers have shown that the effects of material property randomness on dynamic response are much more pronounced in case of composites as compared to conventional materials [2]. It is, therefore, important to consider the material properties as random in the case of composites vis-a-vis the metallic materials as otherwise the predicted response may differ significantly from the observed values and the structures may not be safe.

In spite of the well-developed theory and computational methods for structural responses for deterministic material properties, the random structural analysis where the material properties are considered random remains underdeveloped. Nevertheless, for reliability of design and considering the sensitivity of the application, accurate predictions of the system behavior of structure made up of composites in the presence of the uncertainties favors a probabilistic analysis approach for composites by modeling their properties as random variables(RVs).

1.1 Literature survey

The uncertainties in strength and stiffness properties of composites has been studied by many researchers. Ibrahim [3] reviewed number of topics on structural dynamics with parameter uncertainties. Nakagiri et al.[4] have studied simply supported (SS) graphite/epoxy plates with Stochastic Finite Element Method (SFEM) taking fiber orientation, layer thickness and number of layers as random variables, and found that the overall stiffness of Fiber Reinforced Plastic(FRP) laminated plates is found out to be largely dependent on fiber orientation. Leissa [5] and Martin have analyzed the vibration and buckling of rectangular composite plates and have established that variation in fiber spacing or redistribution of fibers tend to increase the buckling load by 38 percent and the fundamental frequency by 21 percent. Englestad and Reddy [6] studied metal matrix composites (MMC) based on probabilistic micro mechanics nonlinear analysis. They have used Monte Carlo Simulation(MCS), and different probabilistic distributions to incorporate the uncertainty in basic material properties. Vinckenroy and de Wilde [7] in their first part of the work have established a procedure to obtain the best fit for each material property. Further, they have studied the behavior of perforated plate and determined the probability distribution of the response. The input variables have been simulated using MCS and SFEM. Salim et.al [8] studied the statistical response of the system considering the material properties such as, longitudinal modulus, poisson's ratio, transverse elastic modulus, etc., as independent random variables on $[90^0/0^0/90^0]$ and 0^0, rectangular, SS, and CC plates subject to transverse static loads. Salim et.al [9] have shown that there is change in the rate and the order of the natural frequency with SD of input RV and boundary conditions of the plate. Raj et.al [10] studied the response of composite plates with random material properties using FEM and MCS, and found that the longitudinal modulus E_{11} and in-plane shear modulus G_{11} are the most critical material properties influencing the deflection

characteristics of the laminate. Jagdeesh [11] studied the static response of composite laminates with randomness in material properties as well as external loading. There appears to be a very few published literature when both material properties and external loading are modeled as random variables,especially in the area of composites. Salim et.al [12] used the perturbation technique with Rayleigh-Ritz (RR) formulation to analyze the bending, buckling and vibration of composite plates. The RR method can be used only for regular boundary problems. This problem can be over come by using FEM for buckling analysis. Though the perturbation technique though gives acceptable results, the method fails for larger dispersions in the input random variables. The SFEM can handle larger uncertainties in the input parameters. However, it is computationally expensive and being a specialized technique its other applications are limited.

1.2 Present work

With the usage of fiber reinforced and laminated composite materials, the domain of application and range of various shapes of plan forms like plates has enormously increased. Aircraft as well as space vehicles, having plan forms like plates, have been designed and successfully built of high strength temperature resistant composite materials. The skin of aircraft structures are also composed of plate forms, built of stiffened plates and /or composite materials. Thus, with such immense potential of applications in various fields of engineering, the design criteria becomes stringent. Therefore, it is of paramount importance to consider the basic material parameters as random and study their effect on the response characteristics of plate structures. The difficulties in applications of perturbation technique and SFEM to random material properties in problem of composite laminates has motivated the use of a FEM and commercially available NASTRAN software in the present study. The material properties are assumed to vary randomly.

The stiffness properties of lamina such as E_{11}, E_{12}, G_{12} and ν_{12} have been selected to represent its behavior and are taken to be random variables. In the present analysis the buckling of composite laminates due to uniaxial in-plane load has been studied with the above material properties modeled as random variables. MCS and FEM is adopted to obtain the critical load of the laminated plates and its statistics with different input characteristics and cut-out shapes.

1.3 Layout of the thesis

In the present work, the buckling characteristics of the plate with random material properties have been studied. The thesis is organized in the following way. The formulation for buckling analysis has been presented in Chapter 2. The Monte Carlo simulation has been used for random analysis. This has been discussed in Chapter 3. The response characteristics of the plate have been presented in Chapter 4. The conclusions and a few suggestions for further work are given in Chapter 5.

Chapter 2

Formulation for Buckling

2.1 Stress-Strain relations for orthotropic lamina

The constituent equations for kth orthotropic lamina of the laminate in a two-dimensional state of stress along 1 and 2 can be written as

$$\begin{Bmatrix} \sigma_1 \\ \sigma_2 \\ \sigma_{12} \end{Bmatrix}^k = \begin{bmatrix} Q_{11} & Q_{12} & 0 \\ Q_{12} & Q_{22} & 0 \\ 0 & 0 & Q_{66} \end{bmatrix}^k \begin{Bmatrix} \epsilon_1 \\ \epsilon_2 \\ \gamma_{12} \end{Bmatrix}^k \tag{2.1}$$

It can also be written as

$$\begin{Bmatrix} \sigma_1 \\ \sigma_2 \\ \sigma_{12} \end{Bmatrix}^k = [Q_{ij}]^k \begin{Bmatrix} \epsilon_1 \\ \epsilon_2 \\ \gamma_{12} \end{Bmatrix}^k \tag{2.2}$$

where

$[Q_{ij}]_{i,j=1,2,\cdots,6}$ are the stiffness coefficients of the lamina and they are related to the material properties as follows

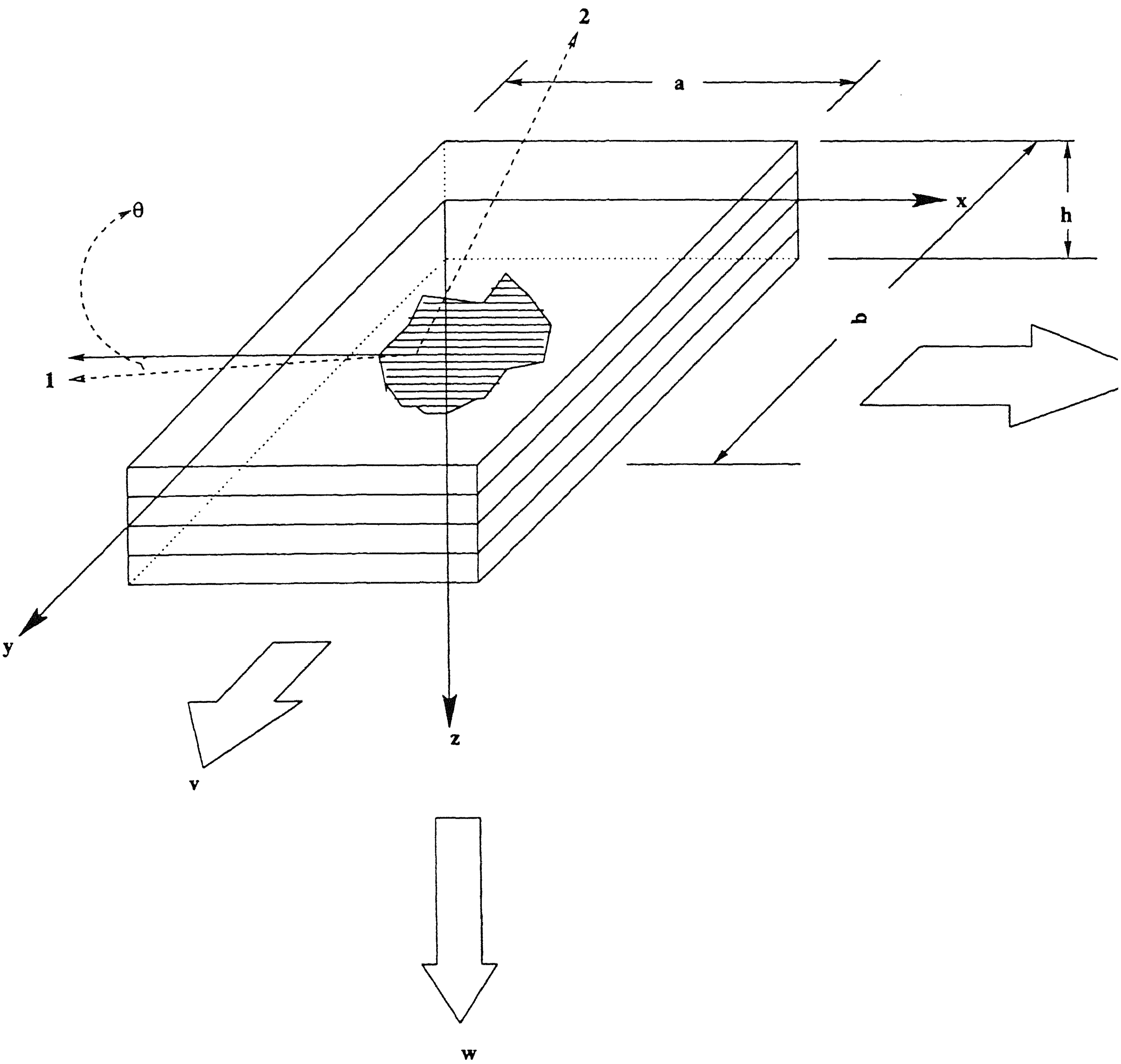

Figure 2.1: Laminated composite rectangular plate

$$
\begin{aligned}
Q_{11} &= \frac{E_{11}}{1-\nu_{12}\nu_{21}} \\
Q_{22} &= \frac{E_{12}}{1-\nu_{12}\nu_{21}} \\
Q_{12} &= \frac{\nu_{12}E_{12}}{1-\nu_{12}\nu_{21}} \\
Q_{66} &= G_{12}
\end{aligned}
\tag{2.3}
$$

Stress-strain relations along x and y axes for the lamina with fiber orientation θ (as shown in Fig. 2.1) are

$$
\left\{\begin{array}{c} \sigma_x \\ \sigma_y \\ \sigma_{xy} \end{array}\right\}^k = \begin{bmatrix} \bar{Q}_{11} & \bar{Q}_{12} & \bar{Q}_{16} \\ \bar{Q}_{21} & \bar{Q}_{22} & \bar{Q}_{26} \\ \bar{Q}_{16} & \bar{Q}_{26} & \bar{Q}_{66} \end{bmatrix}^k \left\{\begin{array}{c} \epsilon_x \\ \epsilon_y \\ \gamma_{xy} \end{array}\right\}^k \tag{2.4}
$$

It can be rewritten as

$$
\left\{\begin{array}{c} \sigma_x \\ \sigma_y \\ \sigma_{xy} \end{array}\right\}^k = \left[\bar{Q}_{ij}\right]^k \left\{\begin{array}{c} \epsilon_x \\ \epsilon_y \\ \gamma_{xy} \end{array}\right\}^k \tag{2.5}
$$

where

$\left[\bar{Q}_{i,j}\right]$ are the transformed stiffness coefficients for the kth lamina

The relations between the elements of the $\left[\bar{Q}\right]$ matrix and the $[Q]$ are [13]

$$
\begin{aligned}
\bar{Q}_{11} &= Q_{11}n^4 + Q_{22}m^4 + 2\left(Q_{12} + 2Q_{66}\right)m^2n^2 \\
\bar{Q}_{22} &= Q_{11}m^4 + Q_{22}n^4 + 2\left(Q_{12} + 2Q_{66}\right)m^2n^2 \\
\bar{Q}_{12} &= \left(Q_{11} + Q_{22} - 4Q_{66}\right)m^2n^2 + Q_{12}\left(m^4 + n^4\right) \\
\bar{Q}_{66} &= \left(Q_{11} + Q_{22} - 2Q_{12} - 2Q_{66}\right)m^2n^2 + Q_{66}\left(m^4 + n^4\right) \\
\bar{Q}_{16} &= \left(Q_{11} - Q_{12} - 2Q_{66}\right)mn^3 - \left(Q_{22} - Q_{12} - 2Q_{66}\right)nm^3 \\
\bar{Q}_{26} &= \left(Q_{11} - Q_{12} - 2Q_{66}\right)nm^3 - \left(Q_{22} - Q_{12} - 2Q_{66}\right)mn^3
\end{aligned}
$$

in which

$m = \sin\theta$ and $n = \cos\theta$.

Considering only the transverse displacement $w(x, y)$, and symmetric laminates, the strain displacement relations are given by

We note, that, for antisymmetric angle-ply laminate, the effect of the coupling terms B_{13} and B_{23} are reduced when the θ^0 and $-\theta^0$ plies are interspersed like $[\theta^0/-\theta^0/\theta^0/-\theta^0]$. Hence, the number of θ^0 and $-\theta^0$ plies in an angle-ply antisymmetric laminate are increasingly interspersed, the laminate behaves as if were predominantly symmetric, and having membrane and bending orthotropy, since the effect of the coupling terms (A_{16}=0, A_{26}=0) and no bend twist terms (D_{16}=0, D_{26}=0) present for any any antisymmetric laminate configuration.

$$\left\{ \begin{array}{c} \epsilon_x \\ \epsilon_y \\ \gamma_{xy} \end{array} \right\} = z \left\{ \begin{array}{c} -\frac{\partial^2 w}{\partial x^2} \\ -\frac{\partial^2 w}{\partial y^2} \\ -2\frac{\partial^2 w}{\partial x \partial y} \end{array} \right\} \tag{2.6}$$

Therefore

the stress-strain relations for the kth lamina are

$$\left\{ \begin{array}{c} \sigma_x \\ \sigma_y \\ \sigma_{xy} \end{array} \right\}^k = z \begin{bmatrix} \bar{Q}_{11} & \bar{Q}_{12} & \bar{Q}_{16} \\ \bar{Q}_{21} & \bar{Q}_{22} & \bar{Q}_{26} \\ \bar{Q}_{16} & \bar{Q}_{26} & \bar{Q}_{66} \end{bmatrix}^k \left\{ \begin{array}{c} -\frac{\partial^2 w}{\partial x^2} \\ -\frac{\partial^2 w}{\partial y^2} \\ -2\frac{\partial^2 w}{\partial x \partial y} \end{array} \right\} \tag{2.7}$$

2.2 Synthesis of Stiffness Matrix

$$\left\{ \begin{array}{c} Mx \\ My \\ Mxy \end{array} \right\} = \sum_{k=1}^{nl} \int_{nk-1}^{nk} \left\{ \begin{array}{c} \sigma_x \\ \sigma_y \\ \sigma_{xy} \end{array} \right\}^k zdz \tag{2.8}$$

By substituting expressions obtained from Eq.(2.7) in Eq.(2.8) the result will be

$$\left\{\begin{array}{c} M_x \\ M_y \\ M_{xy} \end{array}\right\} = \left[\begin{array}{ccc} D_{11} & D_{12} & D_{16} \\ D_{21} & D_{22} & D_{26} \\ D_{16} & D_{26} & D_{66} \end{array}\right] \left\{\begin{array}{c} -\frac{\partial^2 w}{\partial x^2} \\ -\frac{\partial^2 w}{\partial y^2} \\ -\frac{2\partial^2 w}{\partial x \partial y} \end{array}\right\} \tag{2.9}$$

It can also be written as

$$\left\{\begin{array}{c} M_x \\ M_y \\ M_{xy} \end{array}\right\} = [D_{ij}] \left\{\begin{array}{c} -\frac{\partial^2 w}{\partial x^2} \\ -\frac{\partial^2 w}{\partial y^2} \\ -\frac{2\partial^2 w}{\partial x \partial y} \end{array}\right\} \tag{2.10}$$

where

$[D_{ij}] = \frac{1}{3}\sum_{k=1}^{nl} \left[\bar{Q}_{ij}\right]_k \left[h_k^3 - h_{k-1}^3\right]$ called as bending or flexure stiffness matrix.

2.3 Finite Element Formulation

For a two-dimensional state of stress the strain energy stored in the kth lamina can be expressed as

$$U_k = \frac{1}{2}\int_{v_k} \left[\begin{array}{ccc} \sigma_x & \sigma_y & \sigma_{xy} \end{array}\right] \left\{\begin{array}{c} \epsilon_x \\ \epsilon_y \\ \gamma_{xy} \end{array}\right\} dV \tag{2.11}$$

From Eq. (2.7)

$$\left[\begin{array}{ccc} \sigma_x & \sigma_y & \sigma_{xy} \end{array}\right] = \left[\begin{array}{ccc} \epsilon_x & \epsilon_y & \gamma_{xy} \end{array}\right] \left[\bar{Q}_{ij}\right] \tag{2.12}$$

Substituting Eq.(2.12) in Eq.(2.11) we can get

$$U_k = \frac{1}{2}\int_{vk} \left[\begin{array}{ccc} \epsilon_x & \epsilon_y & \gamma_{xy} \end{array}\right] \left[\bar{Q}_{i,j}\right] \left\{\begin{array}{c} \epsilon_x \\ \epsilon_y \\ \gamma_{xy} \end{array}\right\} dV \tag{2.13}$$

We know that

$$\epsilon_x = -z\frac{\partial^2 w}{\partial x^2}$$

$$\epsilon_y = -z\frac{\partial^2 w}{\partial y^2} \tag{2.14}$$

$$\gamma_{xy} = -2z\frac{\partial^2 w}{\partial x \partial y}$$

$$U_k = \int_{vk} \left\{D^2 w\right\}^T \left[\bar{Q}_{ij}\right]_k \left\{D^2 w\right\} dV \tag{2.15}$$

where $\{D^2 w\} = \left\{ \begin{array}{c} -\frac{\partial^2 w}{\partial x^2} \\ -\frac{\partial^2 w}{\partial y^2} \\ -\frac{2\partial^2 w}{\partial x \partial y} \end{array} \right\}$

Integrating over the whole thickness of the laminate, we obtain the total strain energy stored

$$U = \int_A \left\{D^2 w\right\}^T [FS] \left\{D^2 w\right\} dA \tag{2.16}$$

where

$[FS]$= bending stiffness matrix $=[D_{i,j}]$. Work done by the external force

$$W = \frac{1}{2}\int_A N_x \left(\frac{\partial w}{\partial x}\right)^2 dA \tag{2.17}$$

Therefore the variational functional for the present problem

$$I = U - W = \frac{1}{2}\int_A \left[\left\{D^2 w\right\}^T [FS] \left\{D^2 w\right\} - N_x \left(\frac{\partial w}{\partial x}\right)^2\right] dA \tag{2.18}$$

Now

$$\begin{aligned} w &= \{N\}^{e^T} \{\delta\}^e \\ &= \{\delta\}^{e^T} \{N^e\} \end{aligned} \tag{2.19}$$

where

$\{N\}^e$ is the shape function vector and $\{\delta\}^e$ is vector of elemental degrees of freedom.

The shape functions used for a four noded rectangular plate element with four nodal d.o.f (w, θ_x, θ_y, θ_{xy}) are

$$N_1^e = f_1(\xi)\, f_1(\eta)$$

$$N_2^e = a^e g_1(\xi)\, f_1(\eta)$$

$$N_3^e = b^e f_1(\xi)\, g_1(\eta)$$

$$N_4^e = a^e b^e g_1(\xi)\, g_1(\eta)$$

$$N_5^e = f_2(\xi)\, f_1(\eta)$$

$$N_6^e = a^e g_2(\xi)\, f_1(\eta)$$

$$N_7^e = b^e f_2(\xi)\, g_1(\eta)$$

$$N_8^e = a^e b^e g_2(\xi)\, g_1(\eta)$$

$$N_9^e = f_2(\xi)\, f_2(\eta)$$

$$N_{10}^e = a^e g_2(\xi)\, f_2(\eta)$$

$$N_{11}^e = b^e f_2(\xi)\, g_2(\eta)$$

$$N_{12}^e = a^e b^e g_2(\xi)\, g_2(\eta)$$

$$N_{13}^e = f_1(\xi)\, f_2(\eta)$$

$$N_{14}^e = a^e g_1(\xi)\, f_2(\eta)$$

$$N_{15}^e = b^e f_1(\xi)\, g_2(\eta)$$

$$N_{16}^e = a^e b^e g_1(\xi)\, g_2(\eta)$$

$$f_1(s) = \frac{1}{4}\left(2 - 3s + s^3\right)$$

$$f_2(s) = \frac{1}{4}\left(2 + 3s + s^3\right)$$

$$g_1(s) = \frac{1}{4}\left(1 - s - s^2 + s^3\right)$$

$$g_2(s) = \frac{1}{4}\left(-1 - s + s^2 + s^3\right)$$

$$\{B_x\}^e = \frac{\partial \{N\}^e}{\partial x} \tag{2.20}$$

$$\frac{\partial w}{\partial x} = \{B_x\}^{e^T} \{\delta\}^e \tag{2.21}$$

Similarly

$$\left\{D^2 w\right\} = \begin{bmatrix} -\frac{\partial^2 N_1^e}{\partial x^2} & \frac{\partial^2 N_2^e}{\partial x^2} & \cdots \\ -\frac{\partial^2 N_1^e}{\partial y^2} & \frac{\partial^2 N_2^e}{\partial y^2} & \cdots \\ -2\frac{\partial^2 N_1^e}{\partial x \partial y} & \frac{\partial^2 N_2^e}{\partial x \partial y} & \cdots \end{bmatrix} \begin{Bmatrix} \delta_1^e \\ \delta_2^e \\ \vdots \end{Bmatrix} = [C]^e \{\delta\}^e \tag{2.22}$$

For each element, the stiffness matrix and force matrix can be derived as

$$[k^e] = \int_{A^e} [C]^{e^T} [FS] [C]^e \, dA \tag{2.23}$$

and

$$[f^e] = \int_{A^e} N_x \{B_x\}^e \{B_x\}^{e^T} dA \tag{2.24}$$

where $[k^e]$ is the elemental stiffness matrix and $[f^e]$ is the elemental force matrix. Substituting Eq.2.21 and Eq.2.22 in Eq.(2.18) we can get

$$I = \frac{1}{2} \int_A \left[\{\delta\}^{e^T} [C]^{e^T} [FS] [C]^e \{\delta\}^e - N_x \{\delta\}^{e^T} \{B_x\}^e \{B_x\}^{e^T} \{\delta\}^e \right] \tag{2.25}$$

Substituting Eqs.(2.23) and (2.24) in the above equation, we get

$$I = \frac{1}{2} \sum_{e=1}^{ne} \left[\{\delta\}^{e^T} [k]^e \{\delta\}^e - \{\delta\}^{e^T} [f]^e \{\delta\}^e \right] \tag{2.26}$$

The global stiffness matrix, global force matrix and vector global degrees of freedom can be obtained as

$$[K] = \sum_{e=1}^{ne} [k]^e \tag{2.27}$$

$$[F] = \sum_{e=1}^{ne} [f]^e \tag{2.28}$$

$$\{W\} = \sum_{e=1}^{ne} \{\delta\}^e \tag{2.29}$$

where $[K]^e$ are obtained from $[k]^e$ using the following simplified assembly equations.

$$K^e_{4r-3,4s-3} = k^e_{4p-3,4q-3}$$

$$K^e_{4r-3,4s-3} = k^e_{4p-3,4q-2}$$

$$K^e_{4r-3,4s-1} = k^e_{4p-3,4q-1}$$

$$K^e_{4r-3,4s} = k^e_{4p-3,4q}$$

$$K^e_{4r-2,4s-3} = k^e_{4p-2,4q-3}$$

$$K^e_{4r-2,4s-2} = k^e_{4p-2,4q-2}$$

$$K^e_{4r-2,4s-1} = k^e_{4p-2,4q-1}$$

$$K^e_{4r-2,4s} = k^e_{4p-2,4q}$$

$$K^e_{4r-1,4s-3} = k^e_{4p-1,4q-3}$$

$$K^e_{4r-1,4s-2} = k^e_{4p-1,4q-2}$$

$$K^e_{4r-1,4s-1} = k^e_{4p-1,4q-1}$$

$$K^e_{4r-1,4s} = k^e_{4p-1,4q}$$

$$K^e_{4r,4s-3} = k^e_{4p,4q-3}$$

$$K^e_{4r,4s-2} = k^e_{4p,4q-2}$$

$$K^e_{4r,4s-1} = k^e_{4p,4q-1}$$

$$K^e_{4r,4s} = k^e_{4p,4q}$$

when $r = C_{e_p}$ and $s = C_{e_q}$

Otherwise $\qquad [K]^e = 0$

Similar relations are valid for obtaining the $[F]_e$ from $[f]_e$ for determining $\{W\}^e$, the following relations can be used.

$$W^e_{4r-3} = \delta^e_{4p-3}$$

$$W^e_{4r-2} = \delta^e_{4p-2}$$

$$W^e_{4r-1} = \delta^e_{4p-1}$$

$$W^e_{4r} = \delta^e_{4p} \tag{2.30}$$

when $r = C_{e_p}$.

Otherwise $$\{W\}^e = 0$$

where C_{e_p} is the element of the connectivity

$$[C] = \begin{bmatrix} 1 & 2 & 3 & 4 \\ \vdots & \vdots & \vdots & \vdots \end{bmatrix} \tag{2.31}$$

where

the number of rows= number of elements and number of columns =number of nodes per element. In (ξ, η) coordinates

$$[C^e] = [t]\,[C^e] \tag{2.32}$$

where

$$[t] = \begin{bmatrix} \left(\frac{\partial \xi}{\partial x}\right)^2 & 0 & 0 \\ 0 & \left(\frac{\partial \xi}{\partial y}\right)^2 & 0 \\ 0 & 0 & \frac{\partial \xi}{\partial x}\frac{\partial \xi}{\partial y} \end{bmatrix} \tag{2.33}$$

This has been obtained by using the chain rule of differentiation and using the given conversion for rectangular elements from x, y to natural coordinates ξ, η Jacobian matrix $[J] = \begin{bmatrix} \frac{\partial x}{\partial \xi} & 0 \\ 0 & \frac{\partial y}{\partial \xi} \end{bmatrix}$

$$Det\,[J] = a_e.b_e$$

$$x = a_1 + a_e\xi$$

$$y = b_1 + b_e\eta$$

Substituting Eqs.(2.27),(2.28) and (2.29) in Eq.(2.26) we get

$$I = \frac{1}{2}\{W\}^T[K]\{W\} - \{W\}^T[F]\{W\} \tag{2.34}$$

Minimizing the above variational functional

$$\frac{\partial I}{\partial \{W\}} = 0 \tag{2.35}$$

From the above equation, we get

$$[K]\{W\} - [F]\{W\} = 0 \tag{2.36}$$

Thus the final FEM equation for the present problem can be written as

$$[K]\{W\} - [F]\{W\} = 0 \tag{2.37}$$

This is an eigen value problem with characteristic equation $|[K] - [F]| = 0$, which has been solved to obtain the buckling loads and the mode shapes by using NAG routine.

2.4 Buckling analysis using NASTRAN

In the present problem the major analysis is carried out by NASTRAN finite element method analysis. At buckling the determinant of the sum of the elastic stiffness matrix and differential stiffness matrix is equal to zero.

$$\left|K^e + K^d_{cr}\right| = 0 \tag{2.38}$$

Where K^e is the elastic stiffness and K^d_{cr} is the differential stiffness matrix at critical buckling load

$$K^d_{cr}(u) = \lambda \times K^d(u) \tag{2.39}$$

$$\left|K^e + \lambda K^d(u)\right| = 0 \tag{2.40}$$

The above equations is known as the eigen value problem with eigen values $\lambda_1, \lambda_2, \cdots, \lambda_n$ where N is the size of the K^e and K^d matrices (and is equal to the degrees of freedom in the analysis set of the problem). Each value of λ corresponds to a buckling load.

2.5 Methodology for cut-outs

Cut-outs are present in laminated plates in many applications. In the present study three different shapes of cut-outs have been taken namely,

rectangular, circular, and elliptical. For comparison of the plate behavior all the cut-outs have been taken to have the same area.

1. For rectangular cut-out as shown in Fig. 3.1

   $A_c = c \times d$

   Where

   A_c=area of cut-out

   c=length along major axis

   d=length along minor axis

2. For circular cut-out as shown in Fig. 3.1

   $A_c = \pi r^2$

   r=radius of the cut-out

3. For elliptical cut-out as shown in Fig. 3.1

   $A_c = \pi cd/4$

Chapter 3

Solution approach-Monte Carlo simulation technique

The problem of analysis of composite structures with variation in material properties using Monte Carlo simulation approach can be divided in to the following steps.

1. Random input generation.

2. System analysis.

3. Post processing of response behavior.

3.1 Random input generation

3.1.1 Number generation

A set of random numbers are generated of a given sample size, mean, standard deviation and probability distribution. Standard library subroutines are available for this. These can be known as pseudo random numbers as these are artificially generated through numerical subroutines.

3.1.2 Processing of raw data

For getting the random numbers with desired characteristics, the pseudo random numbers generated by G05FDF from NAG library are preprocessed before feeding them as input to the FEM analysis. The samples are checked for shift in the input mean and standard deviation which are usually present in a small amount because of finite length arithmetic of computers. For adjusting these shift these three Arithmetic formulations can be used.

1. Modification of the random numbers to shift the mean.

$$nr_i = x_i - (\mu_e - \mu_r) \tag{3.1}$$

2. Modification of the random number to change the standard deviation (SD)

$$nr_i = \frac{x_i}{\sigma_e} \times \sigma_r \tag{3.2}$$

3. Modification of the random number to change the SD and shift the mean simultaneously.

$$nr_i = \frac{(x_i - \mu_e) \times \sigma_r}{\sigma_e} + \mu_r \tag{3.3}$$

where

$$\mu_e = \frac{\sum_{i=1}^{n} x_i}{n} \tag{3.4}$$

$$\sigma_e = \sqrt{\frac{\sum_{i=1}^{n} (x_i - \mu)^2}{n - 1}} \tag{3.5}$$

μ_r = required mean values

σ_r = required standard deviation values

nr_i=new random numbers.

3.2 System analysis

The governing equation of the buckling analysis of laminated composite has been solved with the help of finite element technique. A 4-DOF C^1 continuity model with 4-noded Lagrangian element has been employed in the present problem. In the finite element program the various stages are.

1. pre-processor
2. processor, and
3. post-processor

3.2.1 pre-processor

It supplies the following data required by the processor

1. Mesh data
   - number of elements
   - number of nodes per element
   - number of DOF per node
   - connectivity matrix
   - vector of nodal co-ordinates
2. vector of nodal values of geometric properties, material properties and other properties.
3. specifying the node numbers and the designated boundary values.

3.2.2 processor

Finite element equations are assembled and solved.

- calculation of elemental coefficient matrix and right side vector
- global assembly

- application of essential boundary conditions
- solving the equations

3.2.3 post-processor

This involves the calculating and plotting of required results. The sample of the buckling response of the plate is obtained from the FEM analyzer and NASTRAN software.Its statistical information is extracted from the Eqns. (3.4) and (3.5).

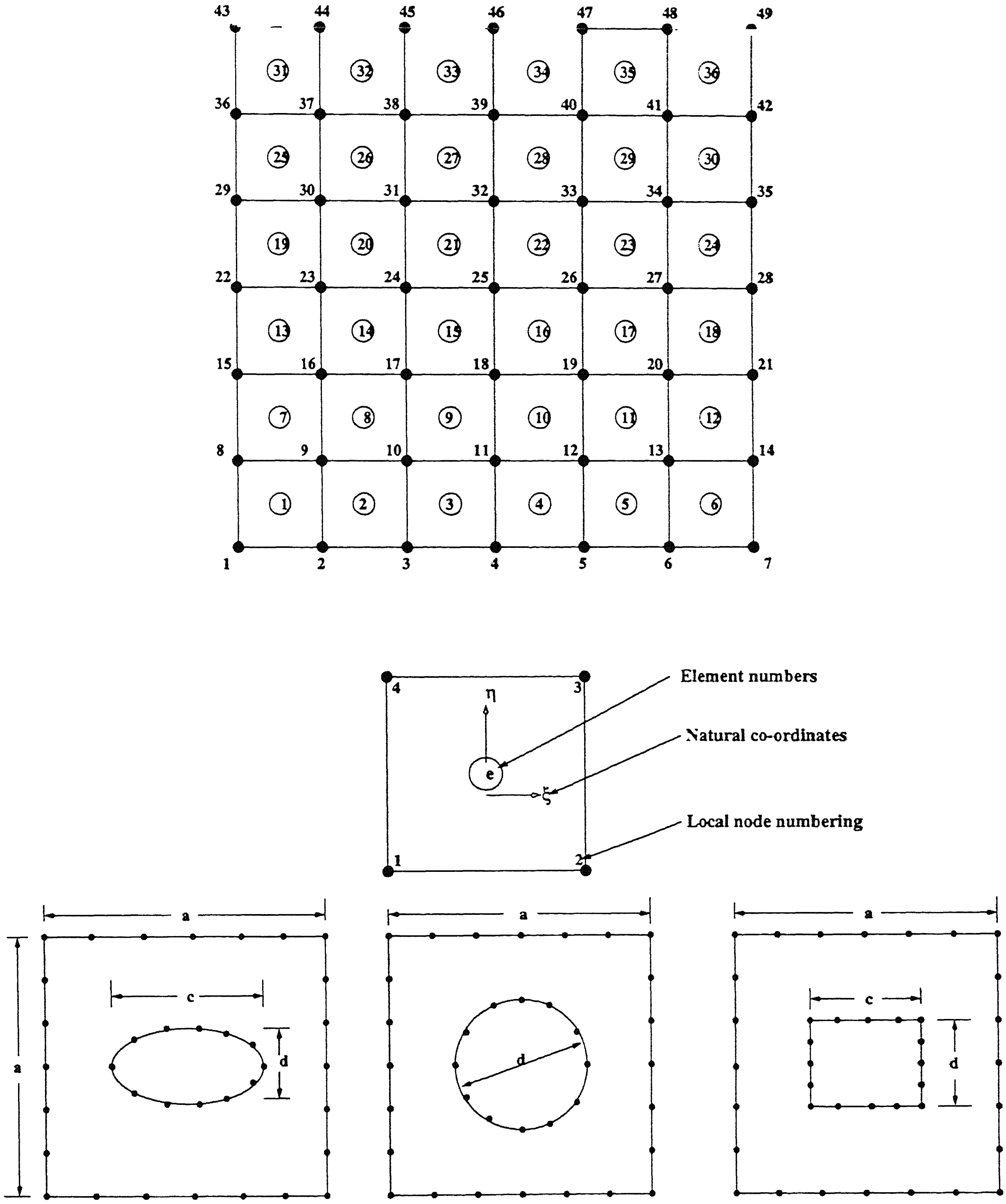

Figure 3.1: Geometry of the plate with nodes on boundaries

Chapter 4

Results and Discussions

4.1 Convergence study

Convergence study has been carried out for three types of plates namely isotropic square plate, composite square plate and composite square plate with circular cut-out. Table 4.1(A) shows the convergence for square isotropic plate with material properties $E = 200GPa$ and $\nu = 0.28$. The convergence study for composite square plate and composite square plate with circular cut-out as shown in Table 4.1(B) and (C) for material properties $E_{11} = 206.8425GPa$, $E_{12} = 5.171GPa$, $\nu_{12} = 0.25$ and $G_{12} = 2.585GPa$. Typical results for a circular cut-out with $a/d = 5.0$ are shown in Table 4.1(C). It it observed that a 6x6 mesh gives sufficient convergence from engineering point. Hence, further computations have been carried out based on 6x6 mesh for the full plate.

4.2 Validation study

Validation studies have been carried for symmetric square cross ply-laminate with simply supported boundary conditions for different mesh sizes. These results are presented in Table 4.2. The material properties used for this are also shown in Table 4.2

From the Table 4.3 it is observed that for all edges simply supported

and all edges clamped for a given minor axis, as the major axis reduces the buckling load increases and then reduces at certain value of a/c which is close to given a/d ratio. Similar observations can be made for a plate which is clamped on two edges and two edges simply supported. In the case of a plate with three edges clamped and one side free, the trend is reverses.

Table 4.1: Convergence study for square isotropic and composite plates

EDGE CONDITIONS	MESH SIZE	CRITICAL LOAD (10^4) N
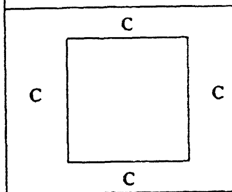	2 X 2	158.5388
	4 X 4	159.4702
	6 X 6	159.5098
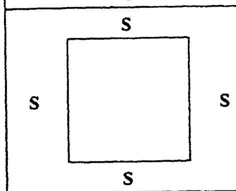	2 X 2	63.2396
	4 X 4	64.2293
	6 X 6	64.2691

(A) : Convergency study for Isotropic square plate

EDGE CONDITIONS	MESH SIZE	CRITICAL LOAD (10^4) N
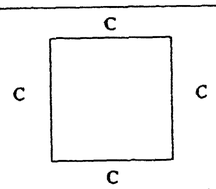	2 X 2	79.13348
	4 X 4	30.58752
	6 X 6	30.58315
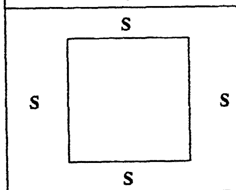	2 X 2	7.932761
	4 X 4	12.40192
	6 X 6	12.40335

(B) : Convergency study for Composite square plate

EDGE CONDITIONS	MESH SIZE	CRITICAL LOAD (10^4) N
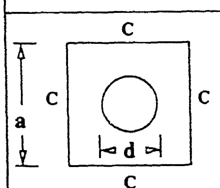	2 X 2	19.705526
	4 X 4	21.386021
	6 X 6	21.391097
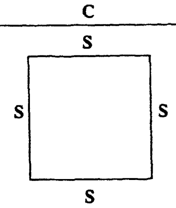	2 X 2	5.2786344
	4 X 4	8.0285583
	6 X 6	8.0310422

(C) : Convergecy study square composite plate with circular cut-out (a/d=5)

Table 4.2: Validation of critical loads for a square simply supported composite plate

Laminate(deg)	Reference [14]	Critical loads (N) Number of elemets in the square plate			
		2 x 2	4 x 4	6 x 6	8 x 8
$[0/90]_s$	18.20341	18.2232534	18.2416366	18.2076981	18.206495
$[0/90/0]_s$	18.19803	18.1270658	18.20268707	18.1991125	18.202405
$[0/90/0/90]_s$	18.19803	18.0794632	18.20167619	18.1987803	18.196925
$[0/90/0/90/0]_s$	18.20098	18.0387587	18.20086620	18.1977916	18.197267

E_{11}=140 GPa, E_{12} =10 GPa, G_{12}=5 GPa and ν_{12}=0.3

Table 4.3: Critical load for elliptic cut-outs with different boundary conditions for deterministic symmetric composite laminate

Critical loads						
geometry	edge conditions notations 1,2,3,4	a/c=4	a/c=5	a/c=6	a/c=7	a/c=8
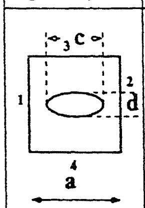	CCCC	5.270304	5.29248	5.6126	5.74887	5.581212
	CCCF	2.66907	2.65275	2.55812	2.36623	2.38523
a/d=10	CCFF	1.982127	2.05487	1.942303	1.88537	1.97432
	CSCS	3.320271	3.4449	3.70915	3.8545	3.79850
	SSSS	2.038672	2.08123	2.1298	2.2038	2.09114

4.3 Plates with random material properties

The approach presented in the previous chapters is used to find the buckling load statistics for rectangular composite plates. In section 4.4 behavior of rectangular plate with different boundary conditions and ply-orientations has been presented assuming the material properties as random. In sections 4.5 - 4.7 results have been presented for the plates with rectangular, circular and elliptical cut-outs respectively. Initially the effect of randomness in individual material property has been investigated to identify the most critical parameter. Subsequently only two parameters E_{11} and G_{12} have been taken as random variables.

- Samples are generated with the standard deviation varying from 5 percent to a 20 percent of their mean values with sample-size 1000 and 10 such samples are used for each study.

- The material properties considered to be random are E_{11},E_{12},ν_{12} and G_{12}.

Results have been computed for graphite/epoxy composites with mean values of the material properties as as given below [14].

$E_{11} = 206.8425 GPa$

$E_{12} = 5.171 GPa$

$\nu_{12} = 0.25$ and

$G_{12} = 2.585 GPa$

4.4 Buckling characteristics of square and rectangular plates

In this section a study of the effect of dispersion in single input random variable while the characteristics of the other input variables are kept constant on plates with different aspect-ratios(AR), boundary conditions and

ply-orientations is carried out. Two classical boundary conditions have been considered namely all edges SS and all edges CC. The critical loads are normalized with respect to the critical loads for$[0^0/90^0/0^0/90^0]$ laminate treating the material properties to be deterministic. Three different lay-ups namely $[45^0/-45^0/-45^0/45^0]$, $[45^0/-45^0/45^0/-45^0]$ and $[0^0/90^0/0^0/90^0]$ laminates have been studied.

Figs. 4.1 to Figs. 4.8 show the mean and standard deviation of normalized critical load corresponding to each input variable as random . Each figure represents six different studies. These presents the effect of the SD of input RV on the buckling load of the plates with different boundary conditions, ARs and ply-orientations.

The Figs. 4.9 and 4.10 show the mean and standard deviation of normalized critical load when both E_{11} and G_{12} are random variables.

4.4.1 Effect of longitudinal elastic modulus E_{11}

Fig 4.1 shows the variation of mean of the buckling load with standard deviation of E_{11}. While Fig 4.2 shows the variation of standard deviation of buckling load with standard deviation of E_{11}. The response shows a generally a linear behavior. The plate with all edges CC is affected more by a change in input randomness compared to a plate with all edges SS. The plate shows least sensitiveness to input dispersion as the aspect ratio increases. From the limited study conducted it is observed that cross-ply laminate is less sensitive compared to angle-ply laminate for all edges SS due to change in σ/μ of E_{11}.

4.4.2 Effect of transverse elastic modulus E_{12}

Fig 4.3 shows the variation of mean of the buckling load with standard deviation of E_{12}. While Fig 4.4 shows the variation of standard deviation of buckling load with standard deviation of E_{12}. The general behavior is almost linear, but unlike the case E_{11}, here the slope of both mean and

standard deviation of normalized critical load curves are decreasing trend. The effect of random variable E_{12} is less compared to random variable E_{11}. As observed in the case of E_{11} here also the plate is less sensitive to input dispersion as aspect ratio increases. All edges CC plate is more affected by dispersion in E_{12} than all edges SS. The cross-ply laminate is least affected compared to angle-ply laminate for all edges SS due to change in σ/μ of E_{12}.

4.4.3 Effect of major Poisson's ratio ν_{12}

Fig 4.5 shows the variation of mean of the buckling load with standard deviation of ν_{12}. While Fig 4.6 shows the variation of standard deviation of buckling load with standard deviation of ν_{12}.

The general nature of the curves are mostly linear. The plate with all edges CC is more affected than plate with all edges SS. From the comparison of all variables it has been found that the random variable ν_{12} has less effect compared to random variables E_{11}, E_{12} and G_{12}. Here too the cross-ply laminate is least affected than angle-ply laminate for all edges SS due to change in σ/μ of ν_{12}.

4.4.4 Effect of rigidity modulus G_{12}

Fig 4.7 shows the variation of mean of the buckling load with standard deviation of G_{12}. While Fig 4.8 shows the variation of standard deviation of buckling load with standard deviation of G_{12}.

Here too the characteristics are mostly linear. The plate with all edges CC is more affected than plate with all edges SS. Here the slope of response characteristic curves have an increasing trend compared to E_{12} and ν_{12} response characteristic curves. Next to the random variable E_{11}, the random variable G_{12} has been found to affect the buckling characteristics.

4.4.5 Combined effect of longitudinal modulus E_{11} and rigidity modulus G_{12}

Fig 4.9 shows the variation of mean of the buckling load with standard deviation of E_{11} and G_{12}. While Fig 4.10 shows the variation of standard deviation of buckling load with standard deviation of E_{11} and G_{12}.

The $[0^0/90^0/0^0/90^0]$ laminate is least affected compared to $[45^0/-45^0/-45^0/45^0]$ and $[45^0/-45^0/45^0/-45^0]$ laminates with all edges SS. The plate with all edges CC is more affected than plate with all edges SS. The general behavior is almost linear, unlike the cases of random variables E_{11}, E_{12}, ν_{12}, G_{12}, here the slope of mean and standard deviation curves are increasing trend.

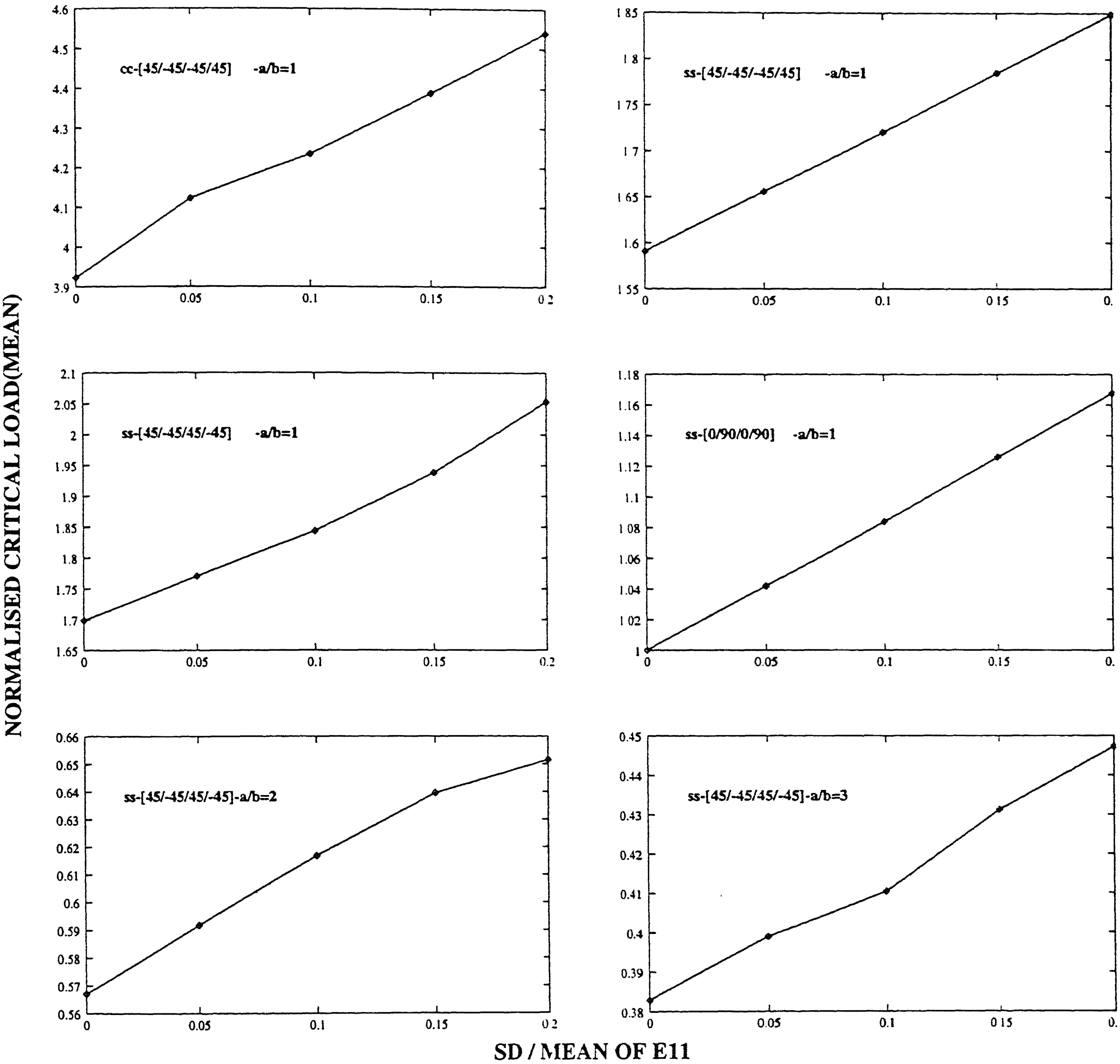

Figure 4.1: Plate buckling(Mean) characteristics with E_{11} as random

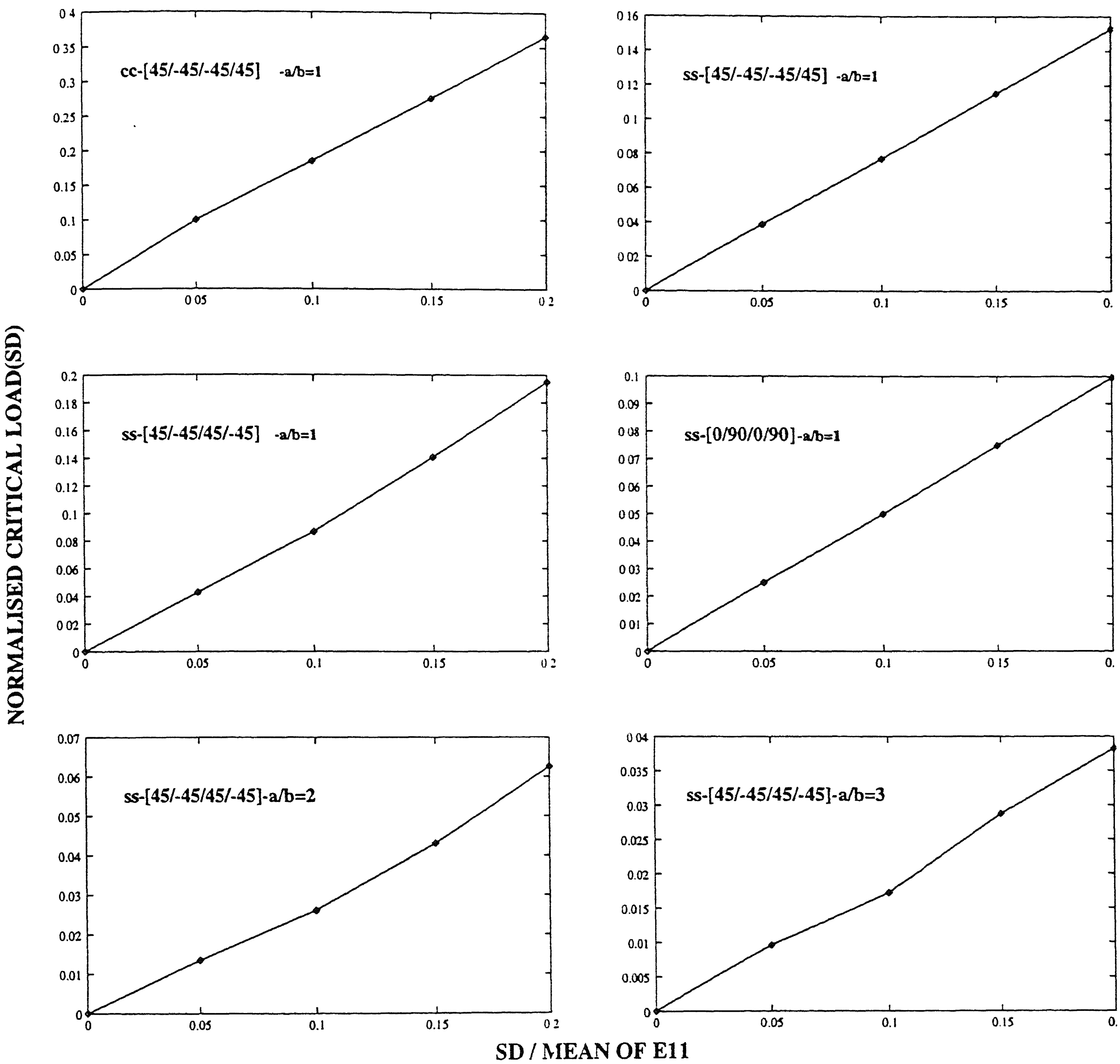

Figure 4.2: Plate buckling(SD) characteristics with E_{11} as random

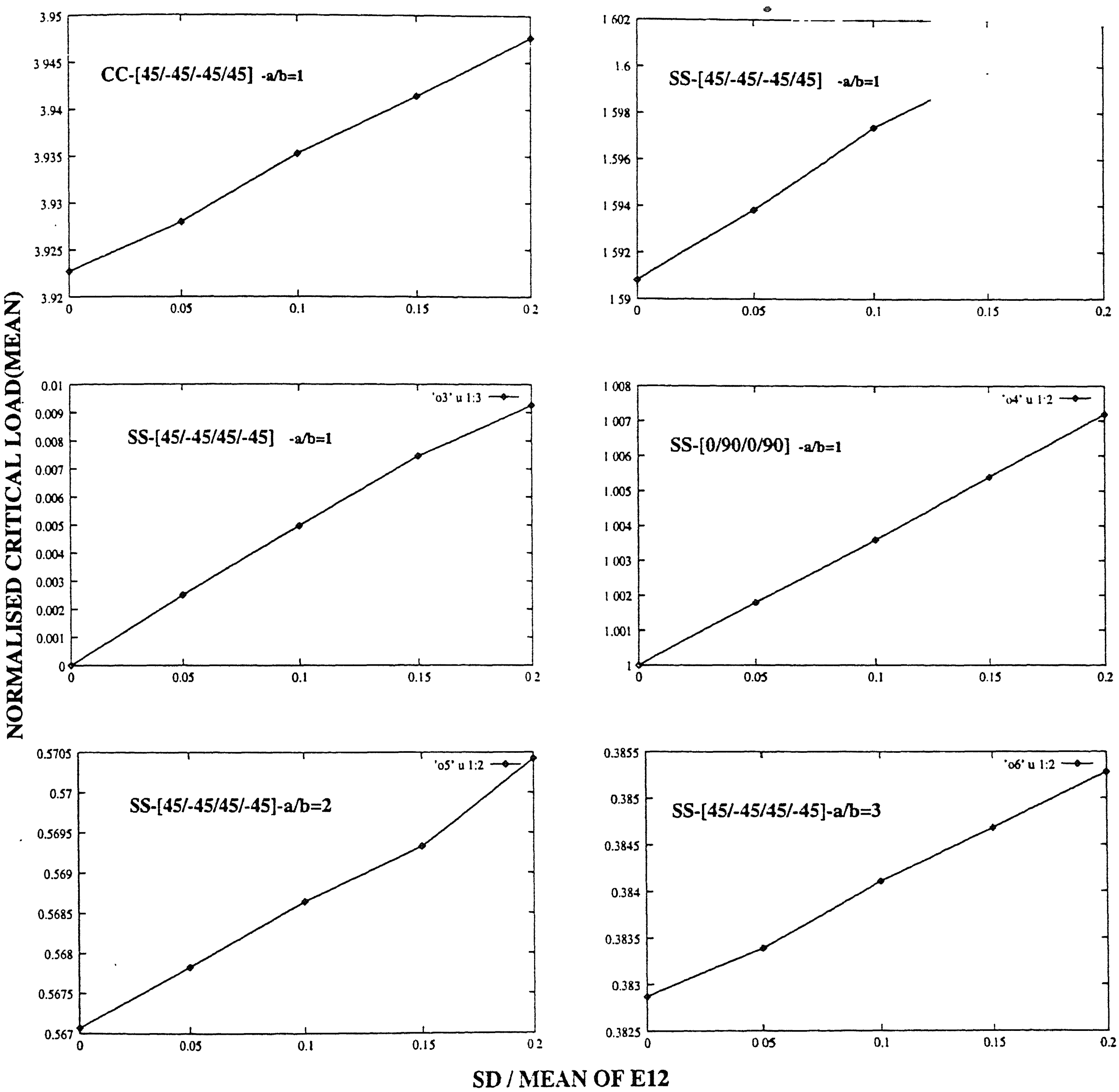

Figure 4.3: Plate buckling(Mean) characteristics with E_{12} as random

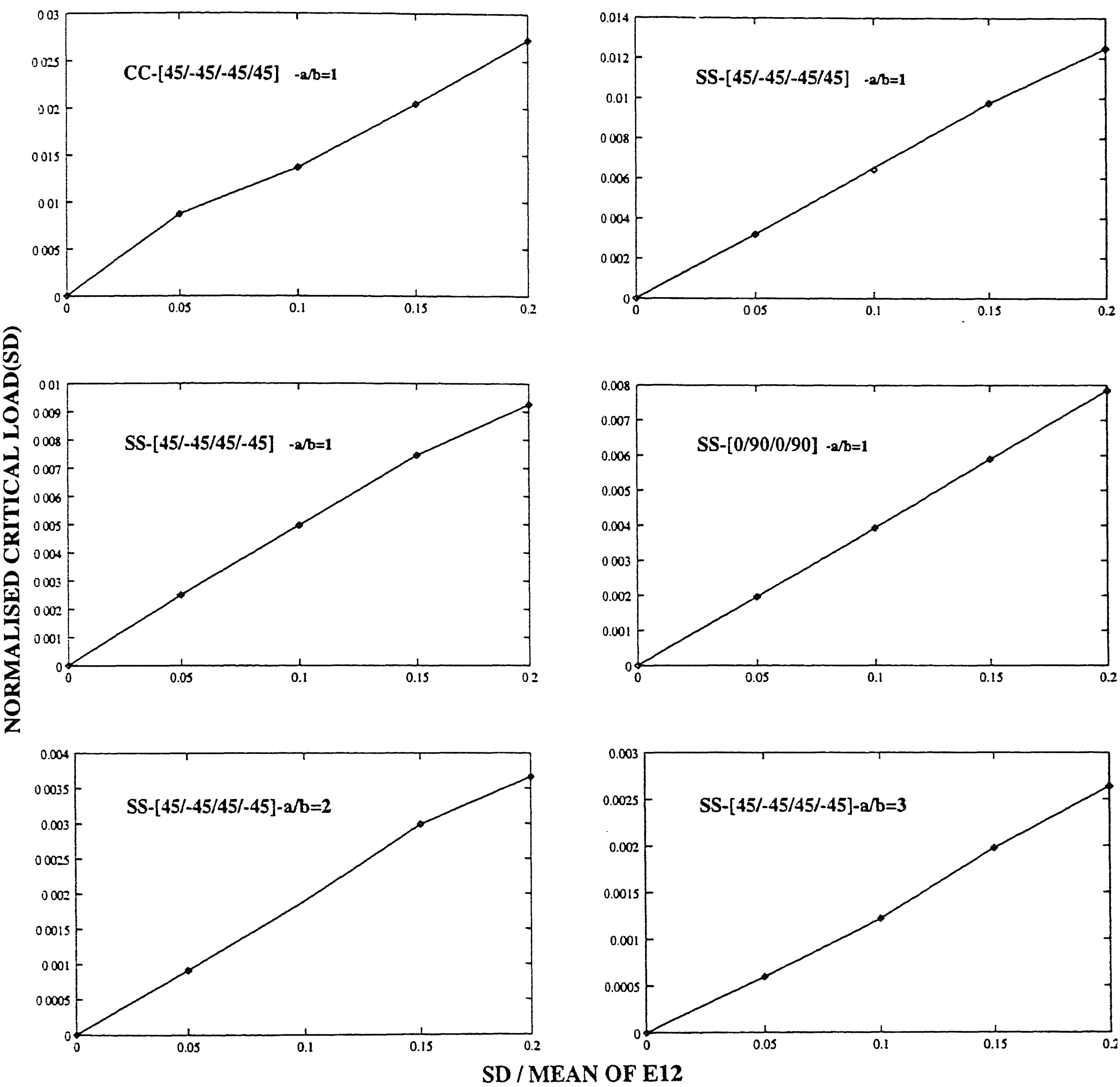

Figure 4.4: Plate buckling(SD)characteristics with E_{12} as random

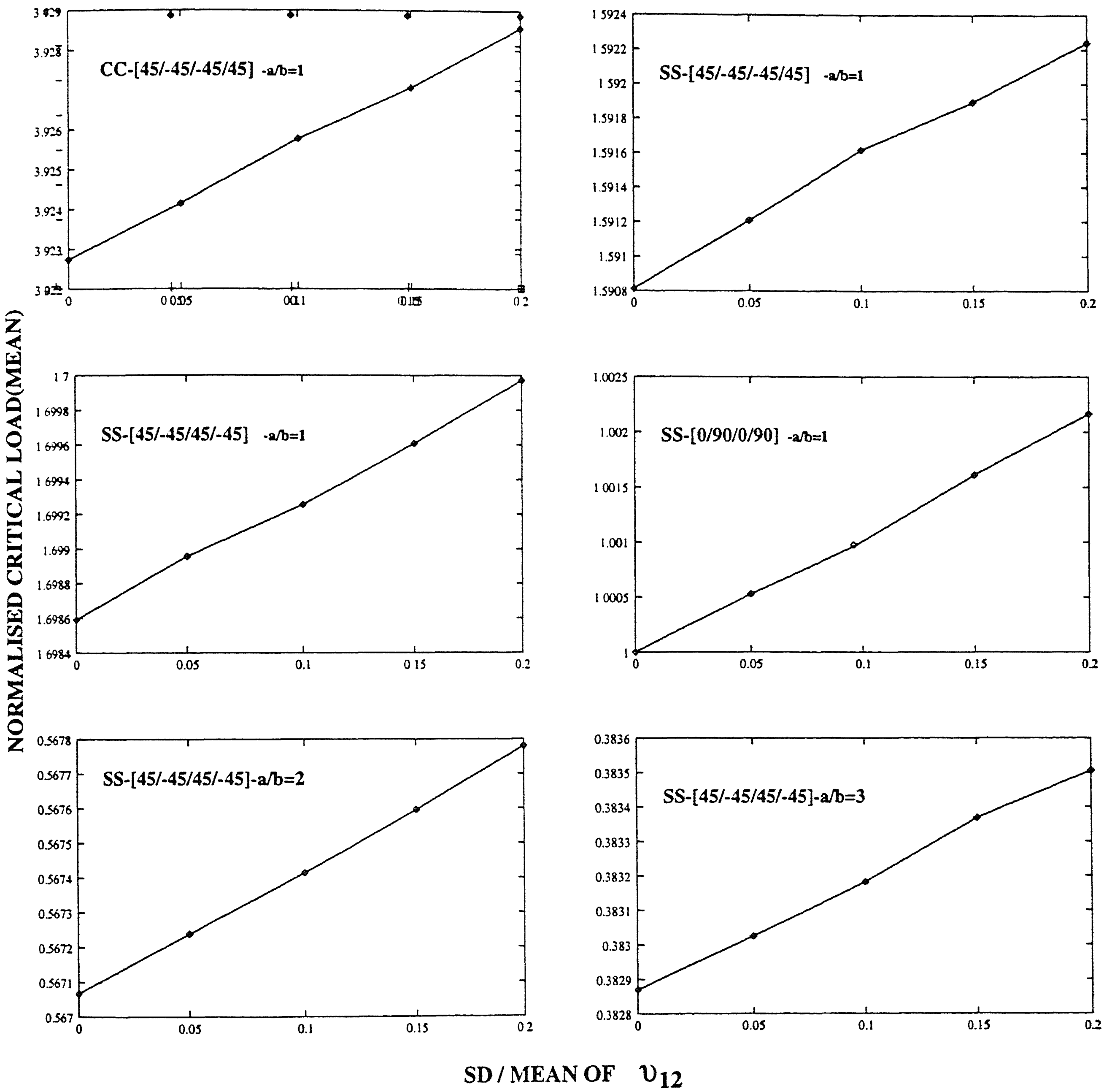

Figure 4.5: Plate buckling(Mean) characteristics with ν_{12} as random

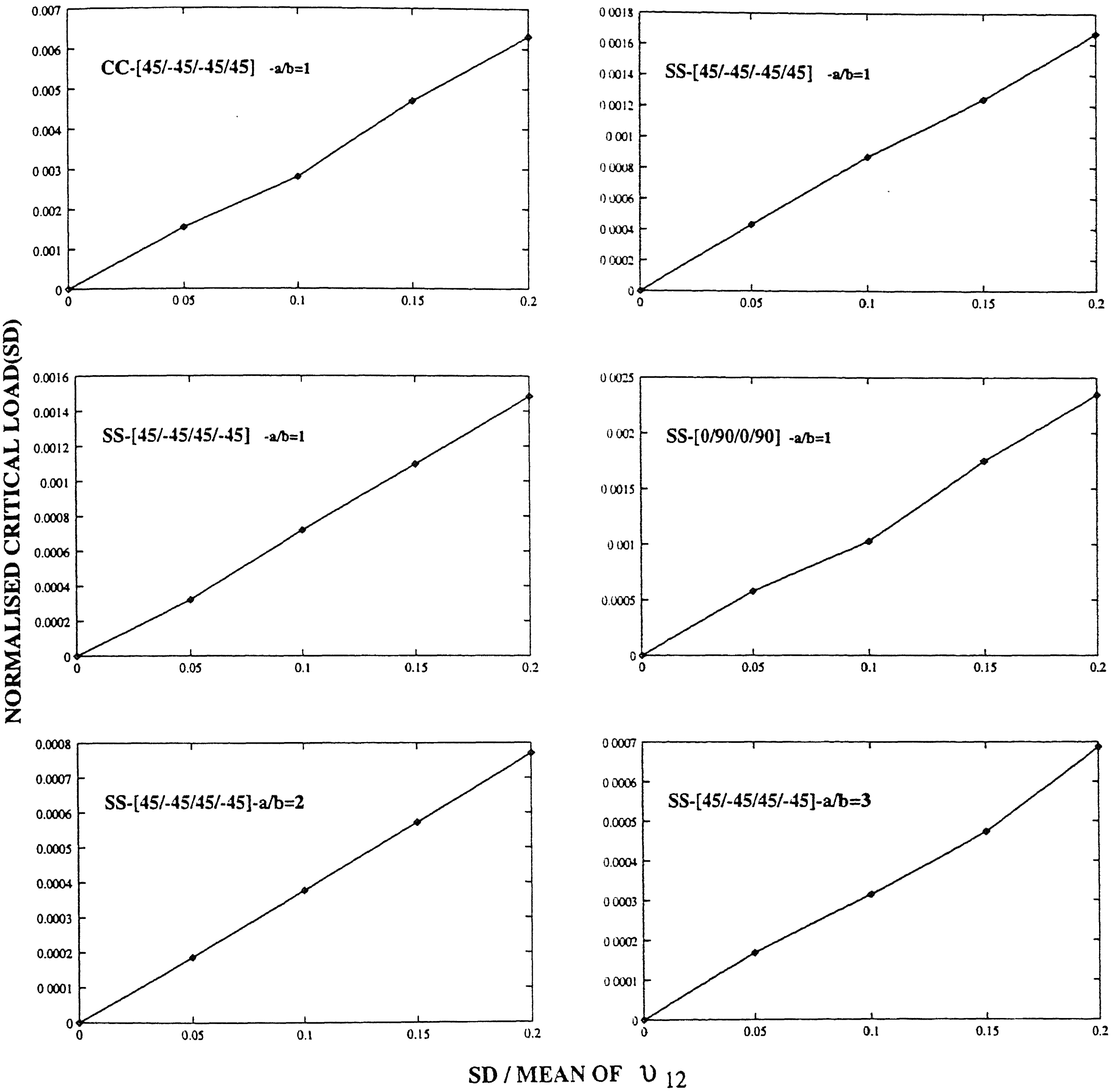

Figure 4.6: Plate buckling(SD) characteristics with ν_{12} as random

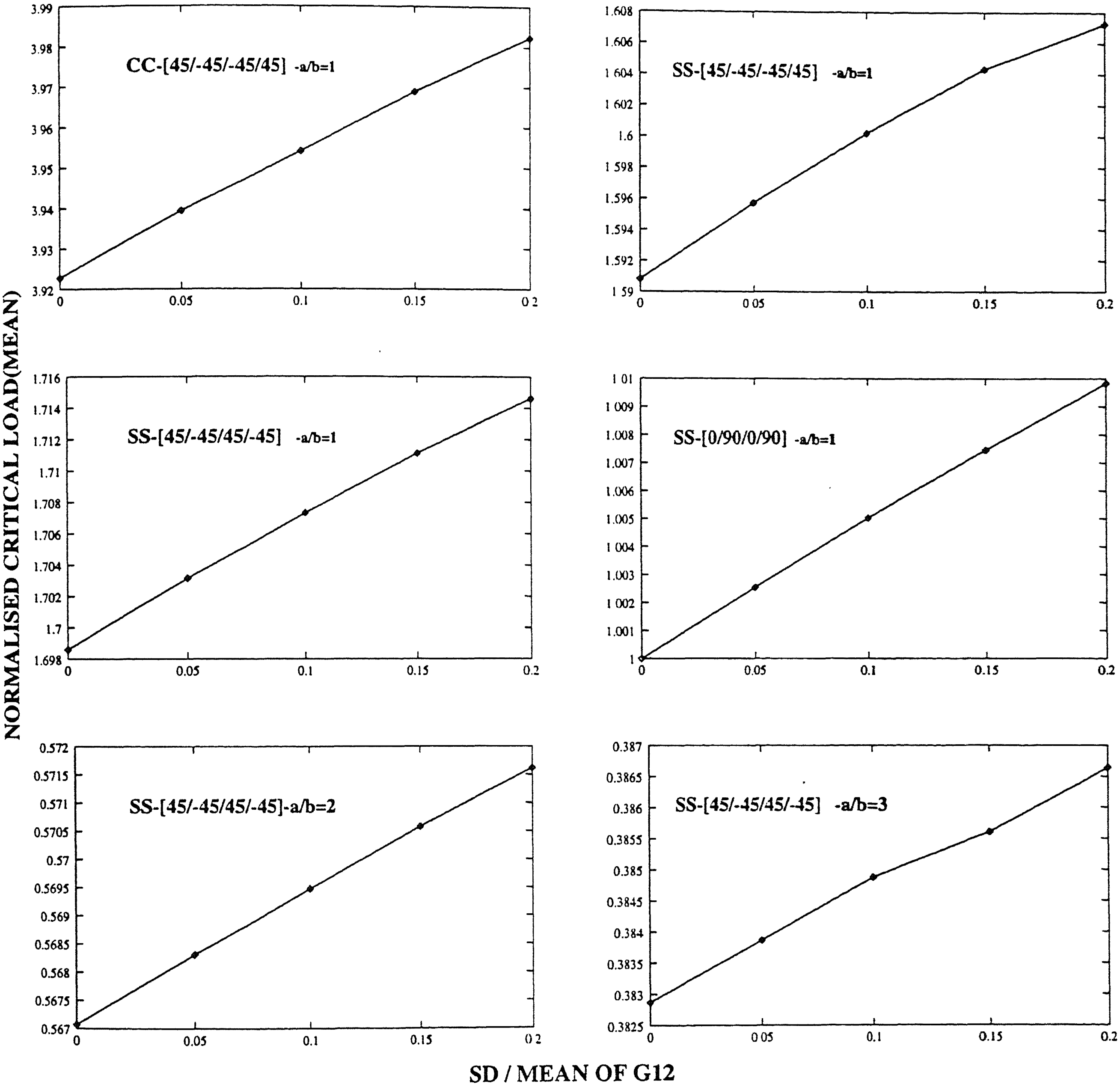

Figure 4.7: Plate buckling(Mean) characteristics with G_{12} as random

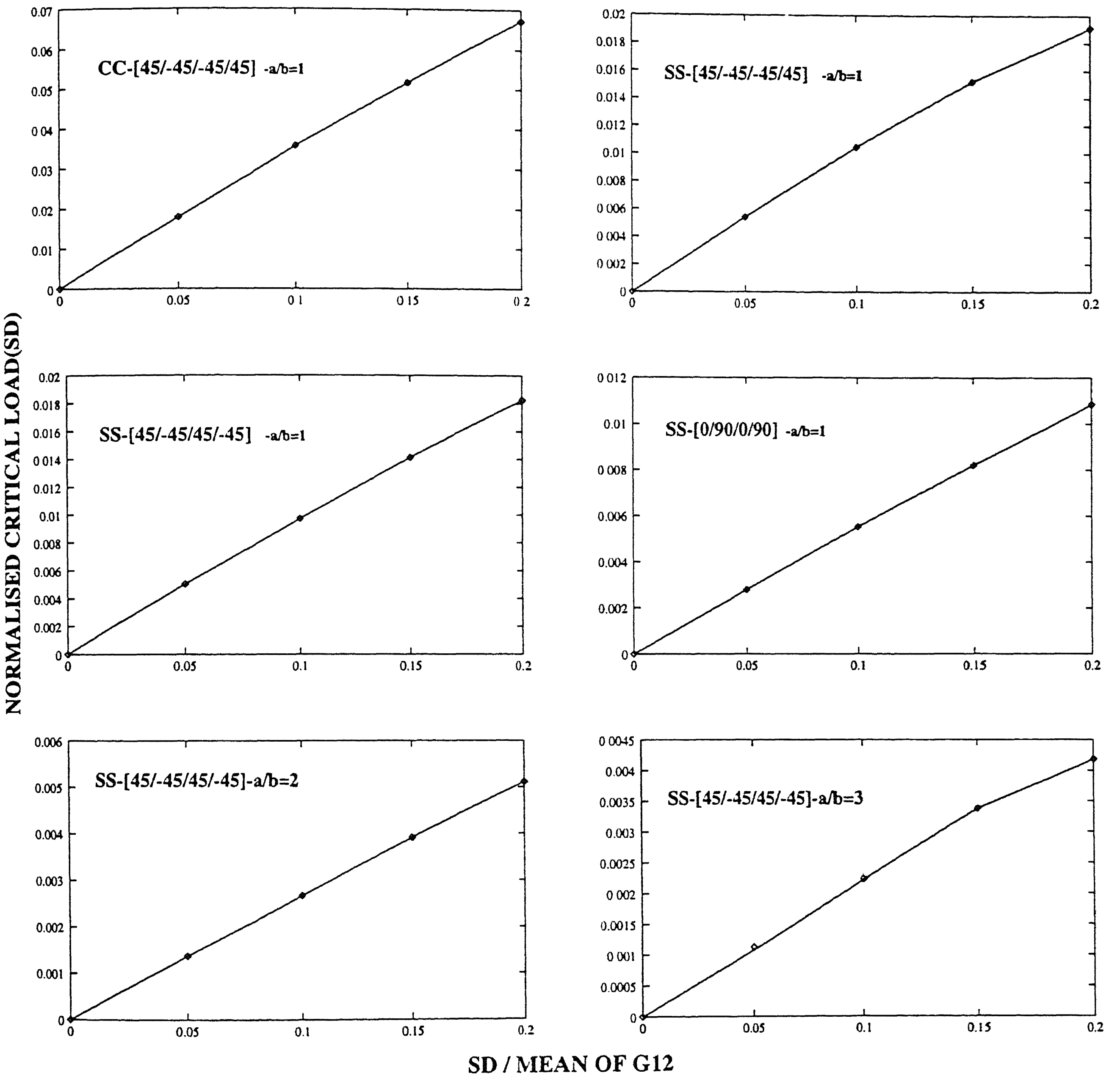

Figure 4.8: Plate buckling(SD) characteristics with G_{12} as random

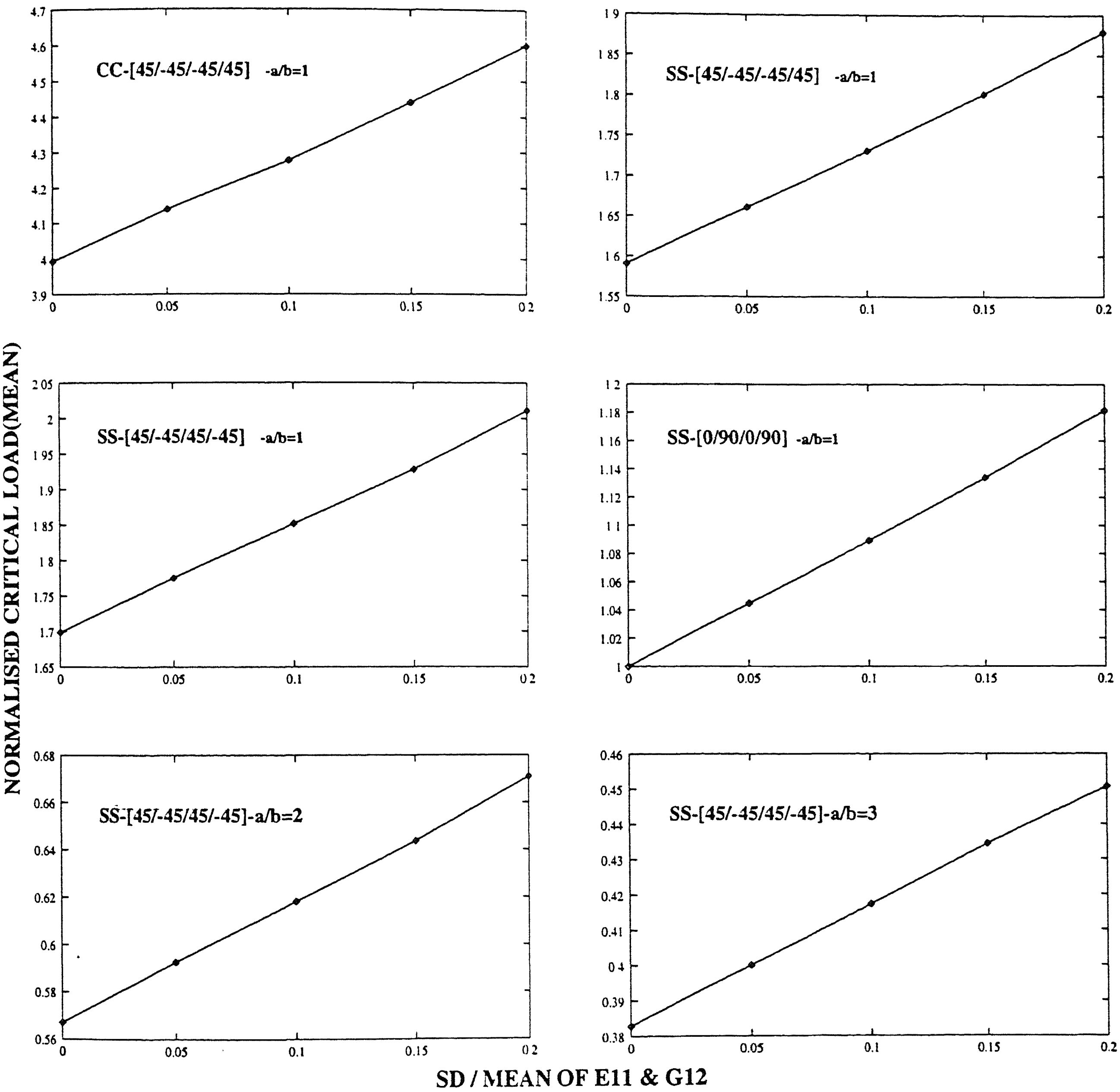

Figure 4.9: Plate buckling(Mean) characteristics with E_{11} and G_{12} as random

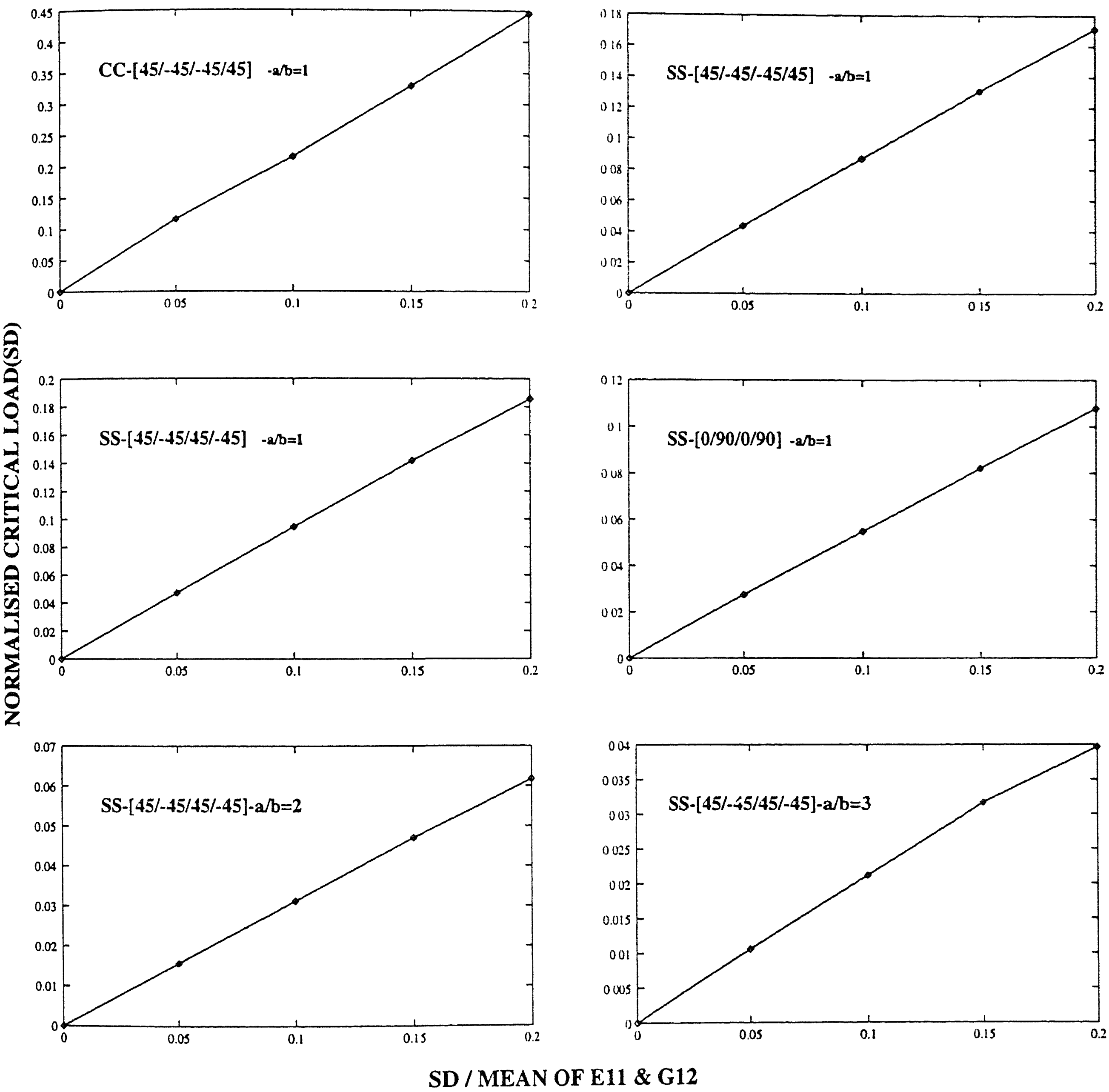

Figure 4.10: Plate buckling(SD) characteristics with E_{11} and G_{12} as random

4.5 Buckling characteristics of plates with rectangular cut-out.

In aerospace structure applications weight reduction is an important design criteria. Besides being required due to functional requirements, cut-out also have relevance to the problem of weight reduction. More and more structures are used with cut-outs. This motivated the study of the behavior of composite plates with cut-outs. A standard plate has been taken with AR=1. Here the cut-out has been used in rectangular plates with cut-out side ratio (c/d) having values 1.15, 0.96 and 0.87. These values have been chosen such that the areas for different shapes of cut-out is constant. The normalization for the mean and SD of critical loads have been done with respect to a cross-ply laminate without cut-out. Results presented graphically to bring out the effect of boundary conditions, ARs and ply-orientation for various c/d ratios mentioned earlier. Three different lay-ups namely $[45^0/-45^0/-45^0/45^0]$, $[45^0/-45^0/45^0/-45^0]$ and $[0^0/90^0/0^0/90^0]$ laminates have been studied.

Figs. 4.11 to Figs. 4.18 show the mean and standard deviation of normalized critical load corresponding to each input variable as random . Each figure represents six different studies. These present the effect of the SD of input RV on the buckling load of the plates with different boundary conditions, ARs and ply-orientations.

The Figs. 4.19 and 4.20 show the mean and standard deviation of normalized critical load when both E_{11} and G_{12} are random variables.

4.5.1 Effect of longitudinal elastic modulus E_{11}

Fig 4.11 shows the variation of mean of the buckling load with standard deviation of E_{11}. Fig 4.12 shows the variation of standard deviation of buckling load with standard deviation of E_{11}. The response shows a generally linear behavior. The plate with all edges CC is more affected by a change in

input randomness compared to a plate with all edges SS. The plate shows least sensitiveness to input dispersion as the aspect ratio increases. From an limited study conducted it is observed that cross-ply laminate is less sensitive compared to angle-ply laminate for all edges SS due to change in σ/μ of E_{11}.

4.5.2 Effect of transverse elastic modulus E_{12}

Fig 4.13 shows the variation of mean of the buckling load with standard deviation of E_{12}. Fig 4.14 shows the variation of standard deviation of buckling load with standard deviation of E_{12}. The general behavior is almost linear, but unlike the case E_{11}, here the slope of both mean and standard deviation of normalized critical load curves are decreasing trend. The effect of random variable E_{12} is less compared to random variable E_{11}. As observed in the case of E_{11} here also the plate is less sensitive to input dispersion as aspect ratio increases. All edges CC plate is more affected by dispersion in E_{12} than all edges SS. The cross-ply laminate is least affected compared to angle-ply laminate for all edges SS due to change in σ/μ of E_{12}.

4.5.3 Effect of major Poisson's ratio ν_{12}

Fig 4.15 shows the variation of mean of the buckling load with standard deviation of ν_{12}. Fig 4.16 shows the variation of standard deviation of buckling load with standard deviation of ν_{12}.

The general nature of the curves are mostly linear. The plate with all edges CC is more affected than plate with all edges SS. From the comparison of all variables it has been found that the random variable ν_{12} has less effect compared to random variables E_{11}, E_{12} and G_{12}. Here too the cross-ply laminate is least affected than angle-ply laminate for all edges SS due to change in σ/μ of ν_{12}.

4.5.4 Effect of rigidity modulus G_{12}

Fig 4.17 shows the variation of mean of the buckling load with standard deviation of G_{12}. Fig 4.18 shows the variation of standard deviation of buckling load with standard deviation of G_{12}.

Here too the characteristics are mostly linear. The plate with all edges CC is more affected than plate with all edges SS. Here the slope of response characteristic curves have an increasing trend compared to E_{12} and ν_{12} response characteristic curves. Next to the random variable E_{11}, the random variable G_{12} has been affected more for buckling characteristics.

4.5.5 Combined effect of longitudinal modulus E_{11} and rigidity modulus G_{12}

Fig 4.19 shows the variation of mean of the buckling load with standard deviation of E_{11} and G_{12}. Fig 4.20 shows the variation of standard deviation of buckling load with standard deviation of E_{11} and G_{12}.

The $[0^0/90^0/0^0/90^0]$ laminate is least affected compared to $[45^0/-45^0/-45^0/45^0]$ and $[45^0/-45^0/45^0/-45^0]$ laminates with all edges SS. The plate with all edges CC is more affected than plate with all edges SS. The general behavior is almost linear, unlike the cases of random variables E_{11}, E_{12}, ν_{12}, G_{12}, here the slope of mean and standard deviation curves are increasing trend.

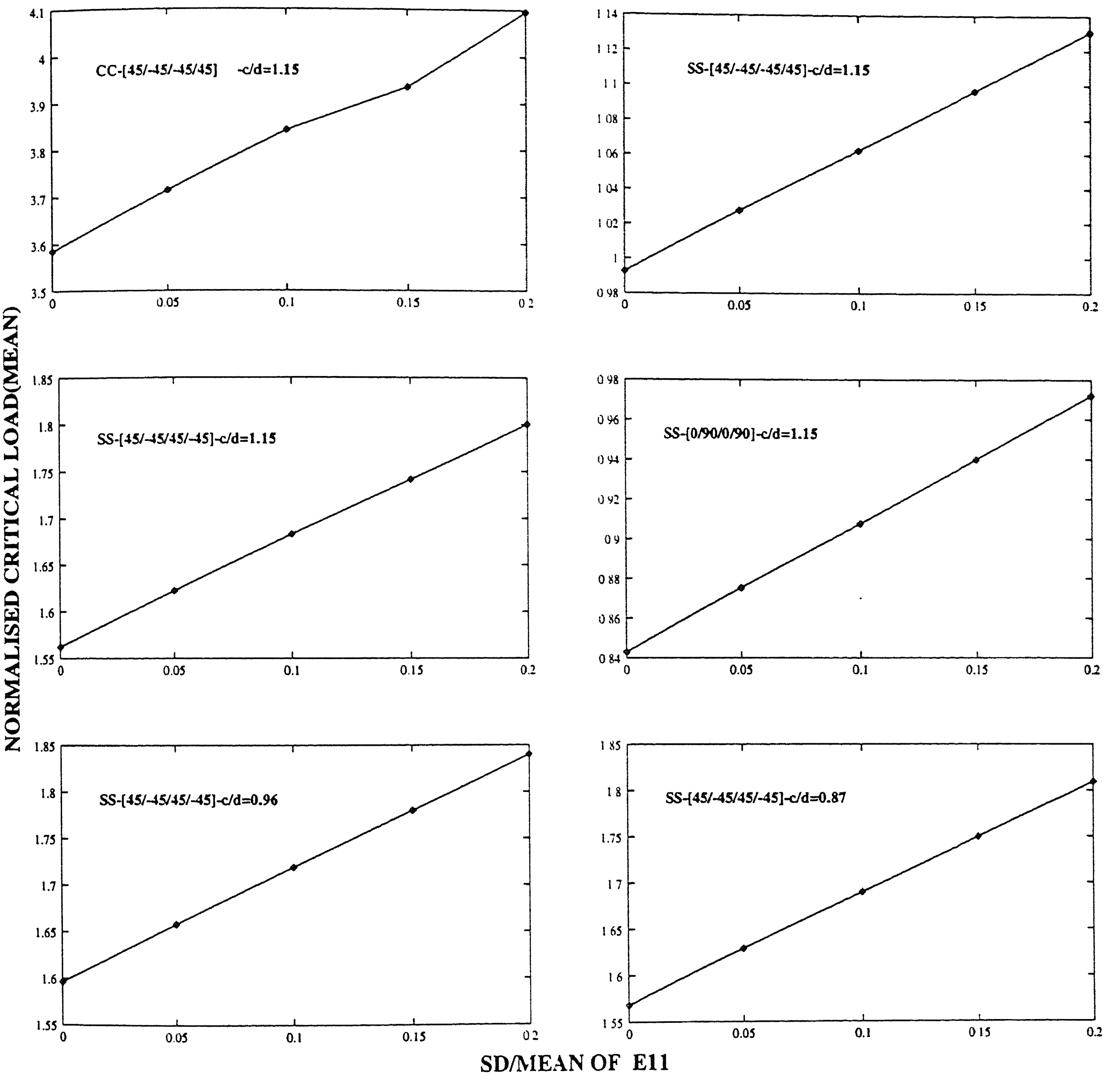

Figure 4.11: Buckling(Mean) characteristics of plate with rectangular cut-out for E_{11} as random

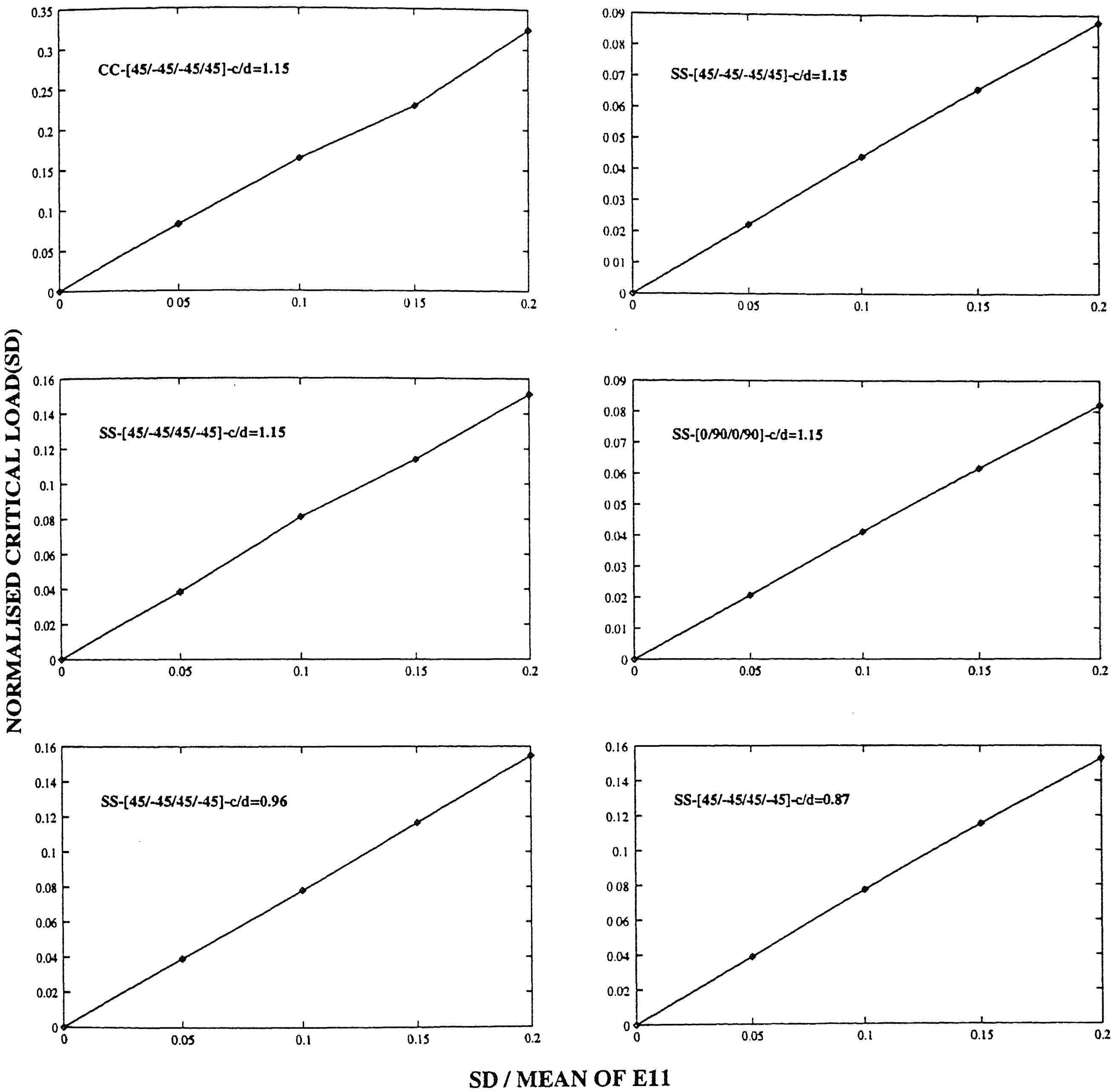

Figure 4.12: Buckling(SD) characteristics of plate with rectangular cut-out for E_{11} as random

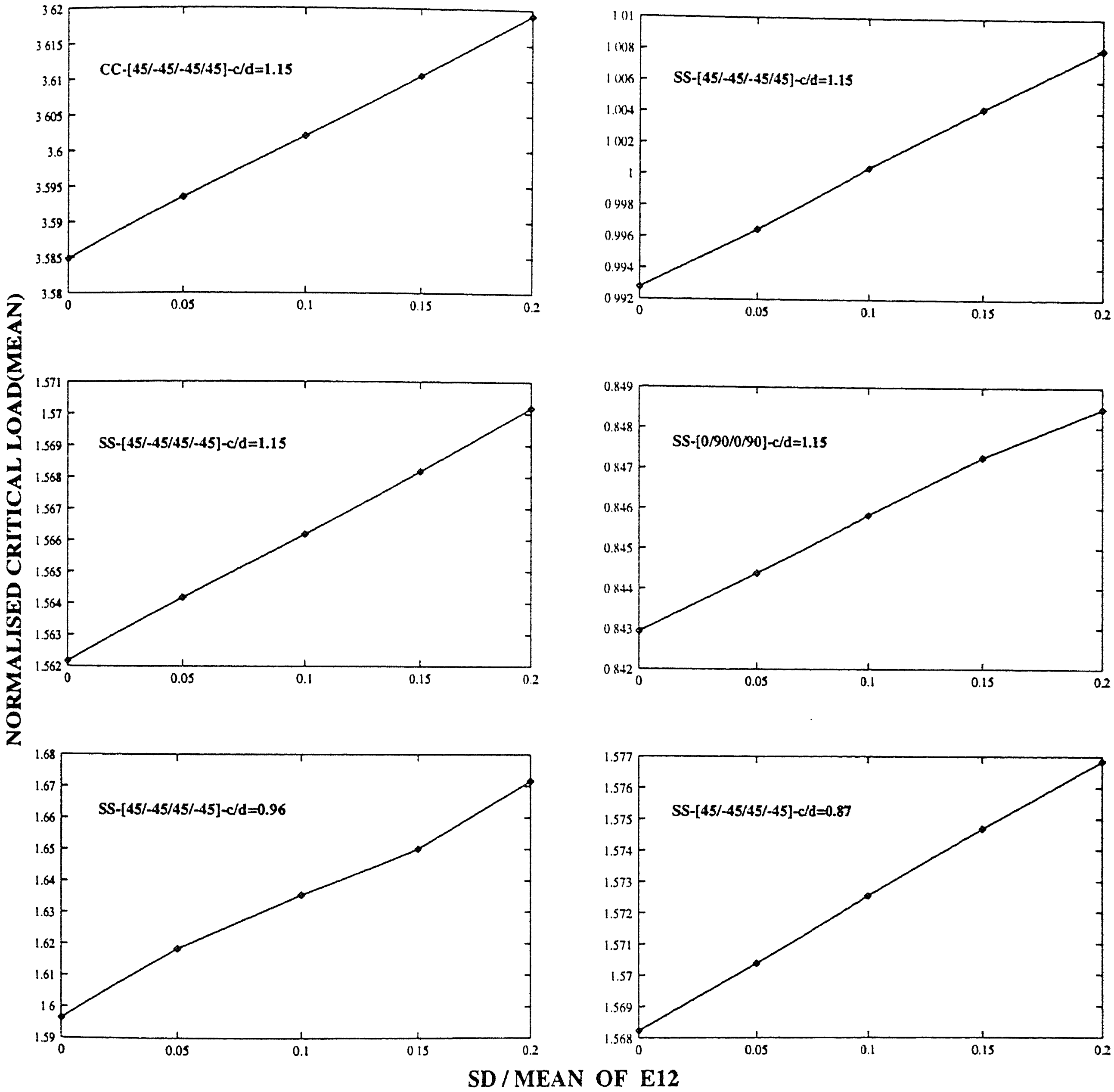

Figure 4.13: Buckling(Mean) characteristics of plate with rectangular cut-out for E_{12} as random

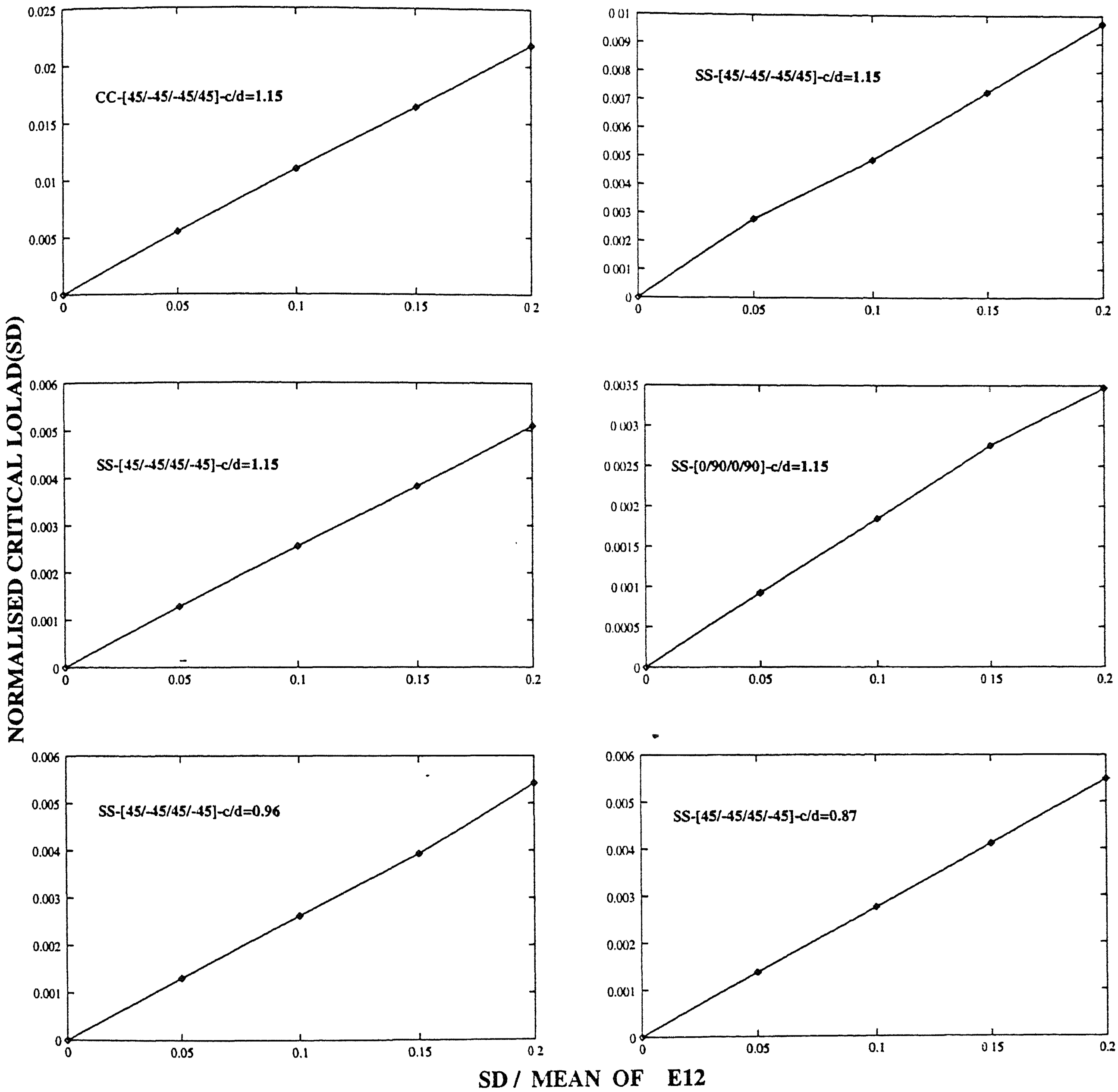

Figure 4.14: Buckling(SD) characteristics of plate with rectangular cut-out for E_{12} as random

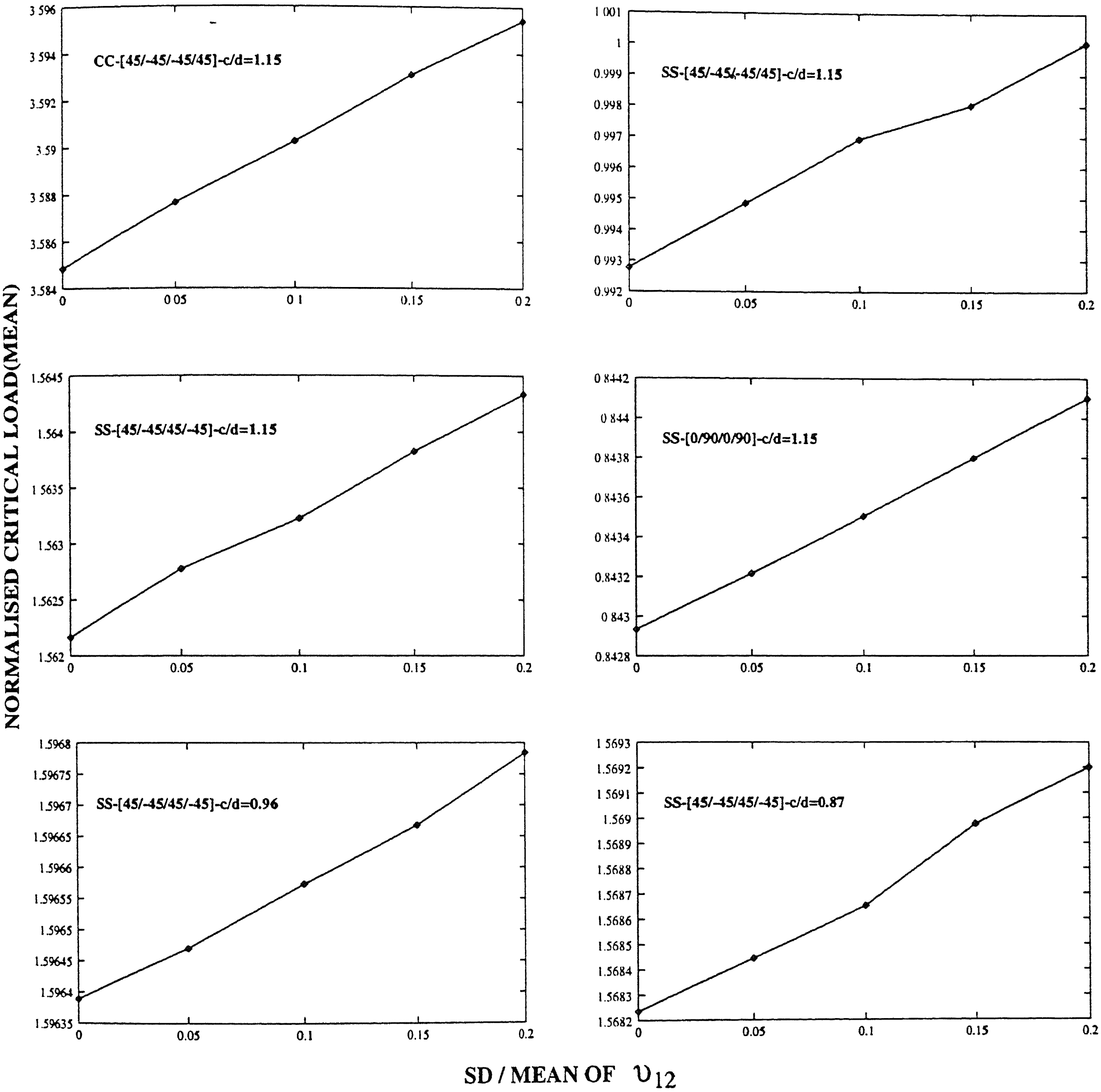

Figure 4.15: Buckling(Mean) characteristics of plate with rectangular cut-out for ν_{12} as random

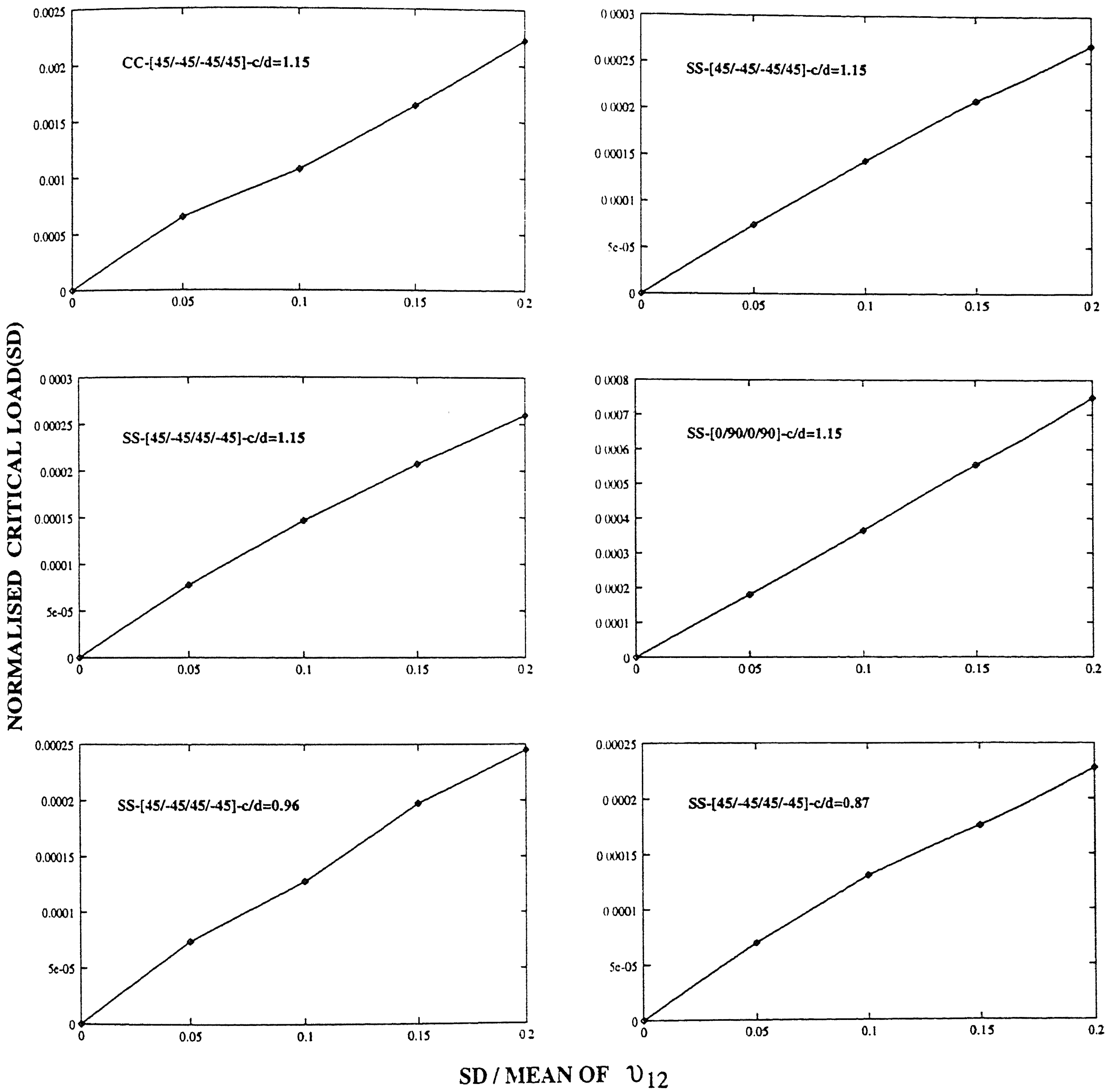

Figure 4.16: Buckling(SD) characteristics of plate with rectangular cut-out for ν_{12} as random

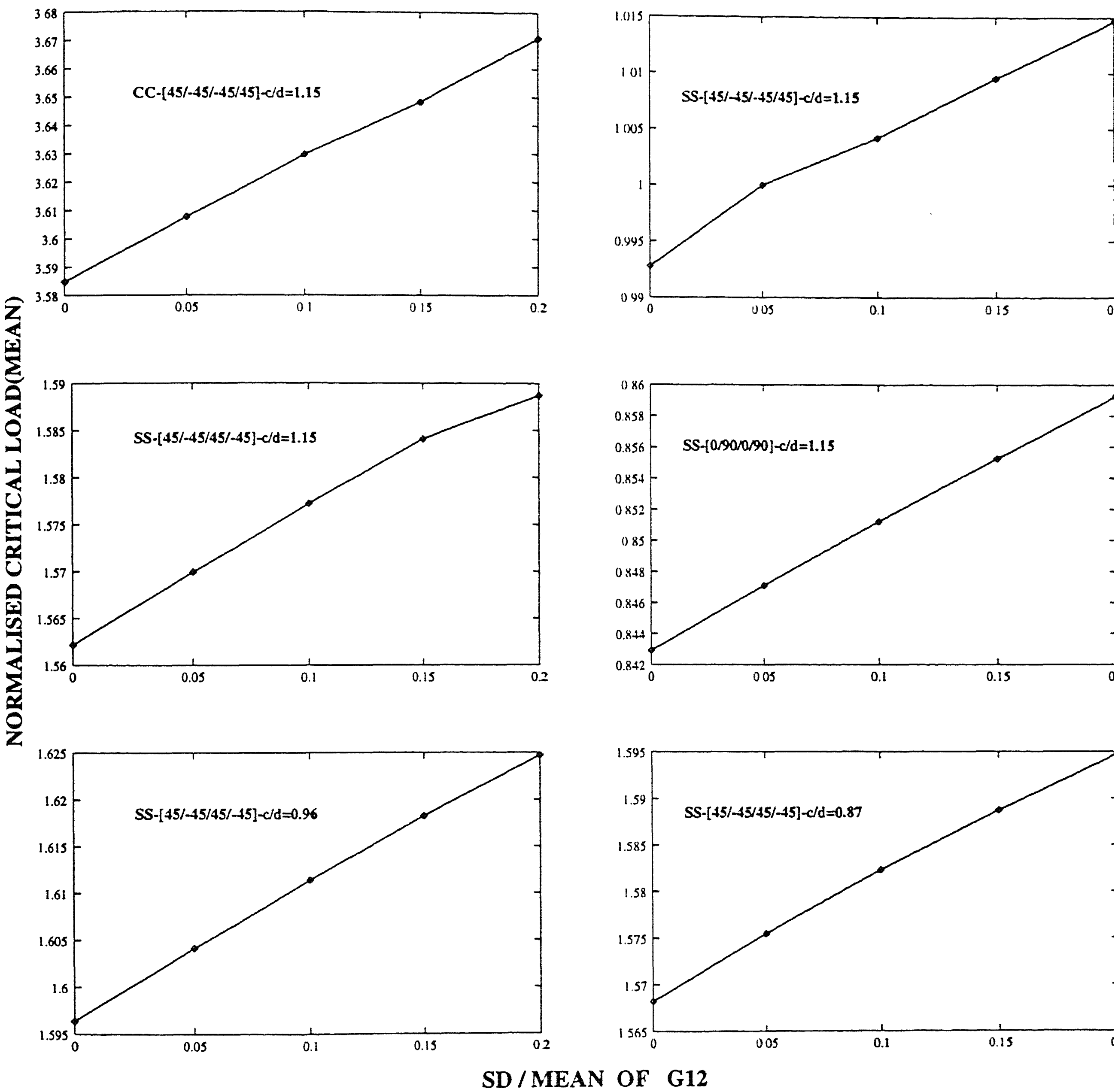

Figure 4.17: Buckling(Mean) characteristics of plate with rectangular cut-out for G_{12} as random

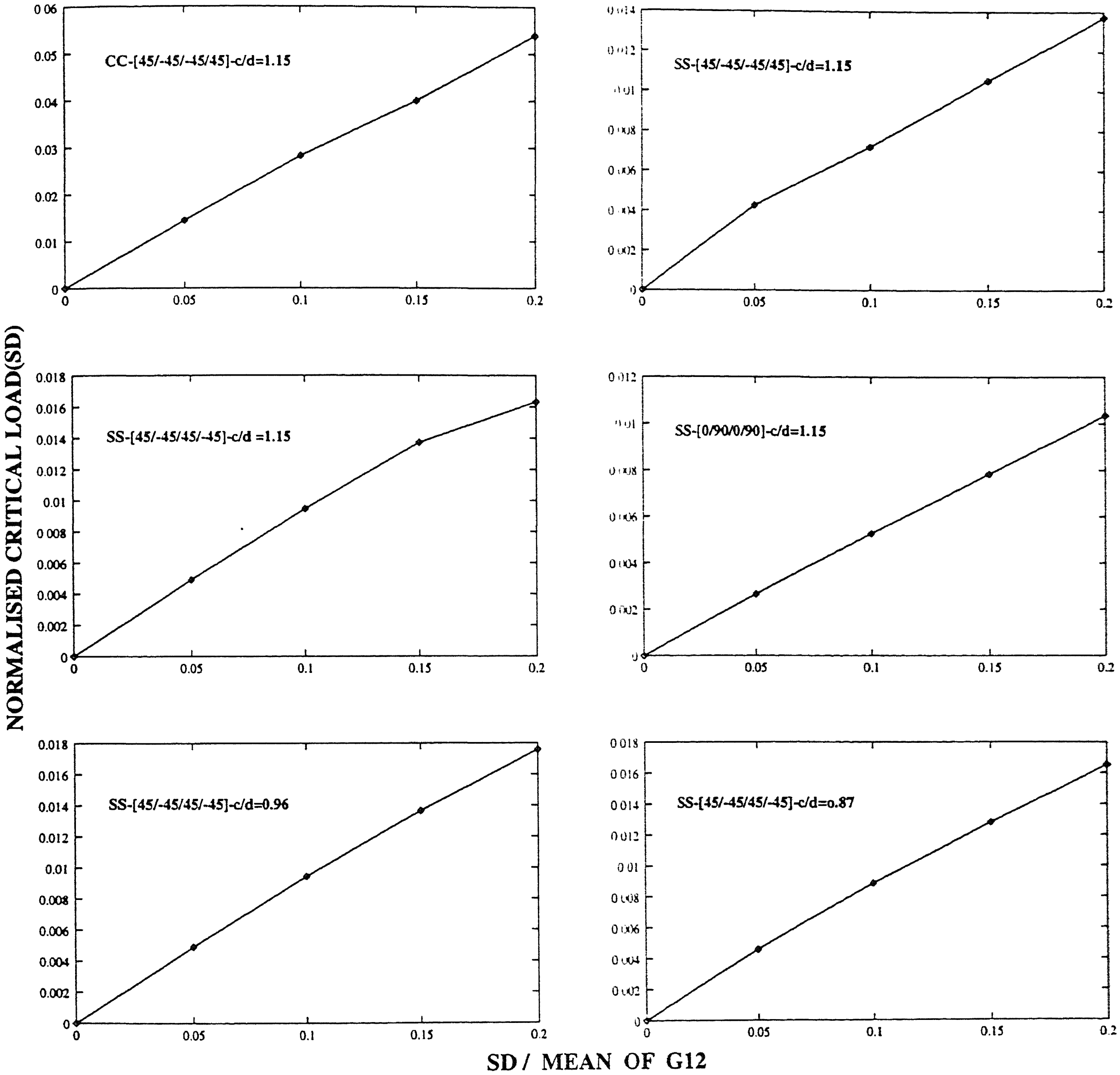

Figure 4.18: Buckling(SD) characteristics of plate with rectangular cut-out for G_{12} as random

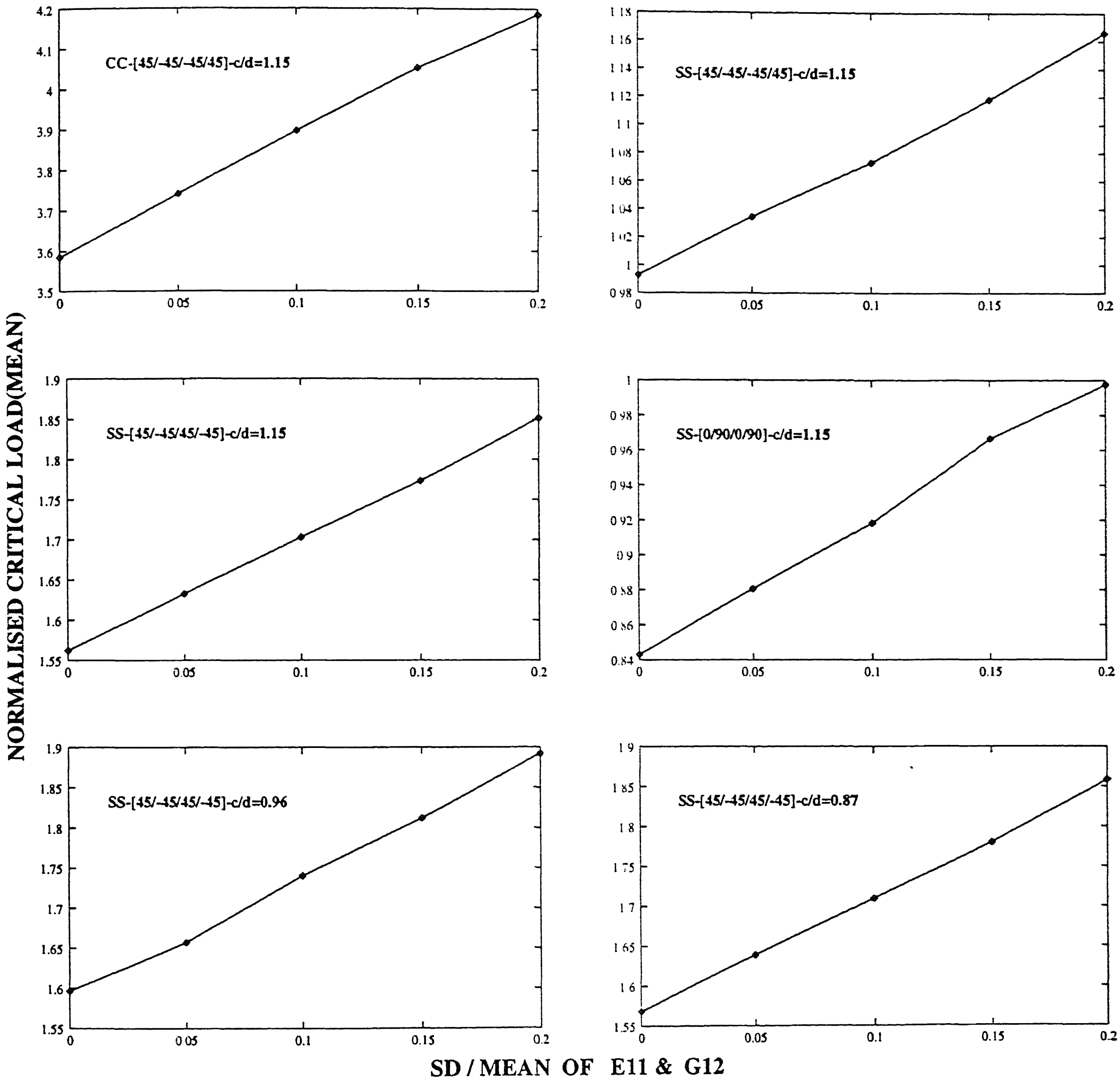

Figure 4.19: Buckling(Mean) characteristics of plate with rectangular cut-out for E_{11} and G_{12} as random

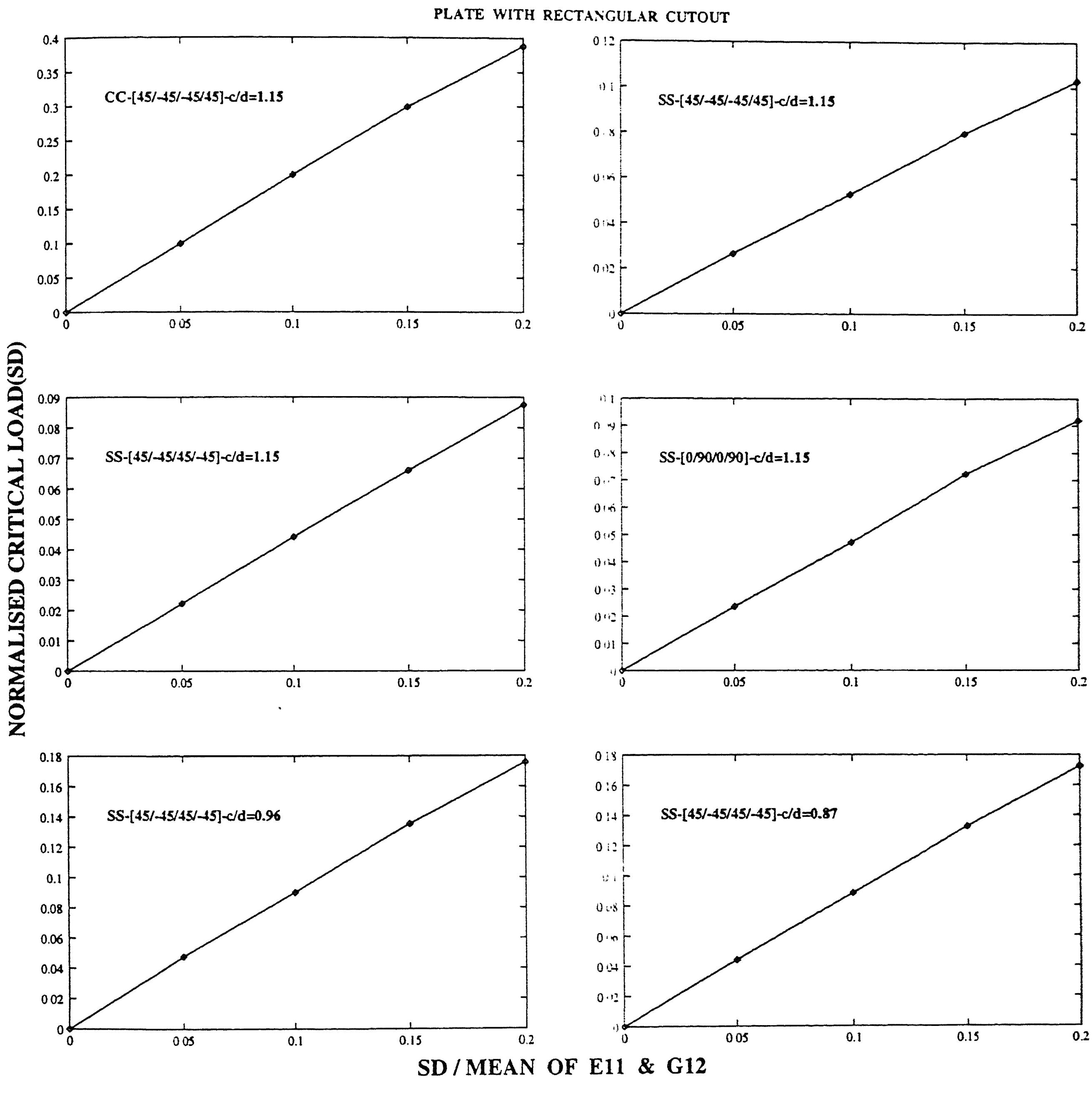

Figure 4.20: Buckling(SD) characteristics of plate with rectangular cut-out for E_{11} and G_{12} as random

4.6 Buckling characteristics of plates with circular cut-out

In this section the circular cutouts has been used in rectangular plates with plate length to cut-out ratio a/d having 1.58. A standard plate is taken with AR = 1. The normalization for the mean and SD of critical loads have been done with respect to a cross-ply laminate without cut-out. Results presented graphically to bring out the effect of boundary conditions, ARs and ply-orientation for various a/d ratio mentioned earlier. Three different lay-ups namely $[45^0/-45^0/-45^0/45^0]$, $[45^0/-45^0/45^0/-45^0]$ and $[0^0/90^0/0^0/90^0]$ laminates have been studied.

The Figs. 4.21 to Figs. 4.28 show the mean and standard deviation of normalized critical load corresponding to each input variable as random . Each figure represents six different studies. These presents the effect of the SD of input RV on the buckling load of the plates with different boundary conditions, ARs and ply-orientations.

The Figs. 4.29 and 4.30 show the mean and standard deviation of normalized critical load when both E_{11} and G_{12} are random variables.

4.6.1 Effect of longitudinal elastic modulus E_{11}

Fig 4.21 shows the variation of mean of the buckling load with standard deviation of E_{11}. Fig 4.22 shows the variation of standard deviation of buckling load with standard deviation of E_{11}. The response shows a generally linear behavior. The plate with all edges CC is more affected by a change in input randomness compared to a plate with all edges SS. The plate shows least sensitiveness to input dispersion as the aspect ratio increases. From an limited study conducted it is observed that cross-ply laminate is less sensitive compared to angle-ply laminate for all edges SS due to change in σ/μ of E_{11}.

4.6.2 Effect of transverse elastic modulus E_{12}

Fig 4.23 shows the variation of mean of the buckling load with standard deviation of E_{12}. Fig 4.24 shows the variation of standard deviation of buckling load with standard deviation of E_{12}. The general behavior is almost linear, but unlike the case E_{11}, here the slope of both mean and standard deviation of normalized critical load curves are decreasing trend. The effect of random variable E_{12} is less compared to random variable E_{11}. As observed in the case of E_{11} here also the plate is less sensitive to input dispersion as aspect ratio increases. All edges clamped plate is more affected by dispersion in E_{12} than all edges SS. The cross-ply laminate is least affected compared to angle-ply laminate for all edges SS due to change in σ/μ of E_{12}.

4.6.3 Effect of major Poisson's ratio ν_{12}

Fig 4.25 shows the variation of mean of the buckling load with standard deviation of ν_{12}. Fig 4.26 shows the variation of standard deviation of buckling load with standard deviation of ν_{12}.

The general nature of the curves are mostly linear. The plate with all edges CC is more affected than plate with all edges SS. From the comparison of all variables it has been found that the random variable ν_{12} has lower effect compared to random variables E_{11}, E_{12} and G_{12}. Here too the cross-ply laminate is least affected than angle-ply laminate for all edges SS due to change in σ/μ of ν_{12}.

4.6.4 Effect of rigidity modulus G_{12}

Fig 4.27 shows the variation of mean of the buckling load with standard deviation of G_{12}. Fig 4.28 shows the variation of standard deviation of buckling load with standard deviation of G_{12}.

Here too the characteristics are mostly linear. The plate with all edges

sponse characteristic curves have an increasing trend compared to E_{12} and ν_{12} response characteristic curves. Next to the random variable E_{11}, the random variable G_{12} has been more affected for buckling characteristics.

4.6.5 Combined effect of longitudinal modulus E_{11} and rigidity modulus G_{12}

Fig 4.29 shows the variation of mean of the buckling load with standard deviation of E_{11} and G_{12}. Fig 4.30 shows the variation of standard deviation of buckling load with standard deviation of E_{11} and G_{12}.

The $[0^0/90^0/0^0/90^0]$ laminate is least affected compared to $[45^0/-45^0/-45^0/45^0]$ and $[45^0/-45^0/45^0/-45^0]$ laminates with all edges SS. The plate with all edges CC is more affected than plate with all edges SS. The general behavior is almost linear, unlike the cases of random variables E_{11}, E_{12}, ν_{12}, G_{12}, here the slope of mean and standard deviation curves are increasing trend.

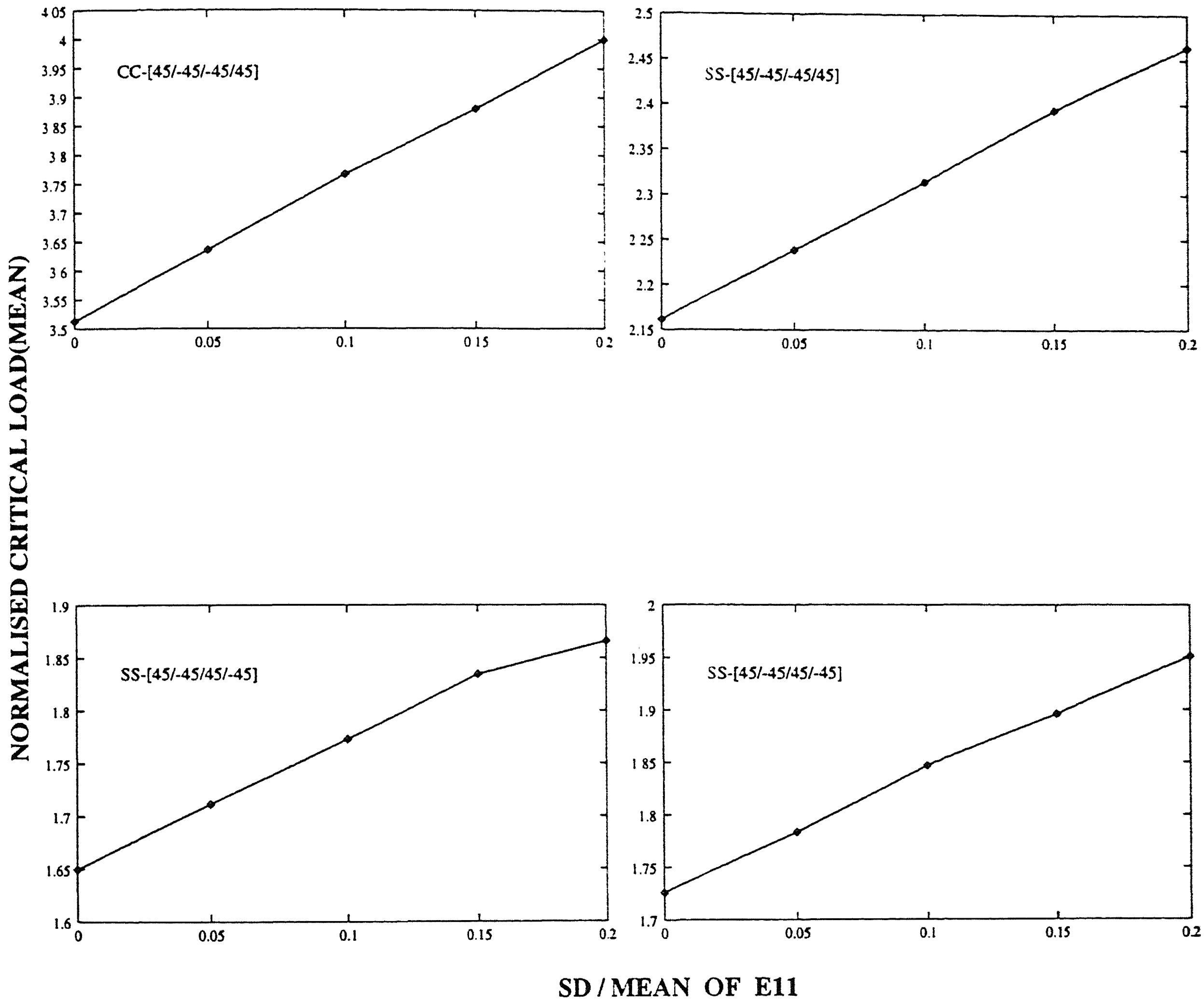

Figure 4.21: Buckling(Mean) characteristics of plate with circular cut-out for E_{11} as random

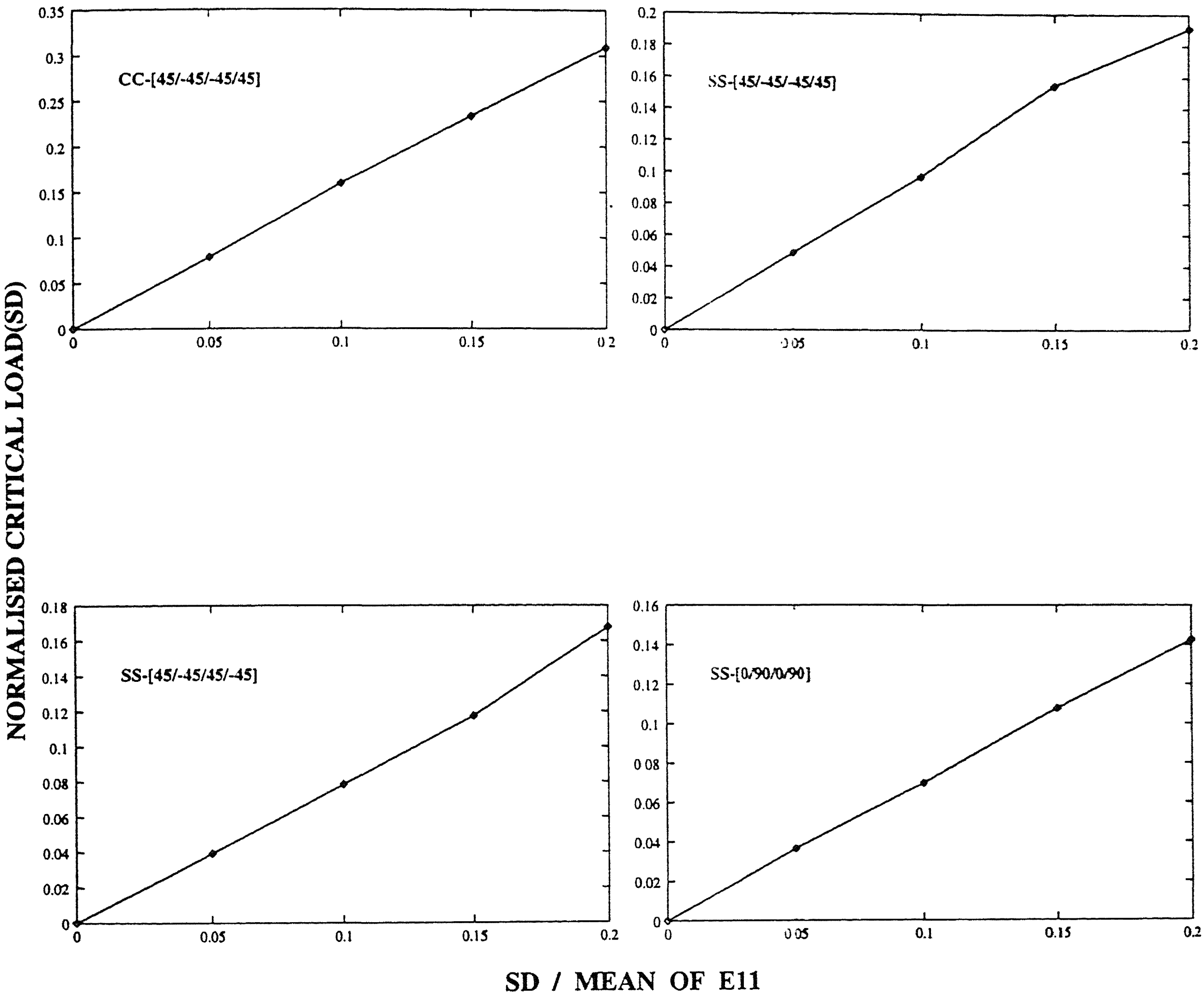

Figure 4.22: Buckling(SD) characteristics of plate with circular cut-out for E_{11} as random

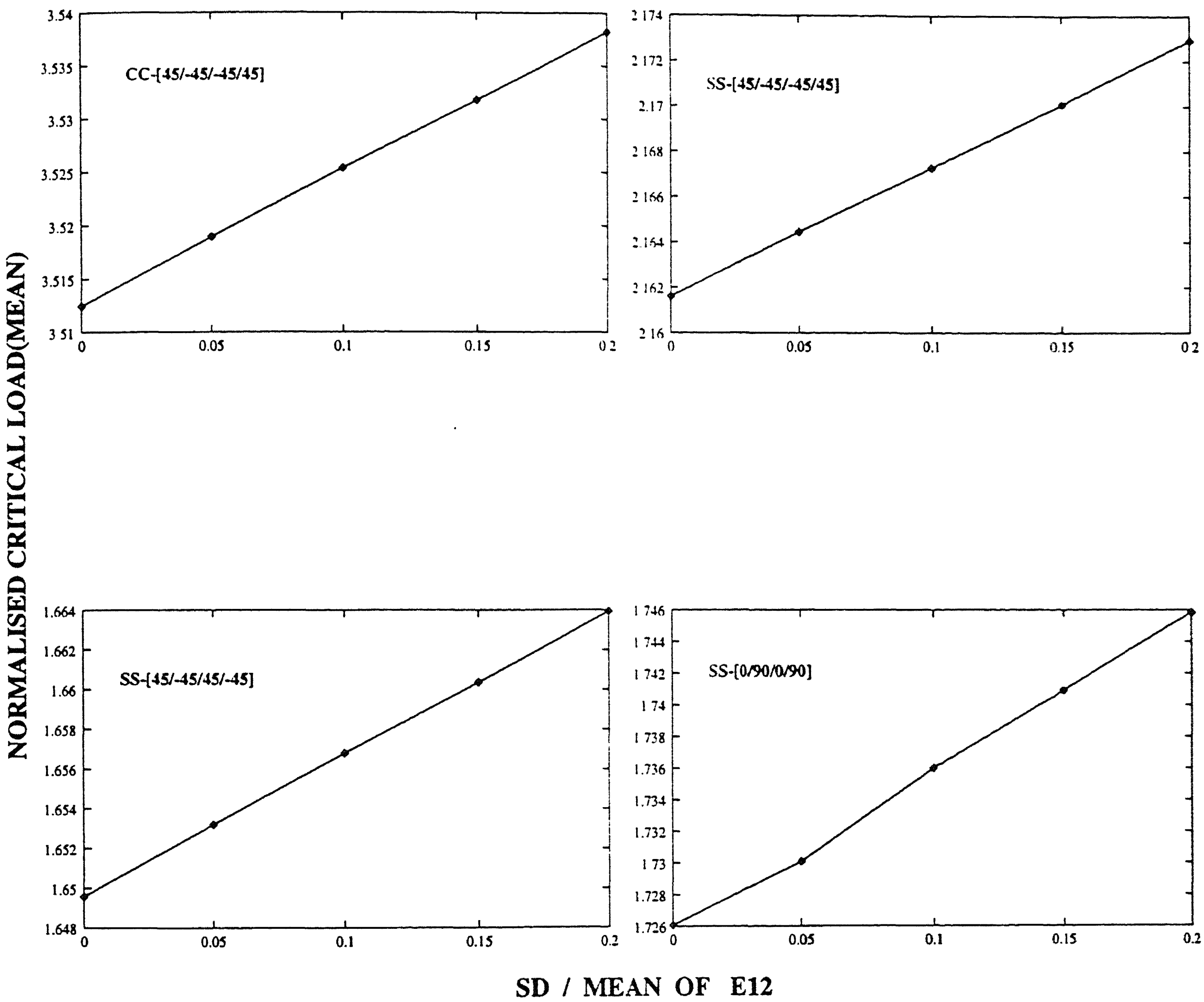

Figure 4.23: Buckling(Mean) characteristics of plate with circular cut-out for E_{12} as random

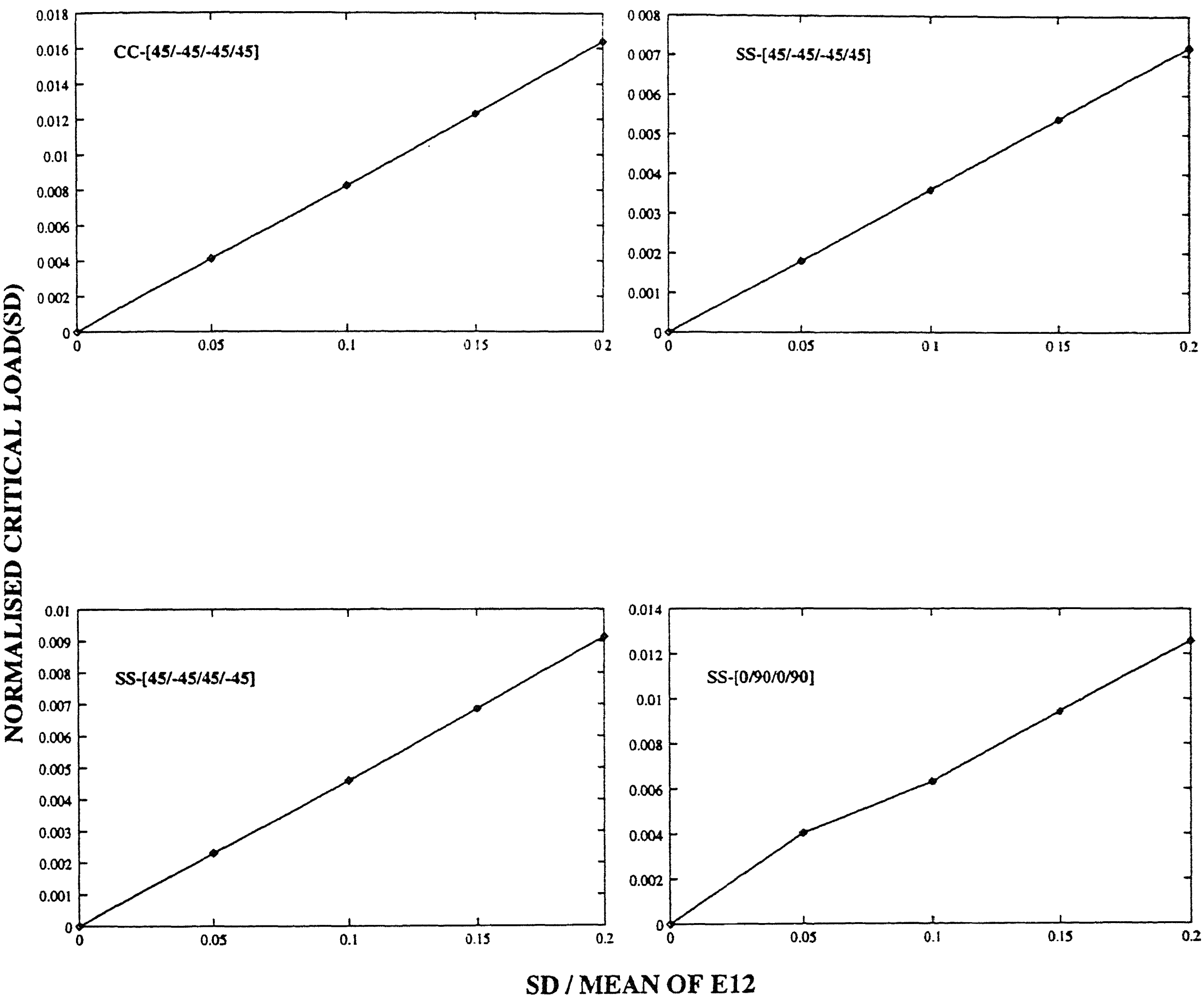

Figure 4.24: Buckling(SD) characteristics of plate with circular cut-out for E_{12} as random

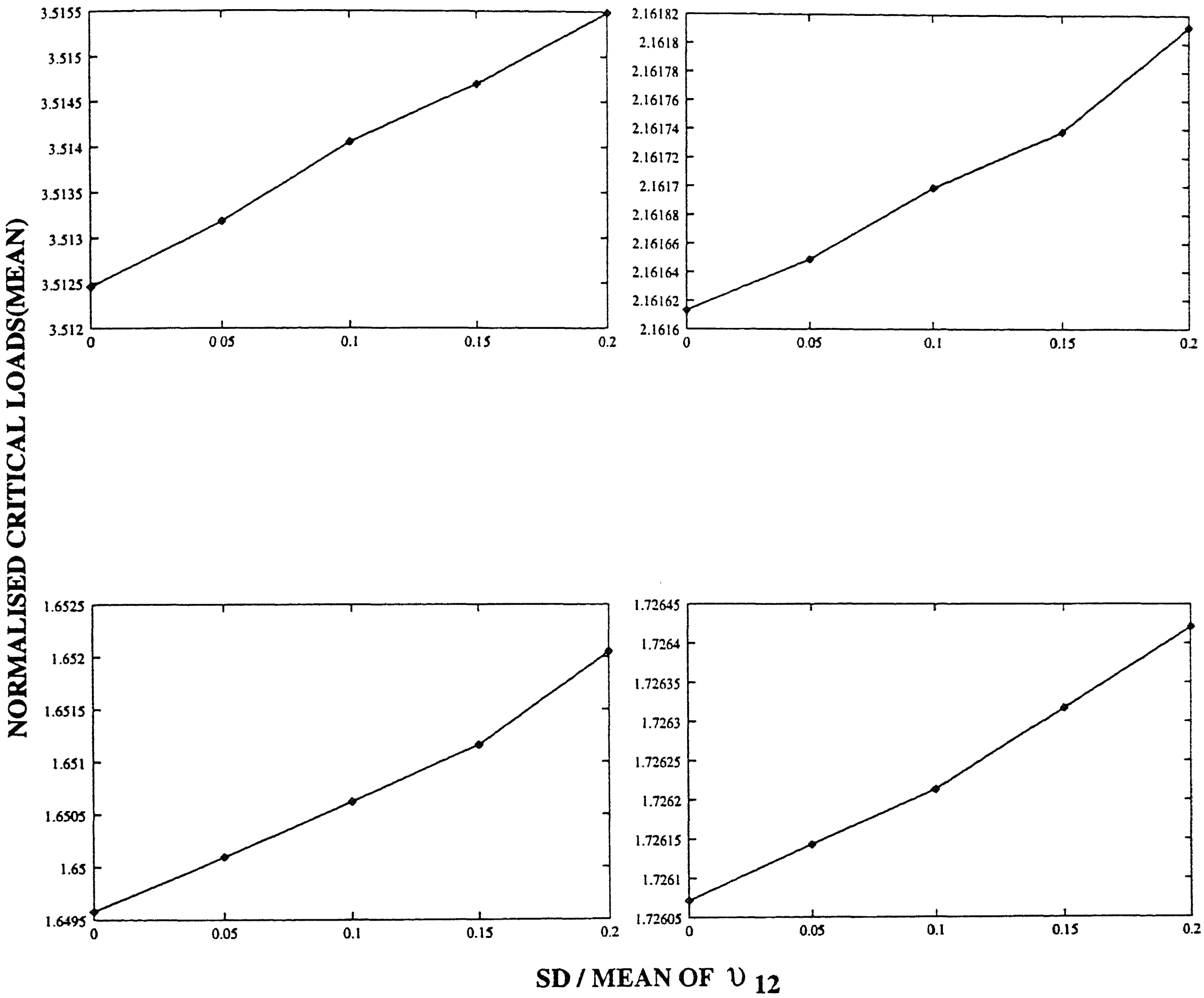

Figure 4.25: Buckling(SD) characteristics of plate with circular cut-out for ν_{12} as random

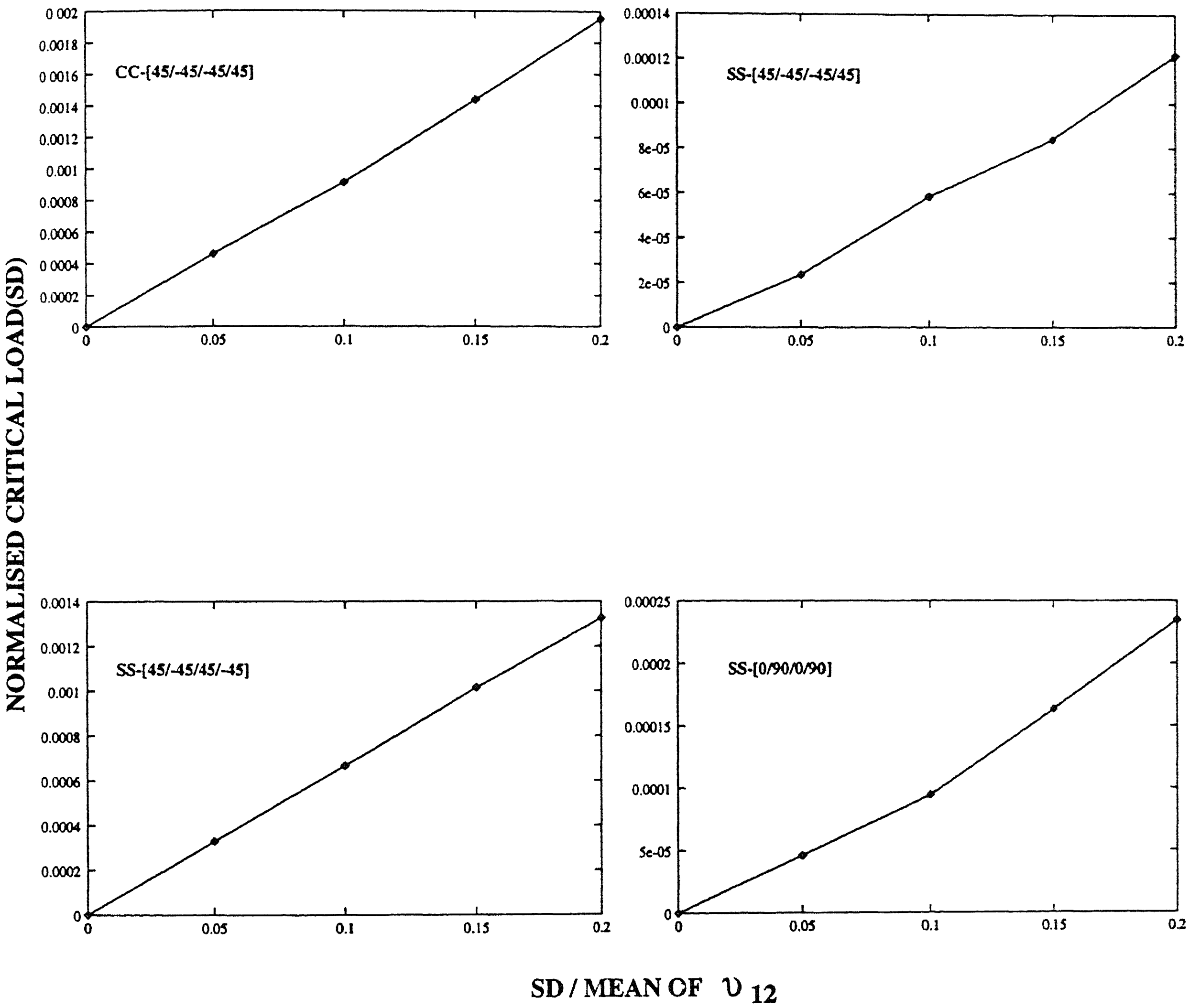

Figure 4.26: Buckling(SD) characteristics of plate with circular cut-out for ν_{12} as random

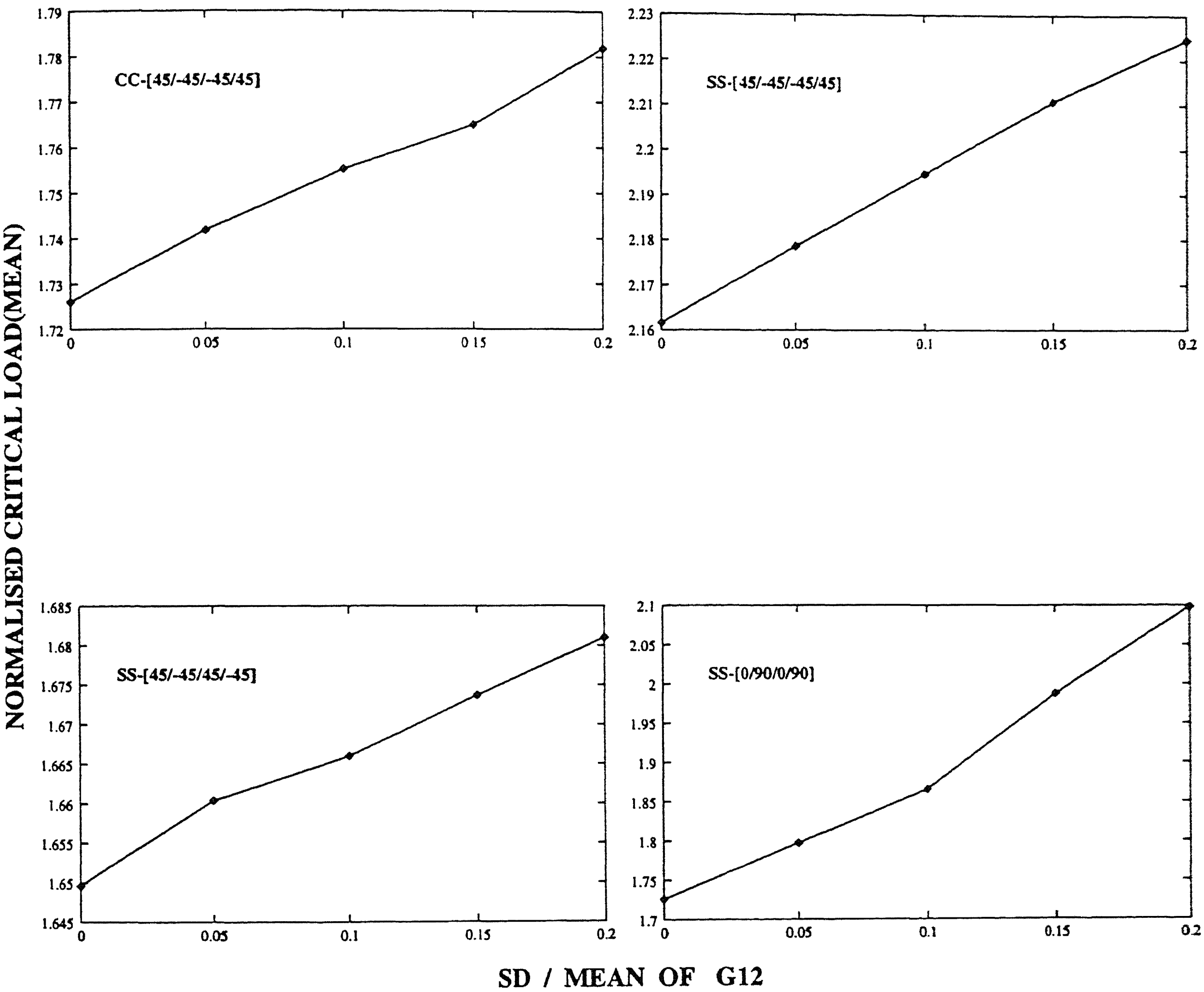

Figure 4.27: Buckling(Mean) characteristics of plate with circular cut-out for G_{12} as random

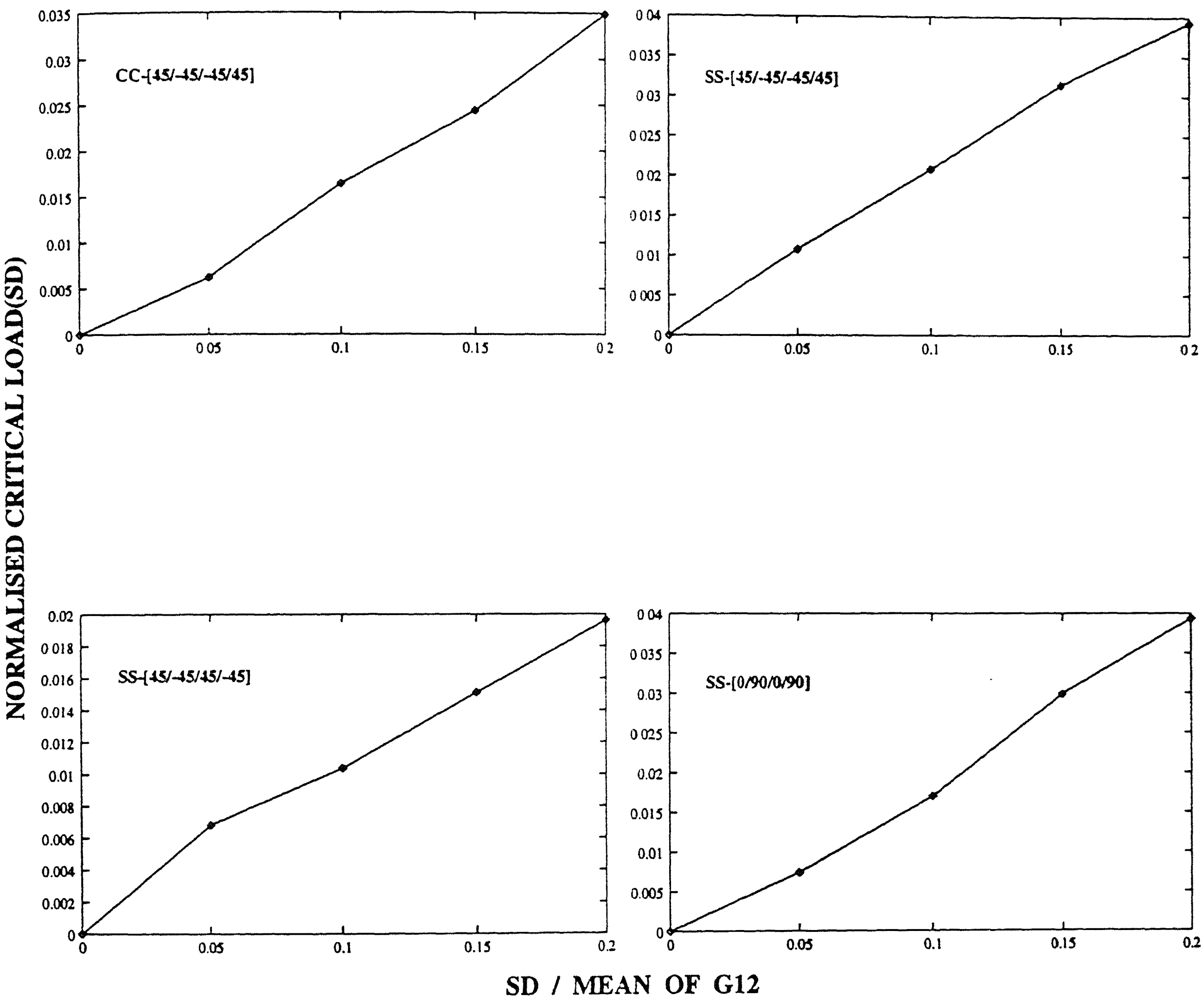

Figure 4.28: Buckling(SD) characteristics of plate with circular cut-out for G_{12} as random

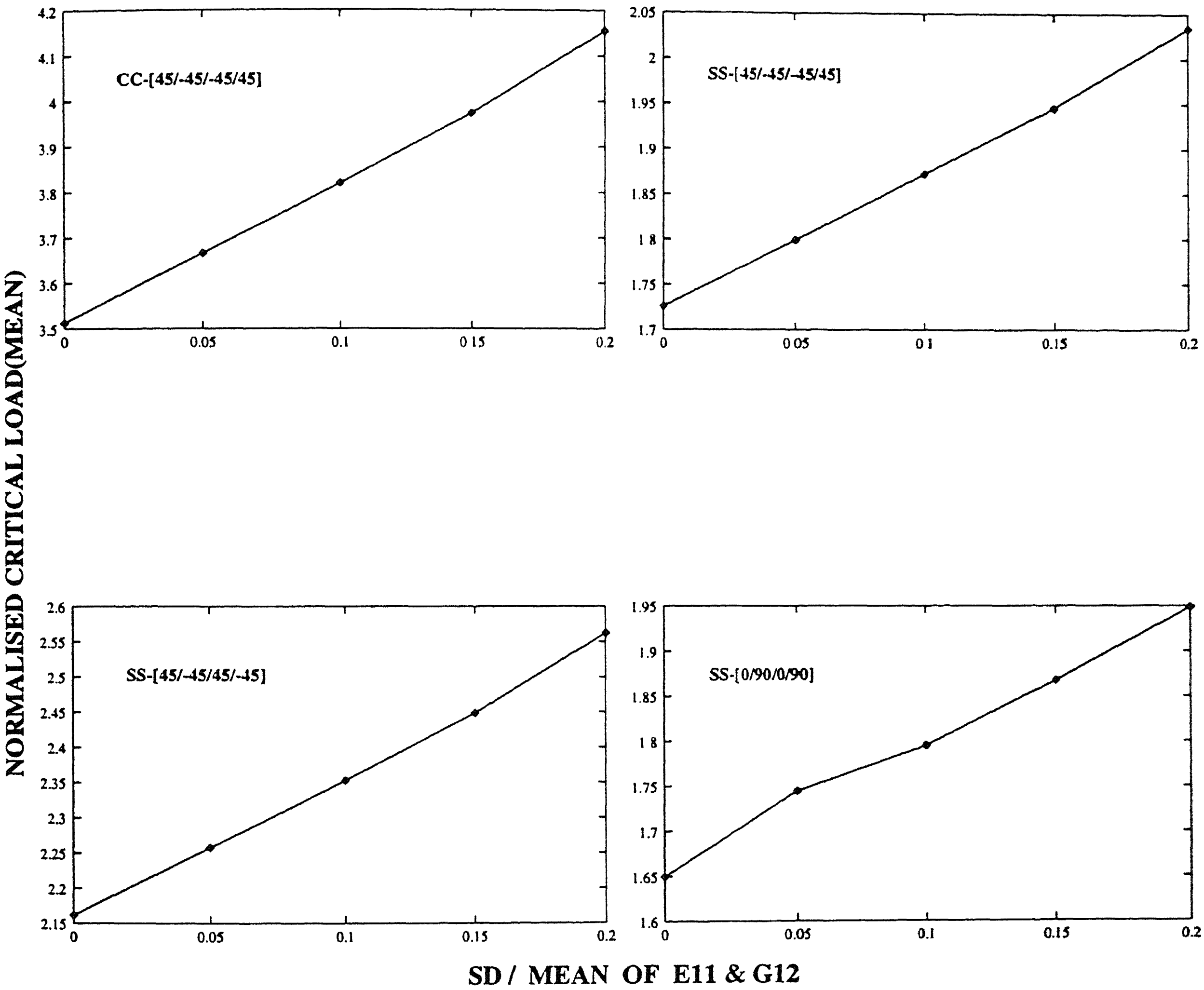

Figure 4.29: Buckling(Mean) characteristics of plate with circular cut-out for E_{11} and G_{12} as random

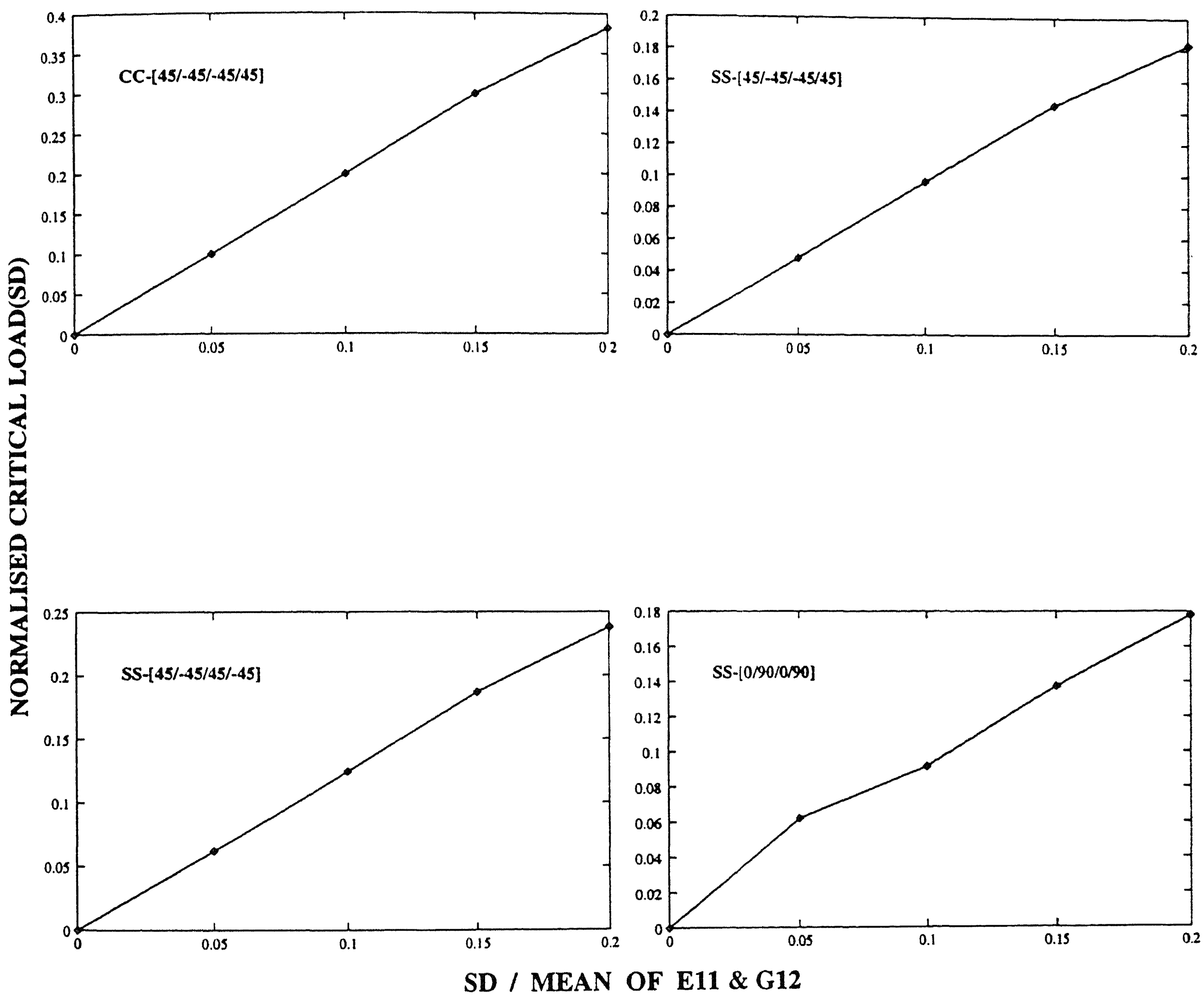

Figure 4.30: Buckling(SD) characteristics of plate with circular cut-out for E_{11} and G_{12} as random

4.7 Buckling characteristics of plates with elliptical cut-out

Results have been obtained for elliptical cut-out in rectangular plates with cut-out ratios (c/d) having values 2.5, 1.225 and 0.4. The area of cut-out has been kept same as that of the circular and rectangular cut-outs. A standard plate is taken with AR = 1. The normalization for the mean and SD of critical loads have been done with respect to a cross-ply laminate without cut-out. Results presented graphically to bring out the effect of boundary conditions, ARs and ply-orientation for various c/d ratios mentioned earlier. Three different lay-ups namely $[45^0/-45^0/-45^0/45^0]$, $[45^0/-45^0/45^0/-45^0]$ and $[0^0/90^0/0^0/90^0]$ laminates have been studied.

The Figs. 4.31 to Figs. 4.38 show the mean and standard deviation of normalized critical load corresponding to each input variable as random . Each figure represents six different studies. These presents the effect of the SD of input RV on the buckling load of the plates with different boundary conditions, ARs and ply-orientations.

The Figs. 4.39 and 4.40 show the mean and standard deviation of normalized critical load when both E_{11} and G_{12} are random variables.

4.7.1 Effect of longitudinal elastic modulus E_{11}

Fig 4.31 shows the variation of mean of the buckling load with standard deviation of E_{11}. Fig 4.32 shows the variation of standard deviation of buckling load with standard deviation of E_{11} . The response shows a linear behavior. The plate with all edges CC is more affected by change in input randomness compared to a plate with all edges SS. The plate shows least sensitiveness to input dispersion for the c/d=1.225. There is a marked increase in sensitiveness of the plate response for c/d=0.4 compared to c/d=1.225. The $[0^0/90^0/0^0/90^0]$ laminate is affected the least compared to angle-ply laminate for all edges SS due to change in SD of E_{11}.

4.7.2 Effect of transverse elastic modulus E_{12}

Fig 4.33 shows the variation of mean of the buckling load with standard deviation of E_{12}. Fig 4.34 shows the variation of standard deviation of buckling load with standard deviation of E_{12} . The general behavior is almost linear, but unlike the case E_{11}, here the slope of both mean and standard deviation of normalized critical load curves are decreasing trend. The effect of random variable E_{12} is less compared to random variable E_{11}. As observed in the case of E_{11} here is again a marked higher sensitiveness for plates with c/d=2.5 as compared to plate with c/d=1.225. All edges CC plate is more affected by dispersion in E_{12} than all edges SS. The $[0^0/90^0/0^0/90^0]$ laminate is affected lesser than $[45^0/-45^0/45^0/-45^0]$ laminate for all edges SS.

4.7.3 Effect of major Poisson's ratio ν_{12}

Fig 4.35 shows the variation of mean of the buckling load with standard deviation of ν_{12}. Fig 4.36 shows the variation of standard deviation of buckling load with standard deviation of ν_{12} . The general nature of the curves are mostly linear.The plate with all edges CC is more affected than plate with all edges SS. From the comparison of all variables it has found that the variable ν_{12} is least effective compared to random variables E_{11}, E_{12} and G_{12}.

4.7.4 Effect of rigidity modulus G_{12}

Fig 4.37 shows the variation of mean of the buckling load with standard deviation of G_{12}. Fig 4.38 shows the variation of standard deviation of buckling load with standard deviation of G_{12}.

Here too the characteristics are mostly linear. The plate with all edges CC is more affected than plate with all edges SS. Next to the random variable E_{11}, the G_{12} is more effective for buckling characteristics.

4.7.5 Combined effect of longitudinal modulus E_{11} and rigidity modulus G_{12}

Fig 4.39 shows the variation of mean of the buckling load with standard deviation of E_{11} and G_{12}. Fig 4.40 shows the variation of standard deviation of buckling load with standard deviation of E_{11} and G_{12}

. The $[0^0/90^0/0^0/90^0]$ laminate is least affected compared to $[45^0/-45^0/-45^0/45^0]$ and $[45^0/-45^0/45^0/-45^0]$ laminates with all edges SS. The plate with all edges CC is more affected than plate with all edges SS. The general behavior is almost linear, unlike the cases of random variables E_{11}, E_{12}, ν_{12}, G_{12}, here the slope of mean and standard deviation curves are increasing trend.

4.8 Normalized Mean and SD of critical loads for various cut-out shapes for antisymmetric angle-ply laminate

The results in Table 4.4 shows the variation of Mean of normalized critical loads with variation of SD. Table 4.5 shows the variation of SD of normalized critical loads with variation of SD. From the above tables, for a given area of the cut-outs, the buckling load for a laminate with elliptical cut-out is lower than circular and rectangular cut-outs. The buckling load with circular cut-out is highest.

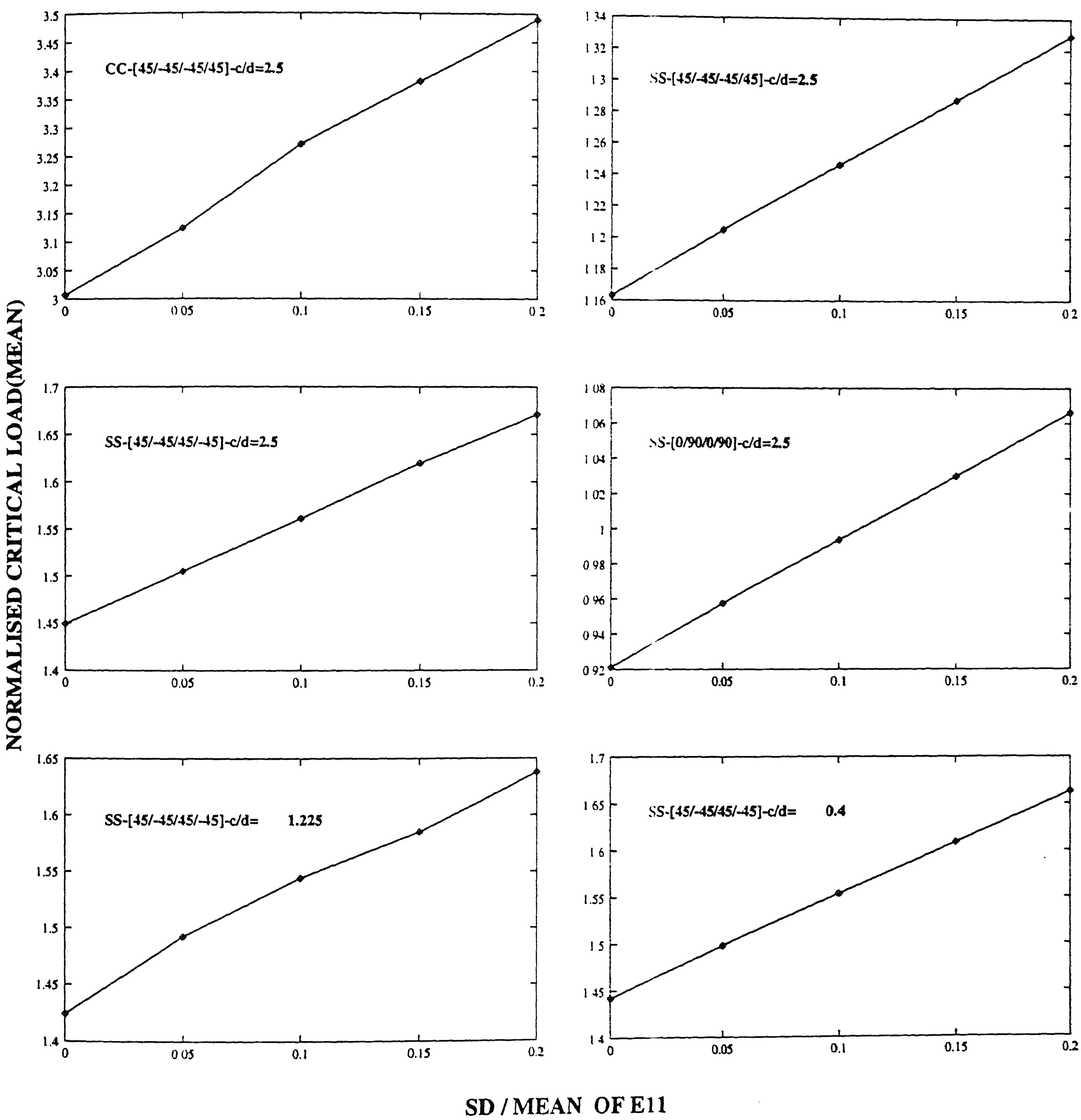

Figure 4.31: Buckling(Mean) characteristics of plate with elliptical cut-out for E_{11} as random

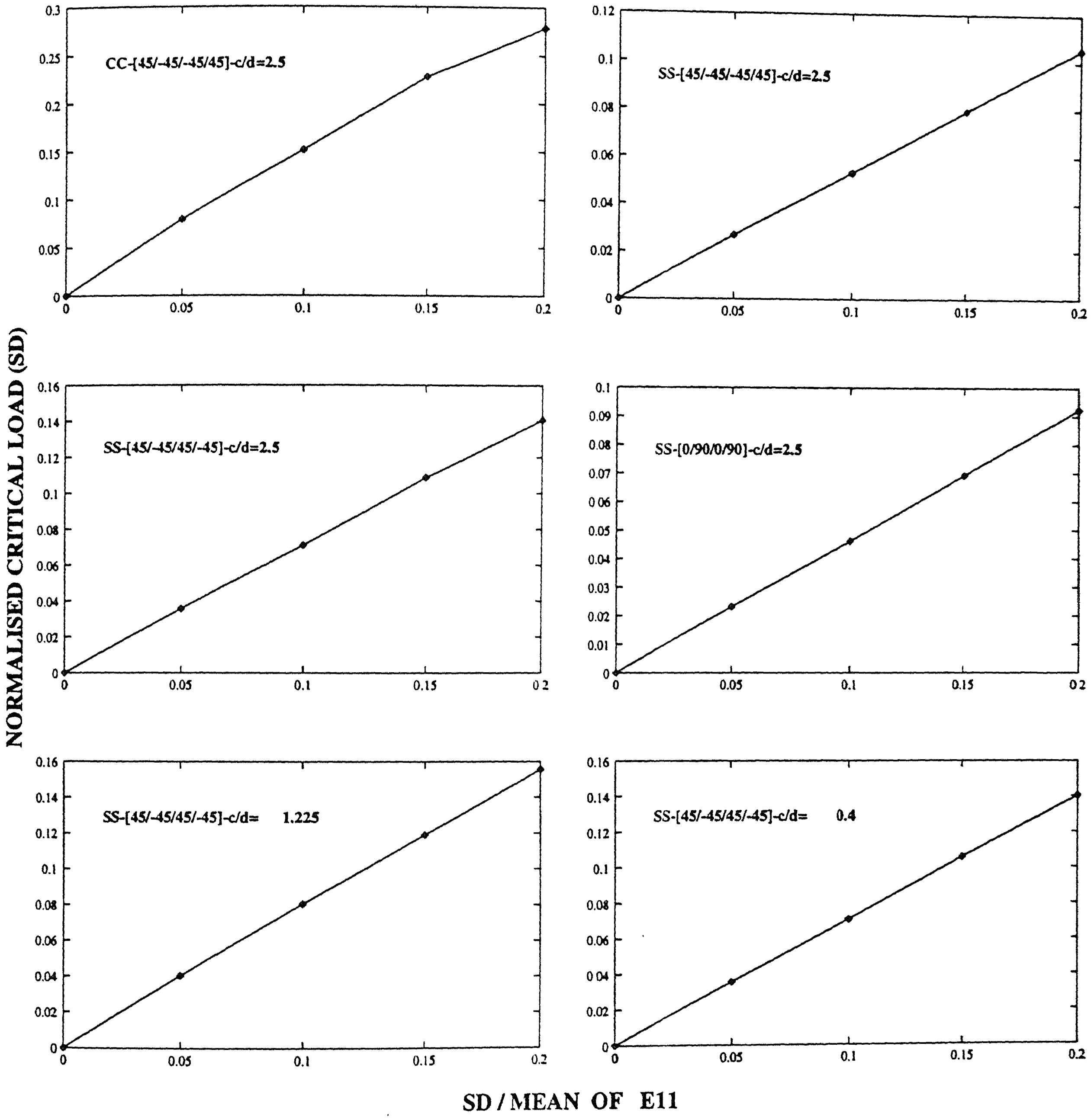

Figure 4.32: Buckling(SD) characteristics of plate with elliptical cut-out for E_{11} as random

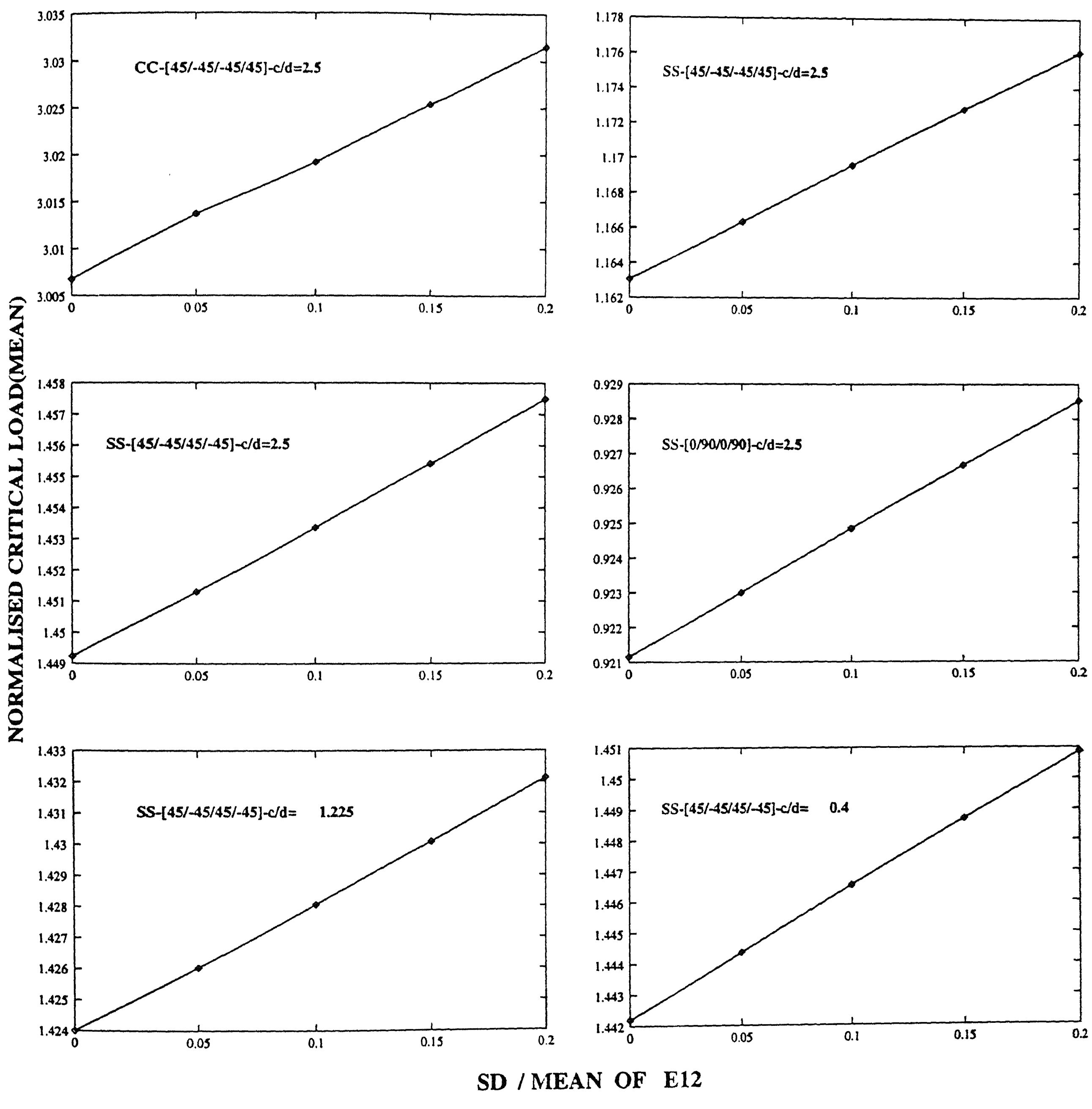

Figure 4.33: Buckling(Mean) characteristics of plate with elliptical cut-out for E_{12} as random

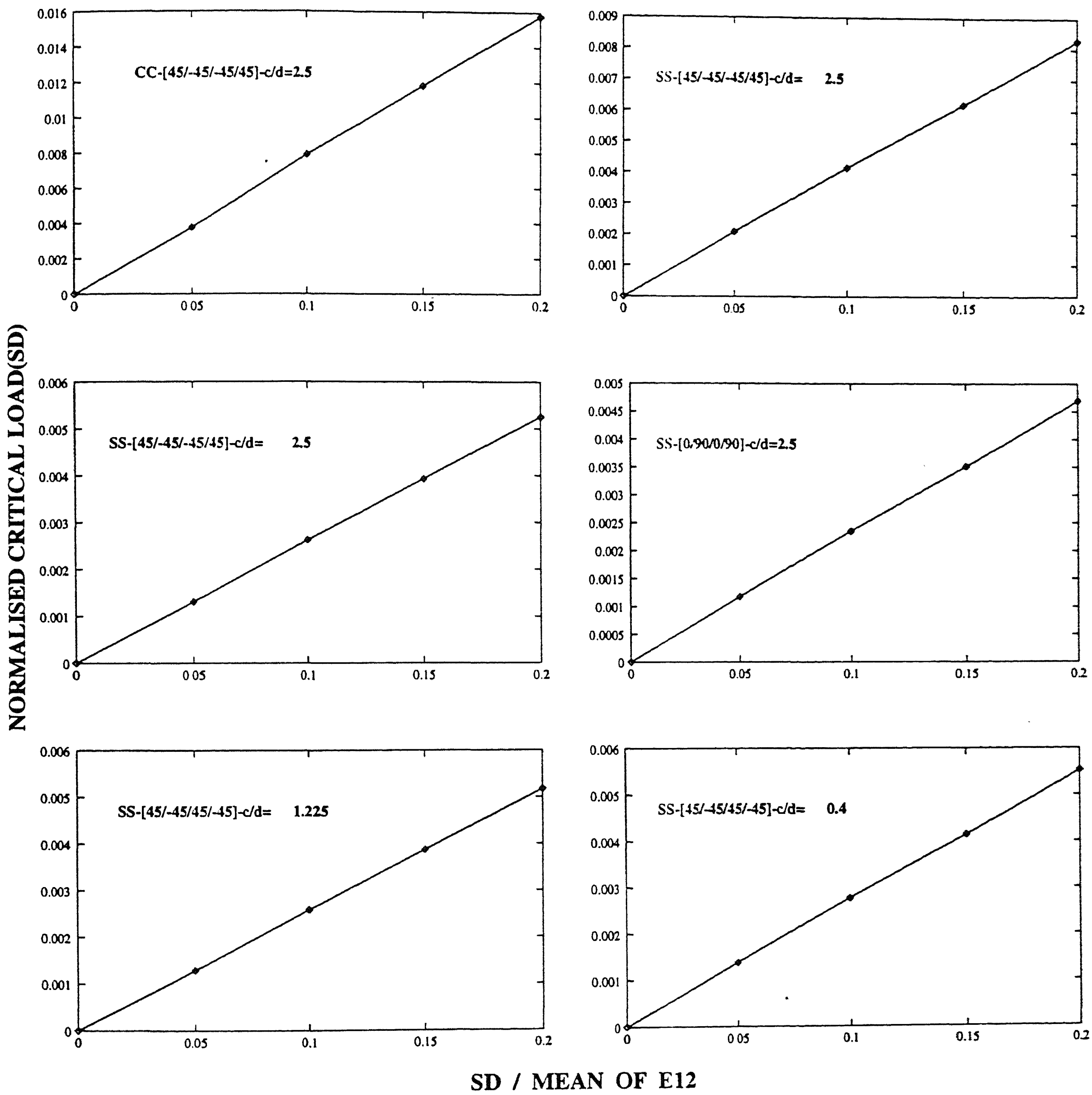

Figure 4.34: Buckling(SD) characteristics of plate with elliptical cut-out for E_{12} as random

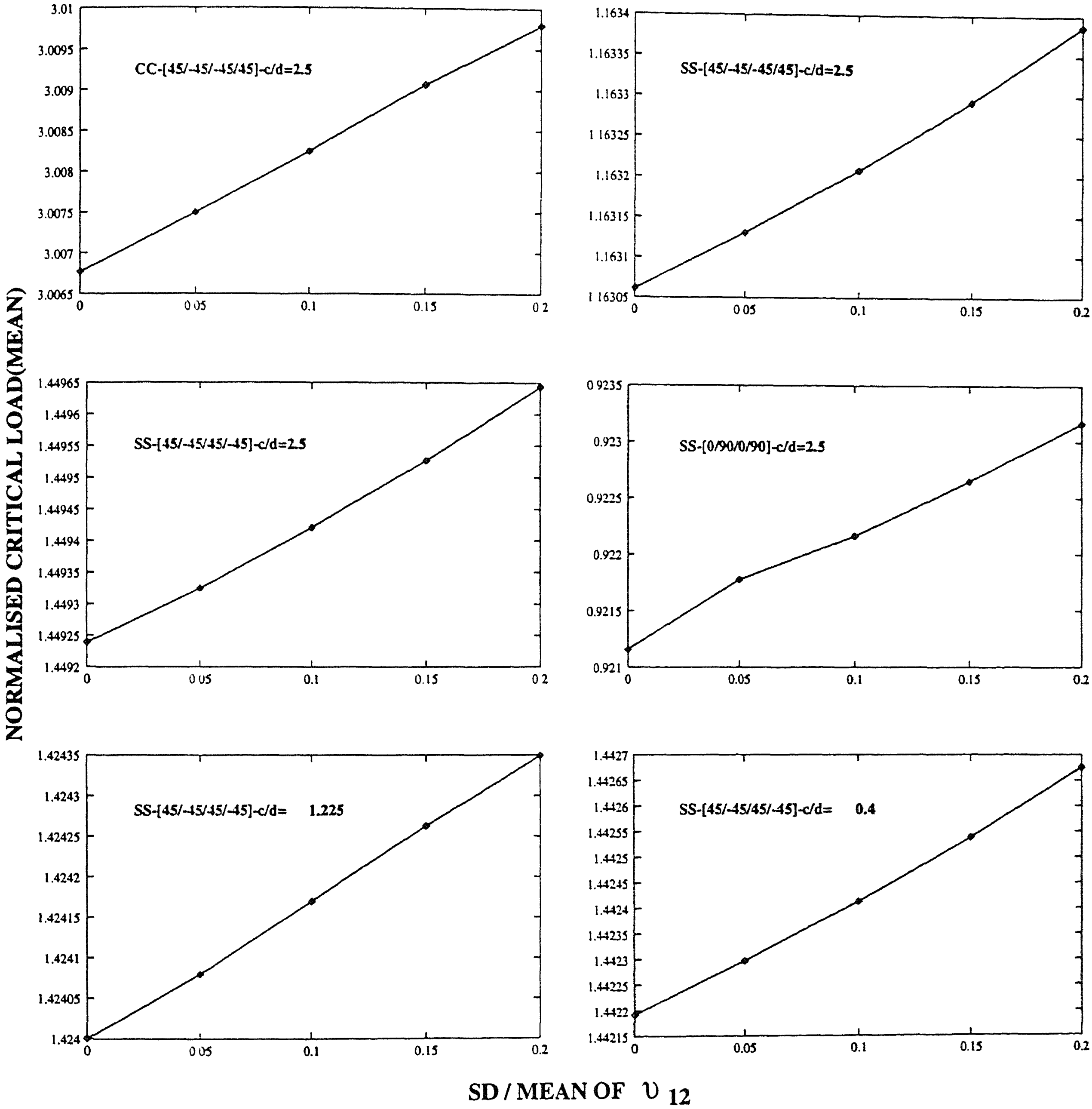

Figure 4.35: Buckling(Mean) characteristics of plate with elliptical cut-out for ν_{12} as random

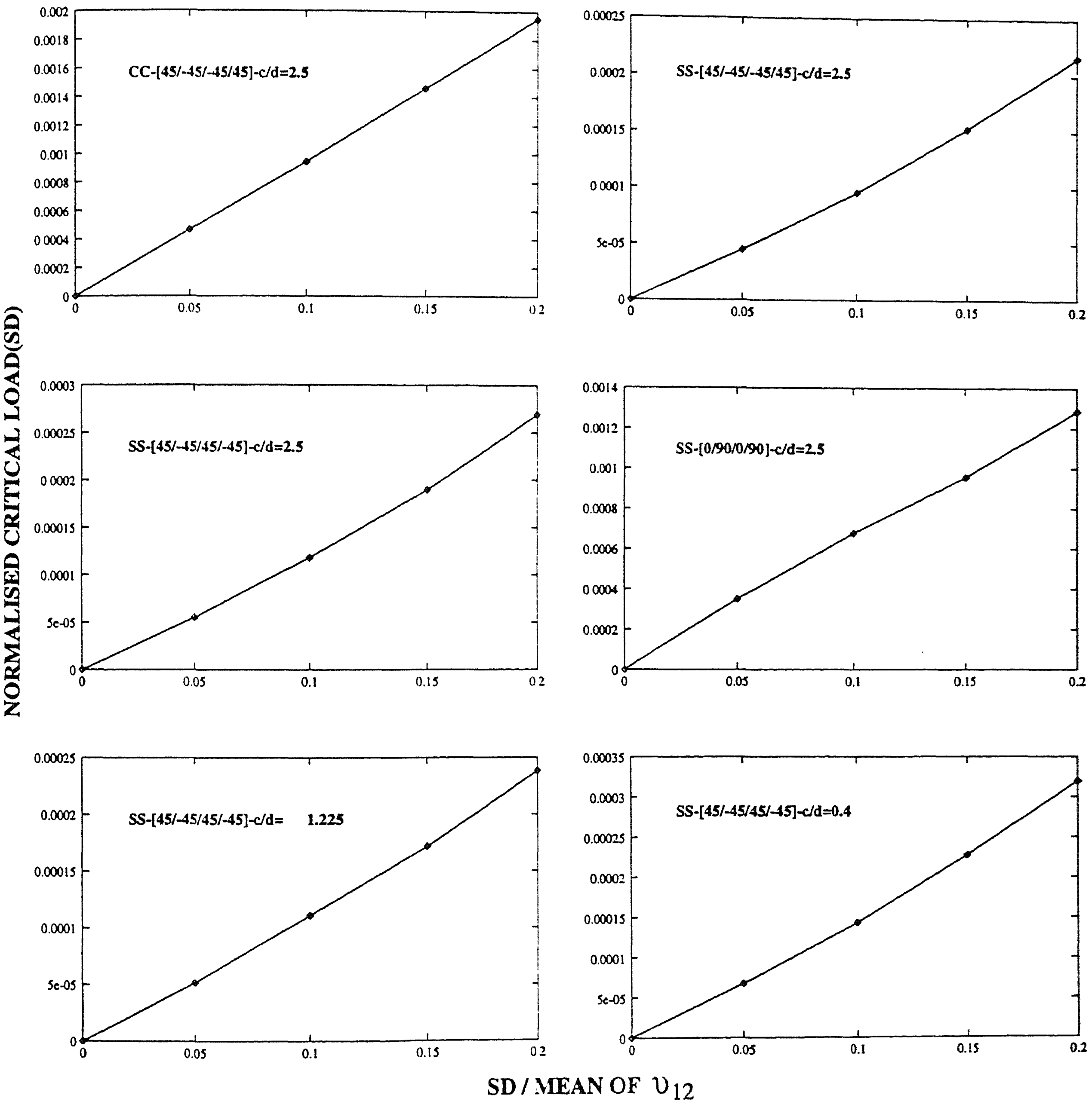

Figure 4.36: Buckling(SD) characteristics of plate with elliptical cut-out for ν_{12} as random

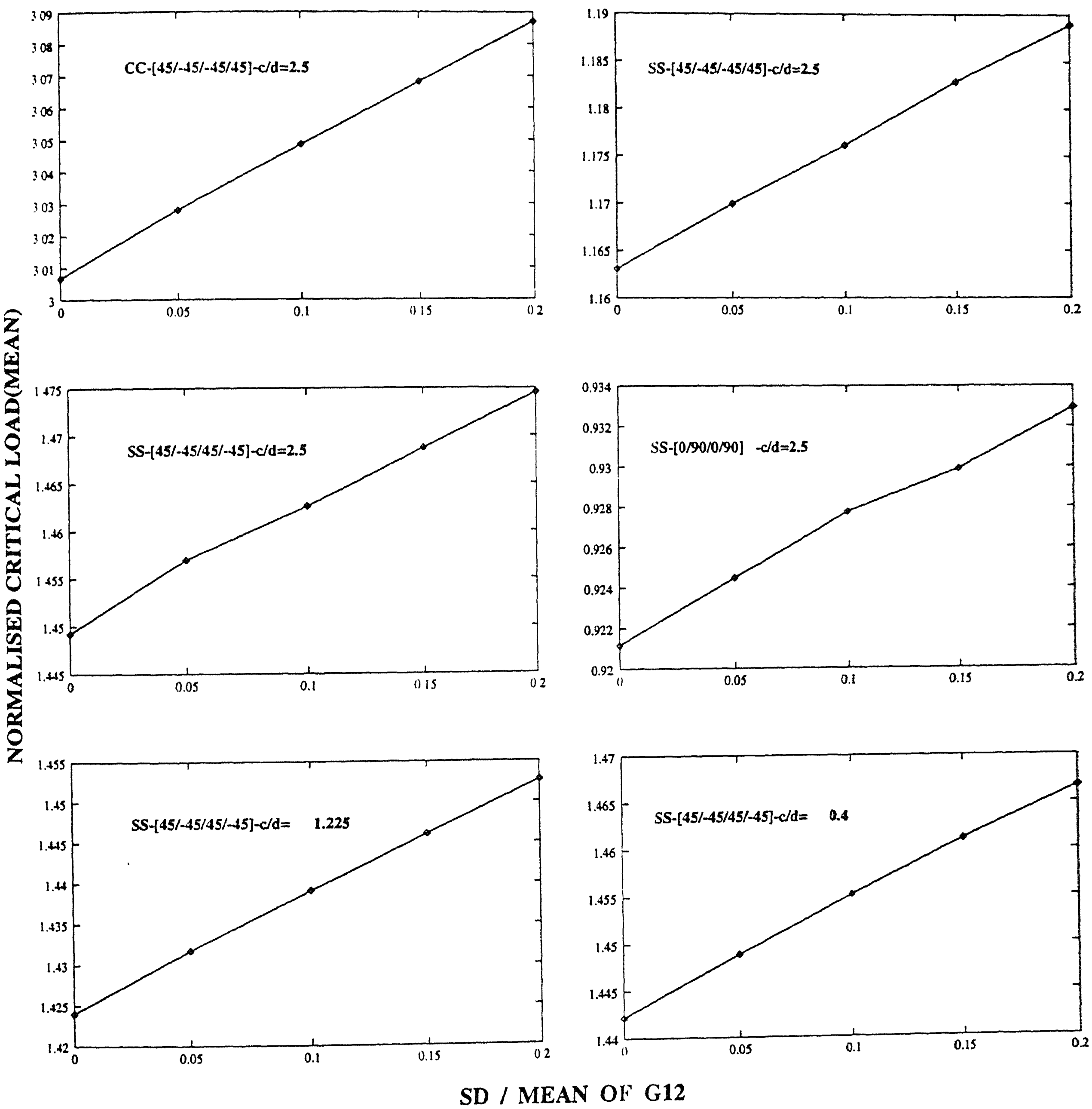

Figure 4.37: Buckling(Mean) characteristics of plate with elliptical cut-out for G_{12} as random

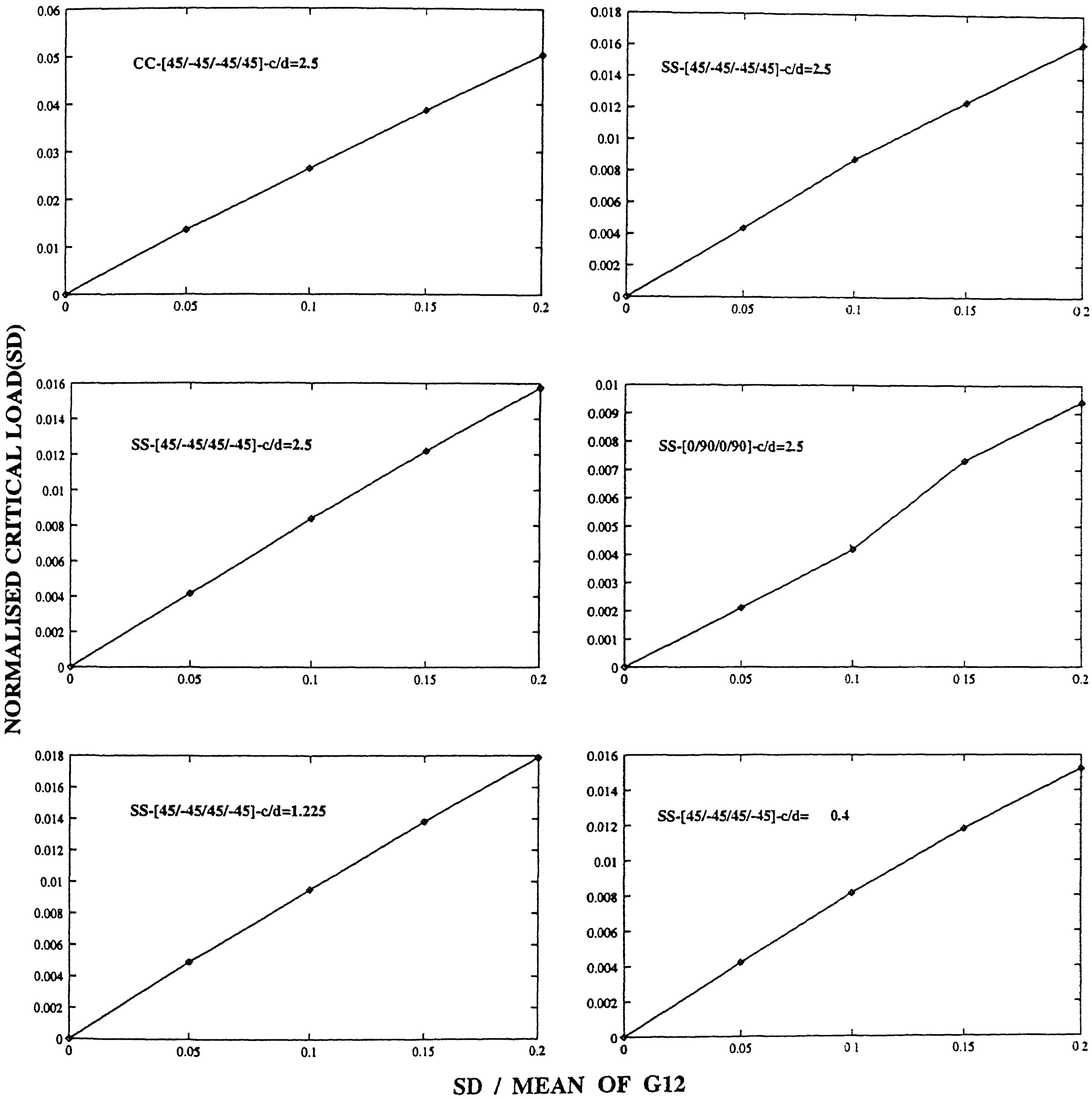

Figure 4.38: Buckling(SD) characteristics of plate with elliptical cut-out for G_{12} as random

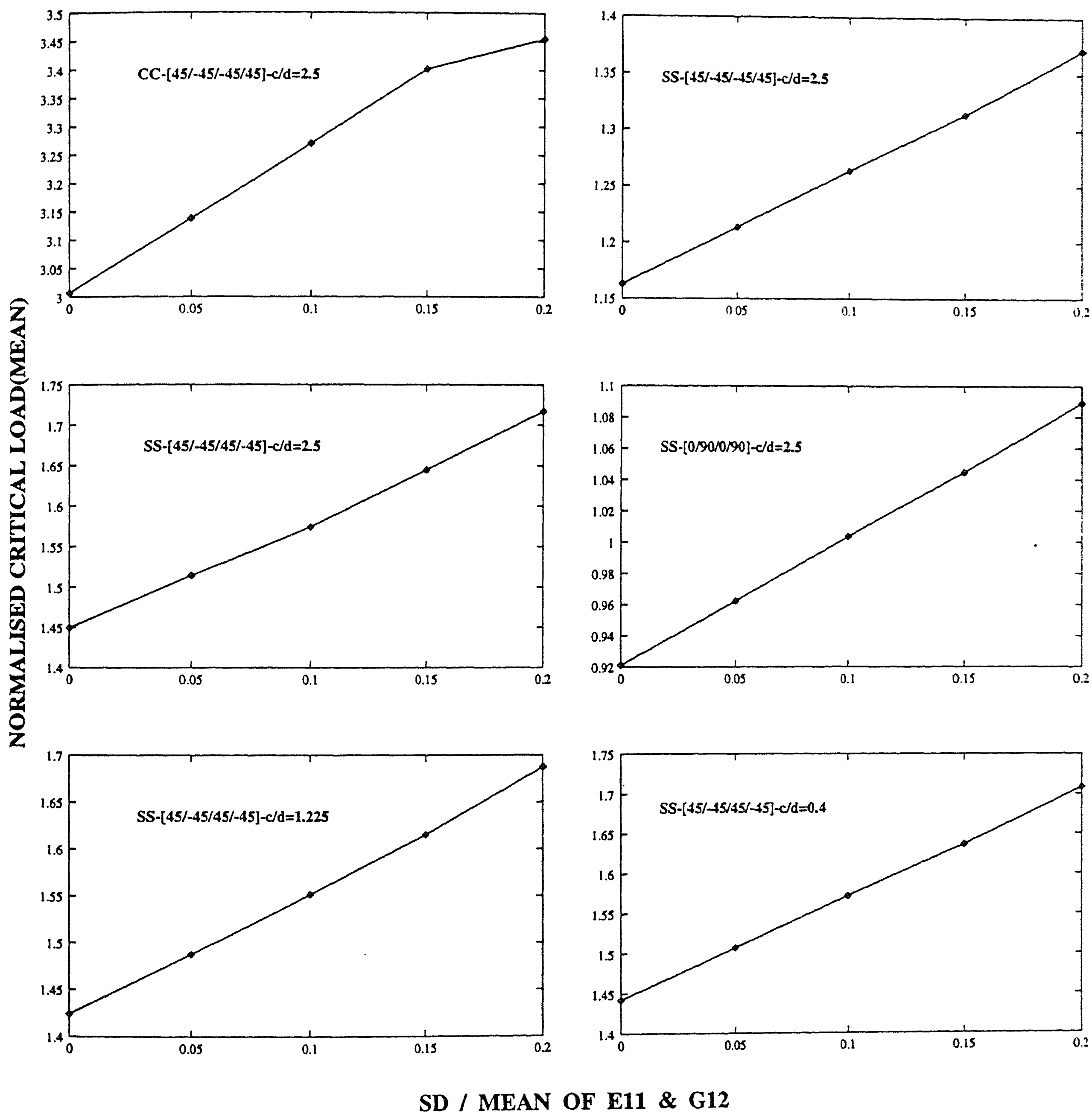

Figure 4.39: Buckling(Mean) characteristics of plate with elliptical cut-out for E_{11} and G_{12} as random

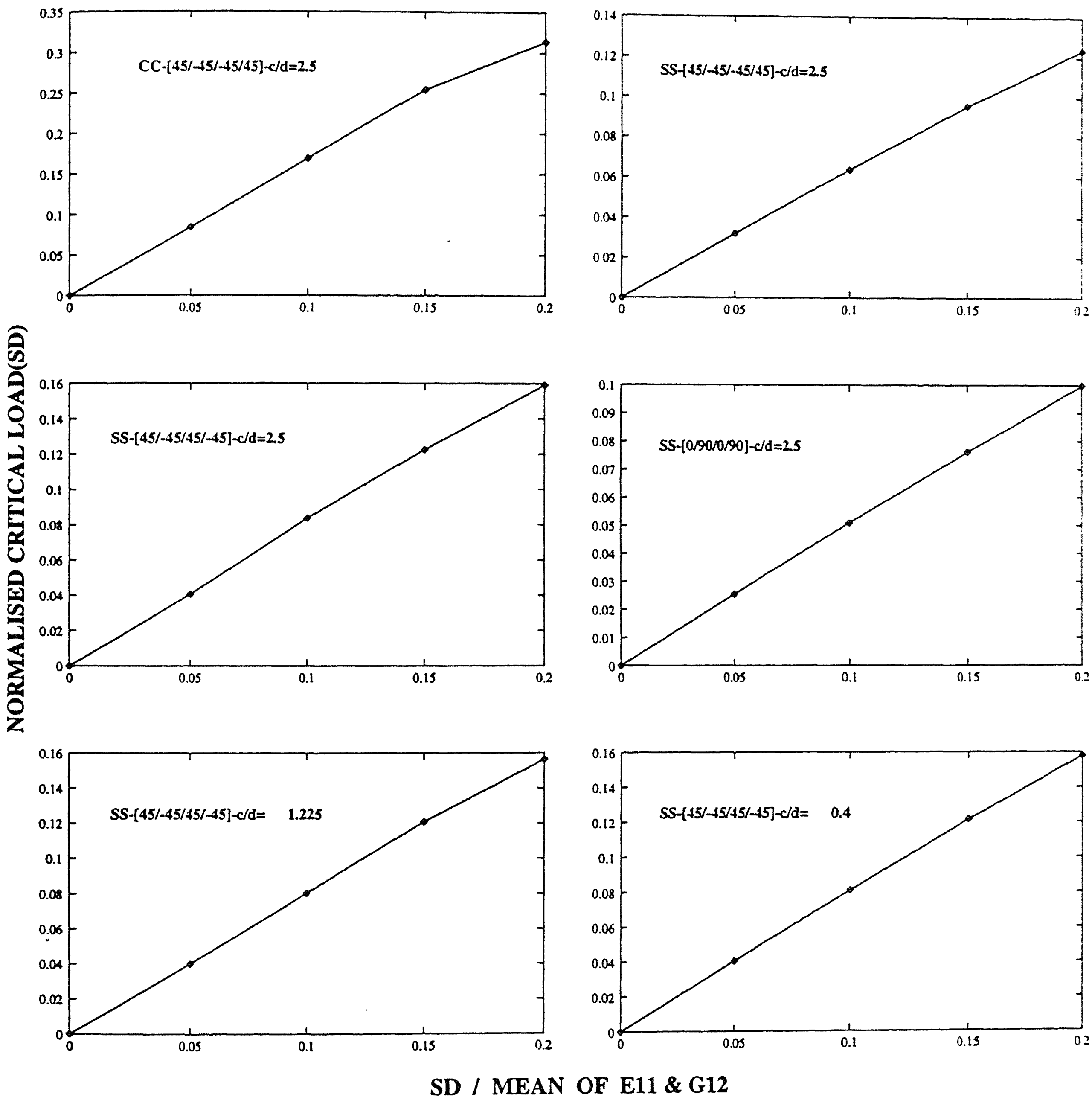

Figure 4.40: Buckling(SD) characteristics of plate with elliptical cut-out for E_{11} and G_{12} as random

Table 4.4: Comparison of normalized (Mean) critical loads for various cut-outs

MATERIAL PROPERTY	σ / μ RATIO	ELLIPTICAL - CUTOUT			RECTANGULAR - CUTOUT			CIRCULAR CUT - OUT
		c/d=2.5	c/d =1.225	c/d=0.4	c/d=1.15	c/d=0.96	c/d=0.87	a/d=1.58
E_{11}	0	1.4492395	1.4240004	1.4421920	1.5621620	1.596388	1.5682254	1.6495797
	5	1.5053510	1.4926805	1.4980849	1.6224700	1.6581648	1.691938	1.7116374
	10	1.5609732	1.5444479	1.5534758	1.6931614	1.7193275	1.6896032	1.7732239
	15	1.6194321	1.5849438	1.6086270	1.7015999	1.7801675	1.7497385	1.8346228
	20	1.6711078	1.6376066	1.6631463	1.8002852	1.8402538	1.8091720	1.9860838
E_{12}	0	1.4492395	1.4240004	1.4421920	1.5621620	1.5963880	1.5682254	1.6495797
	5	1.4513068	1.4260352	1.4443664	1.5641722	1.6184553	1.5703854	1.6532104
	10	1.4533712	1.4280678	1.4465381	1.5661797	1.6355194	1.5725422	1.6568033
	15	1.4554226	1.4300868	1.4486954	1.5681739	1.6500197	1.5746845	1.6603673
	20	1.4574935	1.4321247	1.4508732	1.5701863	1.6716710	1.5768464	1.6639507
G_{12}	0	1.4492395	1.4240004	1.442192	1.5621620	1.5963880	1.5682254	1.6495797
	5	1.4569753	1.4317882	1.4488694	1.5699273	1.6041548	1.5754868	1.6603959
	10	1.4626034	1.4391237	1.4551450	1.5772181	1.6114264	1.5823038	1.6660424
	15	1.4687346	1.4460861	1.4610682	1.5840928	1.6182656	1.5887318	1.6736924
	20	1.4745546	1.4527068	1.4666797	1.5887056	1.6247236	1.5948189	1.6810122
υ_{12}	0	1.4492395	1.4240004	1.4421920	1.5621620	1.5963880	1.5682254	1.6495797
	5	1.4493346	1.4240810	1.4422972	1.5627786	1.5964704	1.5684444	1.6500954
	10	1.4494208	1.4241702	1.4424129	1.5632266	1.5965734	1.56865174	1.6506239
	15	1.4495270	1.4242630	1.4425388	1.5638256	1.5966682	1.5689761	1.6511625
	20	1.4492395	1.4243495	1.4426755	1.5643357	1.5967843	1.5692007	1.6520514
E_{11}& G_{12}	0	1.4492395	1.4240004	1.4421920	1.5621620	1.5983880	1.5682254	1.6495797
	5	1.5145100	1.4878887	1.5070596	1.6326538	1.6571546	1.6389737	1.7446564
	10	1.574315	1.5516605	1.5718314	1.7030315	1.7403914	1.7096150	1.7950891
	15	1.644764	1.6153394	1.6365063	1.7732944	1.8122135	1.7801477	1.8676808
	20	1.7171183	1.6872568	1.7083344	1.8518997	1.8942260	1.8584834	1.9490373

Table 4.5: Comparison of normalized (SD) critical loads for various cut-outs

MATERIAL PROPERTY	σ / μ RATIO	ELLIPTICAL - CUTOUT			RECTANGULAR - CUTOUT			CIRCULAR CUT - OUT
		c/d=2.5	c/d=1.225	c/d=0.4	c/d=1.15	c/d=0.96	c/d=0.87	a/d =1.58
E_{11}	0	0.0000000	0.0000000	0.0000000	0.0000000	0.0000000	0.0000000	0.0000000
	5	0.035745	0.0405153	0.0356054	0.0384147	0.0407634	0.0388382	0.0395384
	10	0.071095	0.0806950	0.0708079	0.0811873	0.0810275	0.0772276	0.0786960
	15	0.108770	0.1192131	0.1057207	0.1139517	0.1207210	0.1152915	0.1175915
	20	0.140840	0.1555576	01402550	0.1511025	0.1557256	0.1529321	0.1678188
E_{12}	0	0.000000	0.0000000	0.0000000	0.0000000	0.0000000	0.0000000	0.0000000
	5	0.001317	0.0012967	0.0013854	0.0013987	0.0013168	0.0013979	0.0023064
	10	0.002632	0.0025914	0.0027686	0.0027990	0.0026317	0.0027930	0.0045980
	15	0.003935	0.0038735	0.0041389	0.0042089	0.0039393	0.0041819	0.0068564
	20	0.005257	0.0051745	0.0055292	0.0056708	0.0054247	0.0055987	0.0091372
G_{12}	0	0.000000	0.0000000	0.0000000	0.0000000	0.0000000	0.0000000	0.0000000
	5	0.004162	0.0049255	0.0042261	0.0049143	0.0050172	0.0045956	0.0068186
	10	0.008409	0.0095218	0.0081467	0.0094676	0.0098529	0.0088526	0.0103780
	15	0.012197	0.0138287	0.0118016	0.0137076	0.0140276	0.0128168	0.0151268
	20	0.015753	0.0178806	0.0152248	0.0163800	0.0182987	0.0165264	0.0196296
υ_{12}	0	0.000000	0.0000000	0.0000000	0.000000	0.0000000	0.0000000	0.0000000
	5	0.000055	0.0000517	0.0000677	0.0000777	0.0000741	0.0000698	0.0003293
	10	0.000118	0.0001111	0.0001433	0.0001467	0.0001281	0.0001503	0.0006673
	15	0.000189	0.0001717	0.0002275	0.0002075	0.0001975	0.0002751	0.0010158
	20	0.000269	0.0002383	0.0003197	0.0003481	0.0002450	0.0003427	0.0013265
E_{11}& G_{12}	0	0.000000	0.0000000	0.0000000	0.0000000	0.0000000	0.0000000	0.0000000
	5	0.040772	0.0402224	0.0404751	0.0441455	0.0477002	0.0441413	0.0619492
	10	0.083770	0.0805695	0.0814567	0.0883622	0.0902348	0.0883475	0.0914177
	15	0.122494	0.1208631	0.1216024	0.1326824	0.1354655	0.1326209	0.1371957
	20	0.159243	0.1564597	0.1581719	0.1721966	0.175937	0.1725041	0.1779614

Chapter 5

Conclusions

In this thesis, a statistical study of the buckling behavior of composite laminated plates with different configurations has been carried out with the help of Monte Carlo simulation, finite element method and commercially available NASTRAN software. The following main conclusions have been drawn from this study.

1. The longitudinal modulus E_{11} and the rigidity modulus G_{12} are the most critical of the material properties. They considerably influence the buckling characteristics of the composite plate.

2. As the AR increases the mean of the buckling load of the plate decreases to the variation in the input material property characteristics.

3. The normalized critical load characteristics of the plate is affected by the edge conditions. The ply-orientation also affects the characteristics but its effect is quite small compared to the effect of the edge conditions.

4. The normalized critical load varies almost linearly with different ARs, boundary conditions and ply-orientations.

5. The CC plate is more sensitive to the changes in material properties compared to SS plate.

6. For a give area of the cut-outs, the buckling load for a laminate with elliptical cut-out is lower than circular and rectangular cut-outs. The buckling load with circular cut-out is the highest.

5.1 Scope for further work

Having worked with this interesting problem for long the author would like to suggest the following for future work.

1. The effect of dispersion in the random material properties on the stresses and dynamics of the plate can be studied.

2. The random material properties were taken to have Normal distribution over lots and was assumed not to vary over the domain of the plate. The problem may be pursued with the material properties having different probability distributions over the domain of the plate as well as varying in lots.

3. Studies to be carried out with bi-axial loading, plate geometry being circular, elliptical etc. The boundary conditions may be fixed, SS, free and in combinations of different boundary conditions. The parameters thickness and ply-orientation, etc. may be taken as random in nature.

4. Studies to be carried out with different cut-out shapes other than regular boundaries with random material properties.

References

[1] C. Zweben, H. T. Habur and T. Chou, "Mechanical behavior and properties of composite materials," *Delaware Composites Design Encyclopedia,* Vol.1, pp. 55-65, New York, Technomic, 1989.

[2] T. Chou, "Mechanical behavior and properties of composite materials," Delaware Composite Design Encyclopedia, Vol.2, pp. 50-55, New York, Technomic, 1989.

[3] R. A. Ibrahim, "Structural dynamics with parameter uncertainties," *Trans., ASME; Applied mechanics review,* Vol. 40, no.3, pp. 309-328, 1987.

[4] S.Nakagiri, H. Takabatake, and S.Tani,"Uncertain eigen value analysis of composite laminated plates by the sfem," *Composite Structures,* Vol.109, pp. 9-12, 1987.

[5] A. W. Leissa and A. F. Martin,"Vibration and buckling of rectangular composite plates with variable fiber spacing," *Composite Structures* , Vol. 14, pp. 339-357, 1990.

[6] S. P. Englestad and J. N. Reddy, "Probabilistic methods for the analysis of metal-matrix composite," *Composite Science and Technology,* Vol. 50, pp. 91-107, 1994

] G. V. Vinckenroy and W. P. de Wilde,"The use of monte carlo techniques in sfem for determination of the structural behavior of composites," *Composite Structures,* Vol. 32, pp. 247-253, 1995

[8] S. Salim, D. Yadav, and N. G. R. Iyengar,"Analysis of composite plates with random material characteristics.,"*Mechanics Research Communication,* Vol. 20, no. 5, pp.405-414, 1993

[9] S. Salim, D. Yadav and N. G. R. Iyengar,"Deflection of composite plates with random material characteristics.,"*Proceedings of Int. Sym. on Aerospace Science and Engineering.,* pp.236-239, Dec 12-15 1992.

[10] B. Navaneetha Raj, N. G. R. Iyengar and D. Yadav,"Analysis of composite laminates with cut-outs and with random material properties using FEM and monte carlo simulation.,"*Proc. the iv world congress as Computational Mechanics.,*pp. 1-9, June 1998.

[11] V. Surya Jagdeesh, "Static response of composite laminates with randomness in material properties and external loading."*M.Tech thesis Dept. of Aerospace Engg., IIT Kanpur.,* May 1998.

[12] S. Salim, D. Yadav and N. G. R. Iyengar,"Free vibration of composite plates with randomness in material properties.," *Proceedings of the Fifth Intl. Conf. on Recent advances in Str. Dynamics,* pp. 814-823, july 18-21 1994.

[13] B. D. Agarwal and L. J. Broutman,"Analysis and Performance of Fiber Composites.,"*John Wiley and sons.,*2nd Edition, 19902nd Edition, 1990.

[14] Jones, R. M.,"Mechanics of Composite Materials.,"*Scripta Book Co.,* 1975